

Wave Propagation in Porothermoelasticity

A Major Research Project Report
(MRP-MAJOR-MATH-2013-2149)

submitted to

University Grants Commission, New Delhi

by

Baljeet Singh

Department of Mathematics,
Post Graduate Government College, Sector-11,
Chandigarh - 160 011, India

E-mail: bsinghgc11@gmail.com

CONTENTS

Chapter No.	Page No.
1. Rayleigh wave in a porothermoelastic solid half-space (Published in Poromechanics VI: Proceedings of the sixth Biot Conference on Poromechanics, ASCE, pp. 1706-1713, 2017)	
2. On Rayleigh wave in a generalized porothermoelastic solid half-space (Published in Research Journal of Engineering and Technology, 9(2) pp. 179-188, 2018)	
3. Reflection of plane waves from surface of a thermoelastic saturated porous solid half-space with impedance boundary conditions (Accepted for publication in Journal of Porous Media, 2018)	
4. Reflection of plane waves from surface of a generalized thermo-viscoelastic porous solid half-space with impedance boundary conditions (Submitted for publication in Computational Methods in Science and Technology)	
5. Summary	

Chapter 1

Rayleigh Wave in a Porothermoelastic Solid Half-space

In this chapter, a problem on the Rayleigh wave at a traction free surface of a generalized porothermoelastic solid half-space is considered. The governing equations of generalized porothermoelasticity are solved for surface wave solutions. The general solutions satisfying the required radiation conditions are obtained in a half-space of the material. These solutions satisfy the suitable boundary conditions at the free surface of the half-space to obtain the secular equation for wave speed of Rayleigh wave. The wave speed of Rayleigh wave is computed for relevant physical constants of material to observe the effects of porosity, frequency, thermal relaxation times, coefficients of thermal expansion and thermoelastic coupling.

1. INTRODUCTION

Linear poroelasticity has important applications in soils and rock materials saturated by groundwater. Fluid-saturated porous materials permeated by groundwater or oil are found on and below the surface of the earth. Water saturated ocean sediments are considered as fluid-saturated porous materials. The theory of poroelasticity was developed by Biot(1956a). A theoretical framework for isothermal wave propagation in fluid-saturated elastic porous media was formulated by Biot (1956b, 1962) for both cases of high and low frequency ranges. Following Biot's theory, many authors have studied problems on propagation of plane and surface waves in fluid-saturated porous materials. Notable among them are Jones (1961), Deresiewicz

and Rice (1962), Hajra and Mukhopadhyay (1982), Tajuddin (1984), Sharma and Gogna (1991), Carcione (1996), Khalili et al. (1999), Berrymann (2005), Tajuddin and Hussaini (2005), Lin et al. (2005), Albers and Wilmanski (2006), Wang et al. (2006), Sharma (2007), Li, et al. (2007), Zyserman and Santos (2007) and Nakagawa and Schoenberg (2007), Lo (2008), Sharma (2012), and many others.

The thermo-mechanical coupling in the poroelastic medium is more complex as compared to classical case due to the fact that the thermal and mechanical coupling occurs between the phases. The problems on wave propagation in saturated thermoelastic porous medium have useful applications in petroleum engineering, chemical engineering, pavement engineering and nuclear waste management. Following Biot (1956c), many researchers including (Schiffman, 1971; Pecker and Dereziwicz, 1973; Mc Tigue, 1986; Coussy, 1989; Kurashige, 1989; Bear et al., 1992; Zhou et al., 1998; Ghassemi and Diek, 2002; Shrefler, 2002; Abousleiman and Ekbote, 2005; Youssef, 2007, Singh, 2011, and Singh, 2013) have contributed various problems in porothermoelastic medium.

The theory of poroelasticity by Biot (1956a, 1962) and the theory of generalized thermoelasticity by Lord and Shulman (1967) inspired Youssef (2007) to develop a generalized theory of porothermoelasticity. In this theory, Youssef (2007) considered a homogeneous, isotropic, elastic matrix whose interstices are filled with a compressible ideal liquid, where both the solid and liquid form continuous and interacting regions and viscous stresses are neglected in the liquid. He assumed that the liquid is capable of exerting a velocity-dependent friction force on the skeleton. This theory was applied by Singh (2011) to show the existence of one shear and four kinds of coupled longitudinal waves in a generalized porothermoelastic solid half-space. Singh (2013) also studied the reflection phenomena in a generalized porothermo-

lastic solid half-space, where the reflection coefficients as well as energy ratios of reflected waves are obtained. In present chapter, the governing equations of generalized porothermoelasticity are solved for surface wave solutions in a half-space. A secular equation for wave speed of Rayleigh wave in the half-space is obtained. The wave speed of Rayleigh wave is computed for a relevant material to show the effects of porosity and various thermal parameters.

2. GOVERNING EQUATIONS

Following Youssef (2007), the linear governing equations of isotropic and homogeneous generalized porothermoelasticity in absence of body forces and heat sources, are

(a) Constitutive equations

$$e_{ij} = \frac{1}{2}(u_{i,j} + u_{j,i}), \quad \epsilon = U_{i,i}, \quad (1)$$

$$\sigma_{ij} = 2\mu e_{ij} + (\lambda e_{kk} + Q\epsilon - R_{11}\Theta^s - R_{12}\Theta^f)\delta_{ij} \quad (2)$$

$$\sigma = Qe_{kk} + R\epsilon - R_{21}\Theta^s - R_{22}\Theta^f \quad (3)$$

$$\rho\eta^s = R_{11}e_{kk} + R_{21}\epsilon + \frac{F_{11}}{T_0}\Theta^s + \frac{F_{12}}{T_0}\Theta^f \quad (4)$$

$$\rho\eta^f = R_{12}e_{kk} + R_{22}\epsilon + \frac{F_{21}}{T_0}\Theta^s + \frac{F_{22}}{T_0}\Theta^f \quad (5)$$

(b) Equations of motion

$$\mu u_{i,jj} + (\lambda + \mu)u_{j,ij} + QU_{j,ij} - R_{11}\Theta_{,i}^s - R_{12}\Theta_{,i}^f = \rho_{11}\ddot{u}_i + \rho_{12}\ddot{U}_i, \quad (6)$$

$$RU_{j,ij} + Qu_{j,ij} - R_{21}\Theta_{,i}^s - R_{22}\Theta_{,i}^f = \rho_{12}\ddot{u}_i + \rho_{22}\ddot{U}_i, \quad (7)$$

(c) Heat Equations

$$K^s \Theta_{,ii}^s = \left(\frac{\partial}{\partial t} + \tau_0^s \frac{\partial^2}{\partial t^2} \right) (F_{11} \Theta^s + F_{12} \Theta^f + T_0 R_{11} e_{ii} + T_0 R_{21} \epsilon), \quad (8)$$

$$K^f \Theta_{,ii}^f = \left(\frac{\partial}{\partial t} + \tau_0^f \frac{\partial^2}{\partial t^2} \right) (F_{21} \Theta^s + F_{22} \Theta^f + T_0 R_{12} e_{ii} + T_0 R_{22} \epsilon), \quad (9)$$

where ρ^{f*} ; ρ^{s*} are the density of the fluid and solid phases, β is the porosity of the material, $\rho^f = \beta \rho^{f*}$ are the density of the fluid phase per unit volume of the bulk, $\rho^s = (1 - \beta) \rho^{s*}$ are the density of the solid phase per unit volume of the bulk, $\rho_{11} = \rho^s - \rho_{12}$ are the mass coefficient of solid phase, $\rho_{22} = \rho^f - \rho_{12}$ are the mass coefficient of fluid phase, ρ_{12} is the dynamic coupling coefficient, u_i ; U_i are the displacements of the skeleton and fluid phases, K^s ; K^f are the thermal conductivities of the solid and fluid phases, τ_0^s ; τ_0^f are the solid and fluid relaxation times, η^s ; η^f are the entropy for the solid and fluid phases, α^s ; α^f are the coefficients of thermal expansion of solid and fluid phases, α^{sf} ; α^{fs} are the thermoelastic coupling between the phases, λ ; μ ; R ; Q , are the poroelastic coefficients, R_{11} ; R_{12} ; R_{21} ; R_{22} , J are the mixed and thermal coefficients, C_E^s ; C_E^f are the specific heat at constant strain of the phases, and $\rho = \rho^s + \rho^f$; $F_{11} = \rho C_E^s$; $F_{22} = \rho C_E^f$; $F_{12} = F_{21} = -JT_0$; $R_{11} = \alpha^s P + \alpha^{fs} Q$; $R_{22} = \alpha^f R + 3\alpha^{sf} Q$; $R_{12} = \alpha^f Q + \alpha^{sf} P$; $R_{21} = 3\alpha^s Q + \alpha^{fs} R$; $\Theta^s = T^s - T_0$, ($|\frac{\Theta^s}{T_0}| \ll 1$); $\Theta^f = T^f - T_0$, ($|\frac{\Theta^f}{T_0}| \ll 1$); where, in the reference state, $T^s = T^f = T_0$.

Using the following Helmholtz's representations

$$u_1 = \phi_{,1}^s - \psi_{,2}^s, \quad u_2 = \phi_{,2}^s + \psi_{,1}^s, \quad (10)$$

$$U_1 = \phi_{,1}^f - \psi_{,2}^f, \quad U_2 = \phi_{,2}^f + \psi_{,1}^f, \quad (11)$$

in the equations (6) to (9), we obtain the following equations in $x_1 - x_2$ plane,

$$(\lambda + 2\mu)(\phi_{,11}^s + \phi_{,22}^s) + Q(\phi_{,11}^f + \phi_{,22}^f) - R_{11} \Theta^s - R_{12} \Theta^f = \rho_{11} \ddot{\phi}^s + \rho_{12} \ddot{\phi}^f, \quad (12)$$

$$R(\phi_{,11}^f + \phi_{,22}^f) + Q(\phi_{,11}^s + \phi_{,22}^s) - R_{21}\Theta^s - R_{22}\Theta^f = \rho_{12}\ddot{\phi}^s + \rho_{22}\ddot{\phi}^f, \quad (13)$$

$$\begin{aligned} & K^s(\Theta_{,11}^s + \Theta_{,22}^s) \\ &= \left(\frac{\partial}{\partial t} + \tau_0^s \frac{\partial^2}{\partial t^2}\right)(F_{11}\Theta^s + F_{12}\Theta^f + T_0 R_{11}(\phi_{,11}^s + \phi_{,22}^s) + T_0 R_{21}(\phi_{,11}^f + \phi_{,22}^f)), \end{aligned} \quad (14)$$

$$\begin{aligned} & K^f(\Theta_{,11}^f + \Theta_{,22}^f) \\ &= \left(\frac{\partial}{\partial t} + \tau_0^f \frac{\partial^2}{\partial t^2}\right)(F_{21}\Theta^s + F_{22}\Theta^f + T_0 R_{12}(\phi_{,11}^s + \phi_{,22}^s) + T_0 R_{22}(\phi_{,11}^f + \phi_{,22}^f)), \end{aligned} \quad (15)$$

$$\mu(\psi_{,11}^s + \psi_{,22}^s) = \rho_{11}\ddot{\psi}^s + \rho_{12}\ddot{\psi}^f, \quad (16)$$

$$0 = \rho_{12}\ddot{\psi}^s + \rho_{22}\ddot{\psi}^f, \quad (17)$$

3. SURFACE WAVE SOLUTIONS

We now consider a porothermoelastic half-space occupying the region $x_2 > 0$ in the reference configuration with boundary $x_2 = 0$ and Rayleigh surface waves propagating along the direction x_1 . The solutions of the equations (12) to (15) are now sought in the form

$$\{\phi^s, \phi^f, \Theta^s, \Theta^f\} = \{\bar{\phi}^s(y), \bar{\phi}^f(y), \bar{\Theta}^s(y), \bar{\Theta}^f(y)\}e^{ik(x_1 - vt)}, \quad (18)$$

in which $y = kx_2$, v is the phase speed, k is the wave number, $\bar{\phi}^s, \bar{\phi}^f, \bar{\psi}^s, \bar{\psi}^f, \bar{\Theta}^s, \bar{\Theta}^f$ are functions of y .

With the help of equation (18), the equations (12) to (15) lead to the following equation,

$$a_0(D^2 - 1)^4 - a_1(D^2 - 1)^3\zeta + a_2(D^2 - 1)^2\zeta^2 - a_3(D^2 - 1)\zeta^3 + a_4\zeta^4 = 0, \quad (19)$$

where $D = d/dx_2, \zeta = v^2$, and the expressions for a_0, a_1, a_2, a_3 and a_4 are given in *Appendix I*. The equation (19) is also written as

$$\begin{aligned}
& a_0 D^8 - (4a_0 + a_1 \zeta) D^6 + (6a_0 + 3a_1 \zeta + a_2 \zeta^2) D^4 \\
& - (4a_0 + 3a_1 \zeta + 2a_2 \zeta^2 + a_3 \zeta^3) D^2 + (a_0 + a_1 \zeta + a_2 \zeta^2 + a_3 \zeta^3 + a_4 \zeta^4) = 0, \quad (20)
\end{aligned}$$

In particular case, if we put $K^s = K^f = 0$; $R_{11} = R_{12} = R_{21} = R_{22} = 0$, the equation (19) or (20) reduces to

$$S_1 D^4 + (S_2 v^2 - 2S_1) D^2 + (S_1 - S_2 v^2 + S_3 v^4) = 0, \quad (21)$$

where

$$S_1 = (\lambda + 2\mu)R - Q^2, \quad S_2 = (\lambda + 2\mu)\rho_{22} + R\rho_{11} - 2Q\rho_{12}, \quad S_3 = \rho_{12}^2 - \rho_{11}\rho_{22}.$$

We require the following radiation conditions on $\bar{\phi}^s, \bar{\phi}^f, \bar{\Theta}^s, \bar{\Theta}^f$ for $x_2 \rightarrow \infty$

$$\bar{\phi}^s(x_2) \rightarrow 0, \quad \bar{\phi}^f(x_2) \rightarrow 0, \quad \bar{\Theta}^s(x_2) \rightarrow 0, \quad \bar{\Theta}^f(x_2) \rightarrow 0, \quad (22)$$

The general solutions $\bar{\phi}^s(y), \bar{\phi}^f(y), \bar{\Theta}^s(y), \bar{\Theta}^f(y)$, which satisfy the radiation conditions (21) are

$$\bar{\phi}^s = \sum_{i=1}^4 A_i \exp(s_i y), \quad \bar{\phi}^f = \sum_{i=1}^4 \xi_i A_i \exp(s_i y), \quad (23)$$

$$\bar{\theta}^s = \sum_{i=1}^4 \eta_i A_i \exp(s_i y), \quad \bar{\theta}^f = \sum_{i=1}^4 \zeta_i A_i \exp(s_i y), \quad (24)$$

The expressions for $\xi_i, \frac{\eta_i}{k^2}, \frac{\zeta_i}{k^2}$, ($i = 1, 2, \dots, 4$) are given in Appendix II.

Similarly, the general solutions $\bar{\psi}^s(y), \bar{\psi}^f(y)$ of equations (16) and (17), which satisfy radiation conditions $\bar{\psi}^s(x_2) \rightarrow 0, \bar{\psi}^f(x_2) \rightarrow 0$, as $x_2 \rightarrow \infty$ are

$$\bar{\psi}^s = B \exp(my), \quad \bar{\psi}^f = \chi B \exp(my), \quad (25)$$

where $m = 1 - \frac{\rho_{11}\rho_{22} - \rho_{12}^2}{\mu\rho_{22}} v^2$ and $\chi = -\rho_{11}/\rho_{22}$.

4. BOUNDARY CONDITIONS

The suitable boundary conditions at free surface $x_2 = 0$ are vanishing of normal stress of solid, tangential stress of solid, liquid stress per unit area, solid heat flux and liquid heat flux

$$\sigma_{22} = 0, \quad \sigma_{12} = 0, \quad \sigma = 0, \quad \frac{\partial \theta^s}{\partial x_2} = 0, \quad \frac{\partial \theta^f}{\partial x_2} = 0, \quad (26)$$

where,

$$\sigma_{22} = \lambda \frac{\partial^2 \phi^s}{\partial x_1^2} + (\lambda + 2\mu) \frac{\partial^2 \phi^s}{\partial x_2^2} + 2\mu \frac{\partial^2 \psi^s}{\partial x_1 \partial x_2} + Q \left(\frac{\partial^2 \phi^f}{\partial x_1^2} + \frac{\partial^2 \phi^f}{\partial x_2^2} \right) - R_{11} \theta^s - R_{12} \theta^f,$$

$$\sigma_{12} = \mu \left(2 \frac{\partial^2 \phi^s}{\partial x_1 \partial x_2} + \frac{\partial^2 \psi^s}{\partial x_1^2} - \frac{\partial^2 \psi^s}{\partial x_2^2} \right),$$

$$\sigma = R \left(\frac{\partial^2 \phi^f}{\partial x_1^2} + \frac{\partial^2 \phi^f}{\partial x_2^2} \right) + Q \left(\frac{\partial^2 \phi^s}{\partial x_1^2} + \frac{\partial^2 \phi^s}{\partial x_2^2} \right) - R_{21} \theta^s - R_{22} \theta^f.$$

The solutions given by (23) to (25) satisfy the boundary conditions (26) and we obtain the following secular equation for Rayleigh wave

$$\begin{aligned} & (1 + m^2) [s_3 s_4 (a_1 b_2 - a_2 b_1) (\eta_3 \zeta_4 - \eta_4 \zeta_3) + s_2 s_4 (a_3 b_1 - a_1 b_3) (\eta_2 \zeta_4 - \eta_4 \zeta_2) \\ & + s_2 s_3 (a_1 b_4 - a_4 b_1) (\eta_2 \zeta_3 - \eta_3 \zeta_2) + s_1 s_4 (a_2 b_3 - a_3 b_2) (\eta_1 \zeta_4 - \eta_4 \zeta_1) \\ & + s_1 s_3 (a_4 b_2 - a_2 b_4) (\eta_1 \zeta_3 - \eta_3 \zeta_1) + s_1 s_2 (a_3 b_4 - a_4 b_3) (\eta_1 \zeta_2 - \eta_2 \zeta_1)] = 0, \end{aligned} \quad (27)$$

where

$$a_i = (\lambda + Q \xi_i) (s_i^2 - 1) + 2\mu s_i^2 - R_{11} \frac{\eta_i}{k^2} - R_{12} \frac{\zeta_i}{k^2}, \quad (i = 1, 2, \dots, 4),$$

$$b_i = (Q + R \xi_i) (s_i^2 - 1) - R_{21} \frac{\eta_i}{k^2} - R_{22} \frac{\zeta_i}{k^2}, \quad (i = 1, 2, \dots, 4).$$

5. RESULTS

The numerical values of the speed of Rayleigh wave is computed for the following values of the relevant parameters at $T_0 = 27 \text{ }^\circ\text{C}$ (Yew and Jogi, 1976),

$$Q = 0.99663 \times 10^{11} \text{ dyne.cm}^{-2}, \quad R = 0.07435 \times 10^{11} \text{ dyne.cm}^{-2},$$

$$\lambda = 0.44363 \times 10^{11} \text{ dyne.cm}^{-2}, \quad \mu = 0.2765 \times 10^{11} \text{ dyne.cm}^{-2},$$

$$\rho_f^* = 0.82 \text{ gm.cm}^{-3}, \quad \rho_s^* = 2.6 \text{ gm.cm}^{-3}, \quad \rho_{11} = 0.002137 \text{ gm.cm}^{-3},$$

$$K^s = 0.4 \text{ cal.cm}^{-1}.\text{s}^{-1}.\text{ }^\circ\text{C}^{-1}, \quad K^f = 0.3 \text{ cal.cm}^{-1}.\text{s}^{-1}.\text{ }^\circ\text{C}^{-1},$$

$$C_E^s = 2.1 \text{ cal.gm}^{-1}.\text{ }^\circ\text{C}^{-1}, \quad C_E^f = 1.9 \text{ cal.gm}^{-1}.\text{ }^\circ\text{C}^{-1},$$

The variation of the speed of Rayleigh wave is shown graphically in figure 1 against the range $0 < \beta \leq 0.8$ of porosity when $\omega = 20Hz$, $\tau_0^s = \tau_0^f = 0.005$, $\alpha^s = \alpha^f = \alpha^{sf} = \alpha^{fs} = 0.01$. It has maximum value $23.3360 \text{ cm.s}^{-1}$ at $\beta = 0.01$. It decreases very sharply to value 2.5825 cm.s^{-1} at $\beta = 0.13$ and then it increases sharply to value $18.6112 \text{ cm.s}^{-1}$ at $\beta = 0.30$. Thereafter, it decreases sharply to its minimum value 1.9220 cm.s^{-1} at $\beta = 0.80$. In absence of thermal effects, this variation reduces to the variation shown by dashed line in figure 1.

The variation of the speed of Rayleigh wave is shown graphically in figure 2 against the range $2 \leq \omega \leq 200Hz$ of frequency when $\beta = 0.25$, $\tau_0^s = \tau_0^f = 0.005$, $\alpha^s = \alpha^f = \alpha^{sf} = \alpha^{fs} = 0.01$. It has its maximum value $34.0043 \text{ cm.s}^{-1}$ at $\omega = 2Hz$. It decreases very sharply to its minimum value 4.2976 cm.s^{-1} at $\omega = 23.6Hz$ and then it increases to value $13.3039 \text{ cm.s}^{-1}$ at $\omega = 200Hz$.

The variation of the speed of Rayleigh wave is shown graphically in figure 3 against the range $0 \leq \tau_0^s \leq 0.005s$ of thermal relaxation in solid when $\beta = 0.25$, $\omega = 20Hz$, $\tau_0^f = 0.005$, $\alpha^s = \alpha^f = \alpha^{sf} = \alpha^{fs} = 0.01$. It has its maximum value 4.3850 cm.s^{-1} at $\tau_0^s = 0$. It decreases to its minimum value 4.3270 cm.s^{-1} at $\tau_0^s = 0.005s$. The variation of the speed of Rayleigh wave is shown graphically in figure 4 against the range $0 \leq \tau_0^f \leq 0.005s$ of thermal relaxation in fluid when $\beta = 0.25$, $\omega = 20Hz$, $\tau_0^s = 0.005$, $\alpha^s = \alpha^f = \alpha^{sf} = \alpha^{fs} = 0.01$. It has its maximum value 4.4902 cm.s^{-1} at $\tau_0^f = 0$. It decreases to its minimum value 4.3270 cm.s^{-1} at $\tau_0^f = 0.005s$.

The variation of the speed of Rayleigh wave is shown graphically in figure 5 against the range $0 \leq \alpha^s \leq 0.01$ of coefficient of thermal expansion in solid when $\beta =$

0.25, $\omega = 20Hz$, $\tau_0^s = \tau_0^f = 0.005s$, $\alpha^f = \alpha^{sf} = \alpha^{fs} = 0.01$. It has its minimum value 3.7536 cm.s^{-1} at $\alpha^s = 0$. It increases to its maximum value 4.3270 cm.s^{-1} at $\alpha^s = 0.01$. The variation of the speed of Rayleigh wave is shown graphically in figure 6 against the range $0 \leq \alpha^f \leq 0.01$ of coefficient of thermal expansion in fluid when $\beta = 0.25$, $\omega = 20Hz$, $\tau_0^s = \tau_0^f = 0.005s$, $\alpha^s = \alpha^{sf} = \alpha^{fs} = 0.01$. It has its maximum value 4.4003 cm.s^{-1} at $\alpha^f = 0$. It decreases to its minimum value 4.3270 cm.s^{-1} at $\alpha^f = 0.01$.

The variation of the speed of Rayleigh wave is shown graphically in figure 7 against the range $0.007 \leq \alpha^{sf} \leq 0.01$ of thermoelastic coupling in solid when $\beta = 0.25$, $\omega = 20Hz$, $\tau_0^s = \tau_0^f = 0.005s$, $\alpha^s = \alpha^f = \alpha^{fs} = 0.01$. It has its maximum value 4.5976 cm.s^{-1} at $\alpha^{sf} = 0.007$. It decreases to its minimum value 4.3270 cm.s^{-1} at $\alpha^{sf} = 0.01$. The variation of the speed of Rayleigh wave is shown graphically in figure 8 against the range $0 \leq \alpha^{fs} \leq 0.01$ of thermoelastic coupling in fluid when $\beta = 0.25$, $\omega = 20Hz$, $\tau_0^s = \tau_0^f = 0.005s$, $\alpha^s = \alpha^f = \alpha^{sf} = 0.01$. It has its minimum value 4.2512 cm.s^{-1} at $\alpha^{fs} = 0$. It increases to its maximum value 4.3270 cm.s^{-1} at $\alpha^{fs} = 0.01$.

6. CONCLUSIONS

The theory of generalized prothermoelasticity is applied to study the Rayleigh wave on a thermally insulated stress free surface of a solid half-space. These theoretical and numerical results may be useful in the detection and study of underground layers of porous solids saturated with oil or groundwater. Water-saturated porous medium can be a more realistic seismic model for oceanic bed. At the ocean bottom, lithosphere is formed by upwelling of hot material at ridges which spreads around and cools with time. The evidences for thermal-mechanical processes that control the formation and evolution of thermoelastic lithosphere below oceans are provided

by the seismological observations. Therefore, the applications of this theoretical and numerical study are geophysical, for example, for the exploration of the oceanic crust, structural engineering or to hydrocarbon/geothermal processes.

ACKNOWLEDGEMENT

Author is highly thankful to University Grants Commission, New Delhi for a Major Research Project on "Wave Propagation in Porothermoelastcity (MRP-MAJOR-MATH-2013-2149).

APPENDIX I.

The expressions for a_0, a_1, a_2, a_3 and a_4 are given as

$$a_0 = \bar{K}^s \bar{K}^f [(\lambda + 2\mu)R - Q^2],$$

$$a_1 = -\bar{K}^s [F_{22}\{(\lambda + 2\mu)R - Q^2\} + T_0\{(\lambda + 2\mu)R_{22}^2 + RR_{12}^2 - 2QR_{12}R_{22}\}]$$

$$-\bar{K}^f [F_{11}\{(\lambda + 2\mu)R - Q^2\} + T_0\{(\lambda + 2\mu)R_{21}^2 + RR_{11}^2 - 2QR_{11}R_{21}\}]$$

$$-\bar{K}^s \bar{K}^f [(\lambda + 2\mu)\rho_{22} + R\rho_{11} - 2Q\rho_{12}],$$

$$a_2 = (F_{11}F_{22} - F_{12}F_{21})[(\lambda + 2\mu)R - Q^2] + (\bar{K}^s F_{22} + \bar{K}^f F_{11})[(\lambda + 2\mu)\rho_{22} + R\rho_{11} - 2Q\rho_{12}]$$

$$+ \bar{K}^s T_0 (\rho_{11}R_{22}^2 + \rho_{22}R_{12}^2 - 2\rho_{12}R_{12}R_{22}) + \bar{K}^f T_0 (\rho_{11}R_{21}^2 + \rho_{22}R_{11}^2 - 2\rho_{12}R_{11}R_{21})$$

$$+ \bar{K}^s \bar{K}^f (\rho_{11}\rho_{22} - \rho_{12}^2) + T_0^2 (R_{11}R_{22} - R_{12}R_{21})^2$$

$$+ T_0 [(\lambda + 2\mu)\{R_{21}^2 F_{22} + R_{22}^2 F_{11} - R_{21}R_{22}(F_{12} + F_{21})\}]$$

$$+ Q\{(F_{12} + F_{21})(R_{11}R_{22} + R_{12}R_{21}) - 2R_{11}R_{21}F_{22} - 2R_{12}R_{22}F_{11}\}$$

$$+ R\{R_{11}^2 F_{22} + R_{12}^2 F_{11} - R_{11}R_{12}(F_{12} + F_{21})\},$$

$$a_3 = (F_{12}F_{21} - F_{11}F_{22})[(\lambda + 2\mu)\rho_{22} + R\rho_{11} - 2Q\rho_{12}]$$

$$+ (\rho_{12}^2 - \rho_{11}\rho_{22})(\bar{K}^s F_{22} + \bar{K}^f F_{11})$$

$$+ T_0 [F_{11}(2\rho_{12}R_{12}R_{22} - \rho_{11}R_{22}^2 - \rho_{22}R_{12}^2)$$

$$+ (F_{12} + F_{21})(\rho_{22}R_{11}R_{12} + \rho_{11}R_{21}R_{22} - \rho_{12}R_{12}R_{21} - \rho_{12}R_{11}R_{22})$$

$$+ F_{22}(2\rho_{12}R_{11}R_{21} - \rho_{22}R_{11}^2 - \rho_{11}R_{21}^2)],$$

$$a_4 = (\rho_{11}\rho_{22} - \rho_{12}^2)(F_{11}F_{22} - F_{12}F_{21}),$$

where, $\bar{K}^s = \frac{K^s}{\tau^{s*}}$ and $\bar{K}^f = \frac{K^f}{\tau^{f*}}$, $\tau^{s*} = \tau_0^s + \frac{i}{\omega}$, $\tau^{f*} = \tau_0^f + \frac{i}{\omega}$.

APPENDIX II.

The expressions for ξ_i , $\frac{\eta_i}{k^2}$, $\frac{\zeta_i}{k^2}$, ($i = 1, 2, \dots, 4$) are given as

$$\xi_i = \frac{(R_{12}q_i - R_{22}p_i) + (R_{11}R_{22} - R_{21}R_{12})\frac{\eta_i}{k^2}}{R_{22}q_i - R_{12}r_i},$$

$$\frac{\eta_i}{k^2} = \frac{f_i(q_i^2 - p_i r_i) - g(R_{22}q_i - R_{12}r_i)}{f_i(R_{21}q_i - R_{11}r_i) - e_i(R_{22}q_i - R_{12}r_i)},$$

$$\frac{\zeta_i}{k^2} = \frac{e_i(q_i^2 - p_i r_i) - g(R_{21}q_i - R_{11}r_i)}{e_i(R_{22}q_i - R_{12}r_i) - f_i(R_{21}q_i - R_{11}r_i)},$$

where

$$p_i = \rho_{11}v^2 + (\lambda + 2\mu)(s_i^2 - 1), \quad q_i = \rho_{12}v^2 + Q(s_i^2 - 1), \quad r_i = [\rho_{22}v^2 + R(s_i^2 - 1)],$$

$$e_i = \tau^{*f}T_0R_{22}[K^s(s_i^2 - 1) + \tau^{*s}v^2F_{11}] - \tau^{*s}\tau^{*f}T_0R_{21}F_{21}v^2,$$

$$f_i = -\tau^{*s}T_0R_{21}[K^f(s_i^2 - 1) + \tau^{*f}v^2F_{22}] + \tau^{*s}\tau^{*f}T_0R_{22}F_{12}v^2,$$

$$g = \tau^{*s}\tau^{*f}T_0v^4(R_{12}R_{21} - R_{11}R_{22}).$$

REFERENCES

- Abousleiman, Y., Ekbote, S., Solutions for the inclined borehole in a porothermoelastic transversely isotropic medium, *J. Appl. Mech.*, vol. **72**, pp. 102-114, 2005.
- Albers, B., Wilmanski, K., Influence of coupling through porosity changes on the propagation of acoustic waves in linear poroelastic materials, *Arch. Mech.*, vol. **58**, pp. 313-325, 2006.
- Bear, J., Sorek, S., Ben-Dor, G., Mazor, G., Displacement waves in saturated thermoelastic porous media. I. Basic equations, *Fluid Dyn. Res.*, vol. **9**, pp. 155-164, 1992.
- Berryman, J.G., Confirmation of Biot's theory, *Appl. Phys. Lett.*, vol. **37**, pp. 382-384, 1980.

- Berryman, J.G., Fluid effects on shear waves in finely layered porous media, *Geophys.*, vol. **70**, N1-N15, 2005.
- Biot, M.A., General solutions of the equations of elasticity and consolidation for a porous material. *J. Appl. Mech.*, vol. **23**, pp. 91-96, 1956a.
- Biot, M.A., Theory of propagation of elastic waves in a fluid-saturated porous solid. I Low frequency range. II. Higher frequency range, *J. Acoust. Soc. Am.*, vol. **28**, pp. 168-191, 1956b.
- Biot, M.A., Mechanics of deformation and acoustic propagation in porous media, *J. Appl. Phys.*, vol. **33**, pp. 1482-1498, 1962.
- Biot, M.A., Thermoelasticity and irreversible thermodynamics. *J. Appl. Phys.*, vol. **27**, pp. 240-253, 1956c.
- Carcione, J.M., Wave propagation in anisotropic, saturated porous media: Plane-wave theory and numerical simulation, *J. Acoust. Soc. Am.*, vol. **99**, pp. 2655-2666, 1996.
- Charlez, P.A., O., Heugas, Measurement of thermoporoelastic properties of rocks: theory and applications. In: Hudson JA, editor, Proceedings of the Eurock 92, ISRM Symposium, pp. 421-446, 1992.
- Coussy, O., A general theory of thermoporoelastoplasticity for saturated porous materials. *Transport in porous media*, vol. **4**, pp. 281-293, 1989.
- Deresiewicz, H., Rice, J.T., The effect of boundaries on wave propagation in a liquid filled porous solid : III. Reflection plane waves at a free plane boundary (General Case), *Bull. Seismo. Soc. Am.*, vol. **52**, pp. 595-625, 1962.
- Gajo, A., Fedel, A., Mongiovi, L., Experimental analysis of the effects of fluid-solid couplings on the velocity of elastic waves in saturated porous media. *Geotech.*, vol. **47**, pp. 993-1008, 1997.

- Ghassemi, A., Diek, A., Porothermoelasticity for swelling shales, *J. Petro. Sci. Eng.*, vol. **34**, pp. 123-135, 2002.
- Hajra, S., Mukhopadhyay, A., Reflection and refraction of seismic waves incident obliquely at the boundary of liquid saturated porous solid, *Bull. Seismo. Soc. Am.*, vol. **72**, pp. 1509-1533, 1982.
- Johnson, D.L., Plona, T.J., Kojima, H., Probing porous media with first and second sound. II. Acoustic properties of water-saturated porous media, *J. Appl. Phys.*, vol. **76**, pp. 115-125, 1994.
- Jones, J.P., Rayleigh wave in a porous elastic saturated solid. *J. Acoust. Soc. Am.* vol. **33**, pp. 959-962, 1961.
- Kelder, O., Smeulders, D.M.J., Observation of the Biot slow wave in water-saturated Nivelsteiner sandstone, *Geophys.*, vol. **62**, pp. 1794-1796, 1997.
- Khalili, N., Yazdchi, M., Valliappan, S., Wave propagation analysis of two-phase saturated porous media using coupled finite-infinite element method, *Soil Dyn. Earth. Eng.*, vol. **18**, pp. 533-553, 1997.
- Kurashige, M., A thermoelastic theory of fluid-filled porous materials. *Int. J. Solids Struct.*, vol. **25**, pp. 1039-1052, 1989.
- Li, Y., Cui, Z.-W., Zhang, Y.-J., Wang, K.-X., Reflection of elastic waves at fluid/fluid saturated poroelastic solid interface *Rock Soil Mech.*, vol. **28**, pp. 1595-1599, 2007.
- Lin, C-H., Lee, V.W., Trifunac, M.D., The reflection of plane waves in a poroelastic half-space saturated with inviscid fluid. *Soil Dyn. Earth. Eng.*, vol. **25**, 205-223, 2005.
- Lo, W.-C., Propagation and attenuation of Rayleigh waves in a semi-infinite unsaturated poroelastic medium. *Adv. Water Resour.* vol. **31**, pp. 1399-1410, 2008.
- Lord, H.W., Shulman, Y., A generalized dynamical theory of thermoelasticity. *J.*

- Mech. Phys. Solids* , vol. **15**, pp. 299-309, 1967.
- Mc Namee, J., Gibson, R.E., Displacement functions and linear transforms applied to diffusion through porous elastic medium. *Quart. J. Mech. Appl. Math.*, vol. **13**, pp. 98-111, 1960.
- McTigue, D., Thermoelastic response of fluid-saturated porous rock. *J. Geophys. Res.*, vol. **91**, pp. 9533-9542, 1986.
- Nakagawa, N.K., Soga, K., Mitchell, J.K., Observation of Biot compressional wave of the second kind in granular soils. *Geotech.*, vol. **47**, pp. 133-147, 1997.
- Nakagawa, S., Schoenberg, M.A., Poroelastic modeling of seismic boundary conditions across a fracture, *J. Acoust. Soc. Am.*, vol. **122**, pp. 831-847, 2007.
- Pecker, C., Deresiewicz, H., Thermal effects on waves in liquid-filled porous media. *Acta Mech.*, vol. **16**, pp. 45-64, 1973.
- Plona, T.J., Observation of a second bulk compressional wave in a porous medium at ultrasonic frequencies, *Appl. Phys. Lett.*, vol. **36**, pp. 259-261, 1980.
- Schiffman, R.L., A thermoelastic theory of consolidation. In Environmental and Geophysical Heat Transfer, *ASME*, New York, vol. **99**, pp. 78-84, 1971.
- Shrefler, B.A. Mechanics and thermodynamics of saturated/unsaturated porous materials and quantitative solutions. *Appl. Mech. Rev.*, **55**, pp. 351-389, 2002.
- Sharma, M.D. and Gogna, M.L., Wave propagation in anisotropic liquid-saturated porous solids, *J. Acoust. Soc. Am.*, vol. **90**, pp. 1068-1073, 1991.
- Sharma, M.D., Wave propagation in a general anisotropic poroelastic medium: Biot's theories and homogenization theory, *J. Earth Syst. Sci.*, vol. **116**, pp. 357-367, 2007.
- Sharma, M.D., Rayleigh waves in a partially-saturated poroelastic solid. *Geophys. J. Int.* vol. **189**, pp. 1203-1214, 2012.

- Singh, B., On propagation of plane waves in generalized porothermoelasticity, *Bull. Seismo. Soc. Am.*, **101**, pp. 756-762, 2011.
- Tajuddin, M. Rayleigh waves in a poroelastic half-space. *J. Acoust. Soc. Am.* vol. **75**, pp. 682-684, 1984.
- Tajuddin, M., Hussaini, S.J., Reflection of plane waves at boundaries of a liquid filled poroelastic half-space, *J. Appl. Geophys.*, vol. **58**, pp. 59-86, 2005.
- Wang, D., Zhang, H.-L., Wang, X.-M., A numerical study of acoustic wave propagation in partially saturated poroelastic rock, *Chinese J. Geophys.*, vol. **49**, pp. 524-532, 2006.
- Yew, C.H., Jogi, P.N., Study of wave motion in fluid-saturated porous rocks, *J. Acoust. Soc. Am.*, vol. **60**, pp. 2-8, 1976.
- Youssef, H.M., Theory of generalized porothermoelasticity, *Int. J. Rock Mech. Min. Sci.*, vol. **44**, pp. 222-227, 2007.
- Yin, S., Dusseault, M.B., Rothenburg, L., Fully coupled numerical modeling of ground surface uplift in steam injection. *J. Can. Petro. Tech.* vol. **49**, pp. 16-21, 2010.
- Yin, S., Dusseault, M.B., Rothenburg, L., Thermal reservoir modelling in petroleum geomechanics. *Int. J. Numer. Analyt. Methods Geomech.* vol. **33**, pp. 449-485, 2009.
- Yin, S., Dusseault, M.B., Rothenburg, L., Multiphase poroelastic modeling in semi-space for deformable reservoirs. *J. Petro. Sci. Eng.* vol. **64**, pp. 45-54, 2009.
- Yin, S., Towler, B.F., Dusseault, M.B., Rothenburg, L., Numerical experiments on oil sands shear dilation and permeability enhancement in a multiphase thermoporoelastoplasticity framework. *J. Petro. Sci. Eng.* vol. **69**, pp. 219-226, 2009.
- Zhou, Y., Rajapakse, R.K.N.D., Graham, J., A coupled thermoporoelastic model

with thermo-osmosis and thermal-filtration. *Int. J. Solids Struct.*, vol. **35**, pp. 4659-4683, 1998.

Zyserman, F.I., Santos, J.E., Analysis of the numerical dispersion of waves in saturated poroelastic media, *Comput. Methods Appl. Mech. Eng.*, vol. **196**, pp. 4644-4655, 2007.

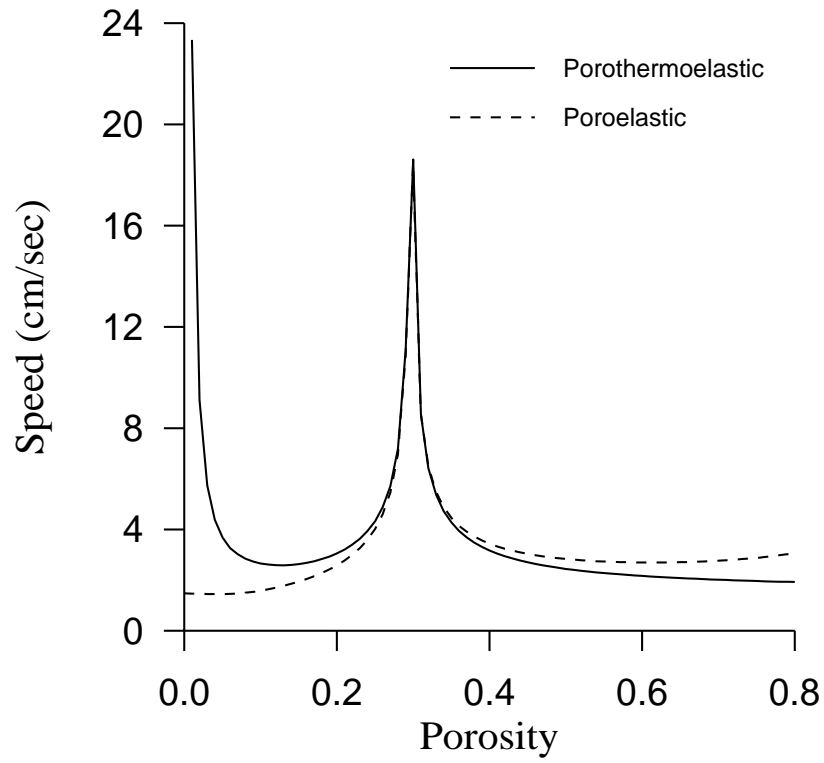


Figure 1. Variation of the speed of Rayleigh wave against porosity (β). (The values on vertical axis are without the multiplier 10^5)

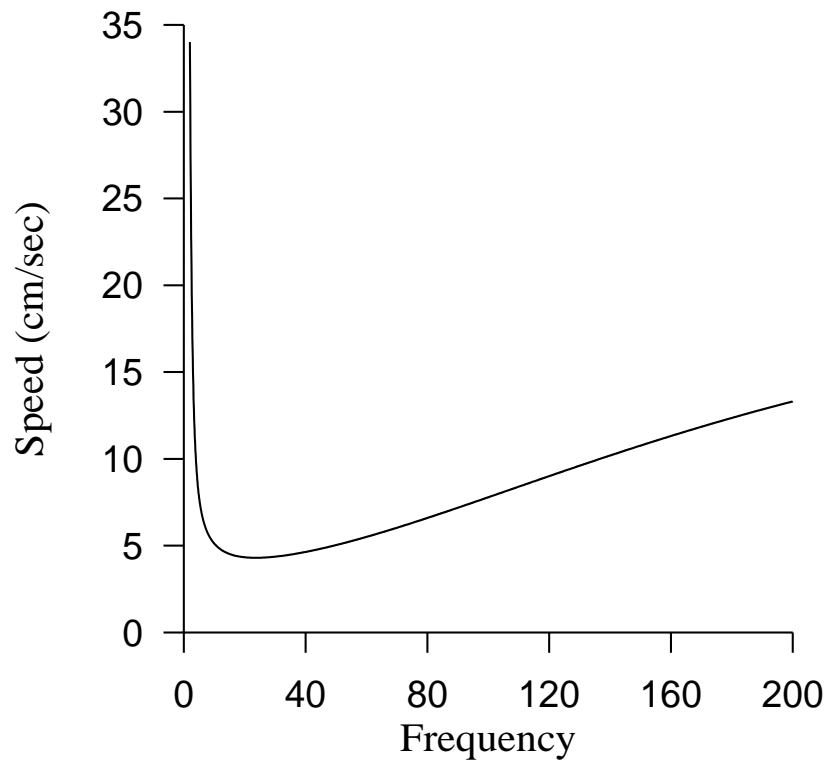


Figure 2. Variation of the speed of Rayleigh wave against frequency (ω). (The values on vertical axis are without the multiplier 10^5)

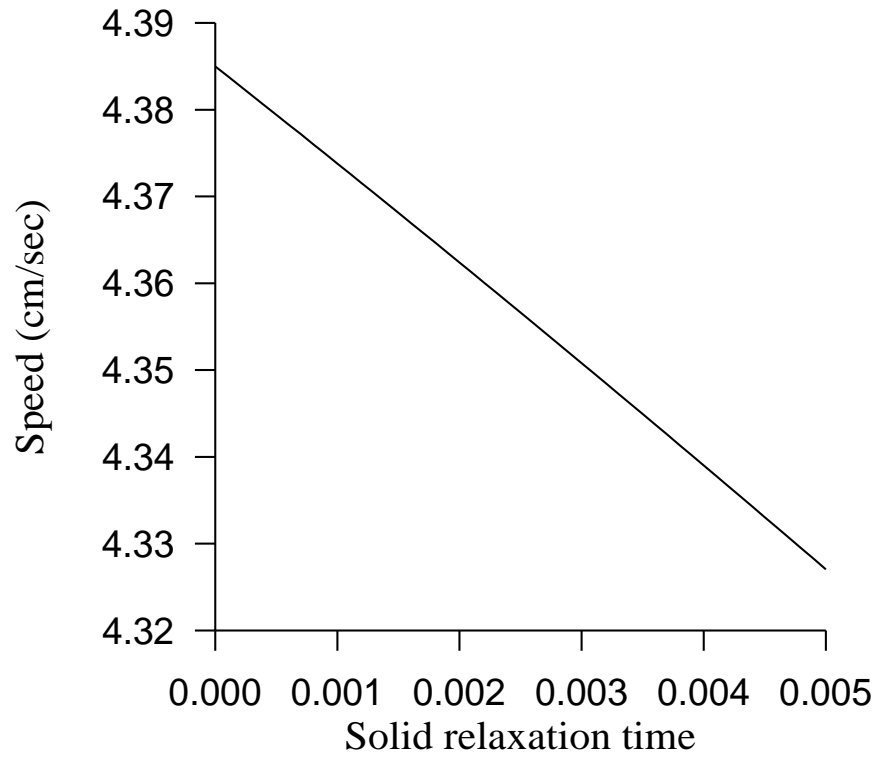


Figure 3. Variation of the speed of Rayleigh wave against thermal relaxation in solid (τ_0^S).
(The values on vertical axis are without the multiplier 10^5)

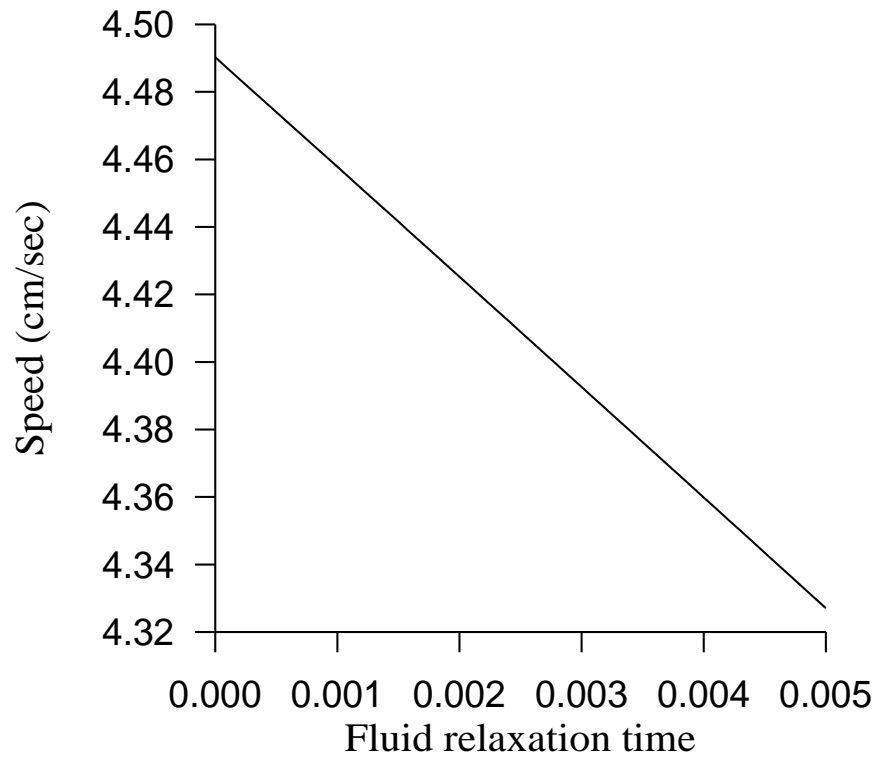


Figure 4. Variation of the speed of Rayleigh wave against thermal relaxation in fluid (τ_0^f).
(The values on vertical axis are without the multiplier 10^5)

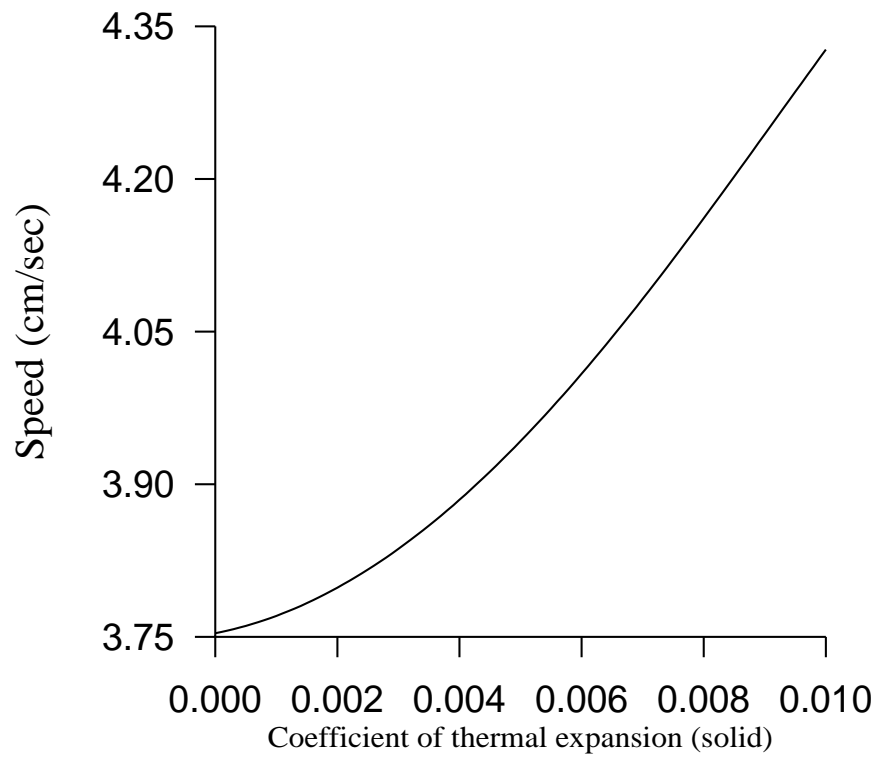


Figure 5. Variation of the speed of Rayleigh wave against coefficient of thermal expansion in solid (α^s). (The values on vertical axis are without the multiplier 10^5)

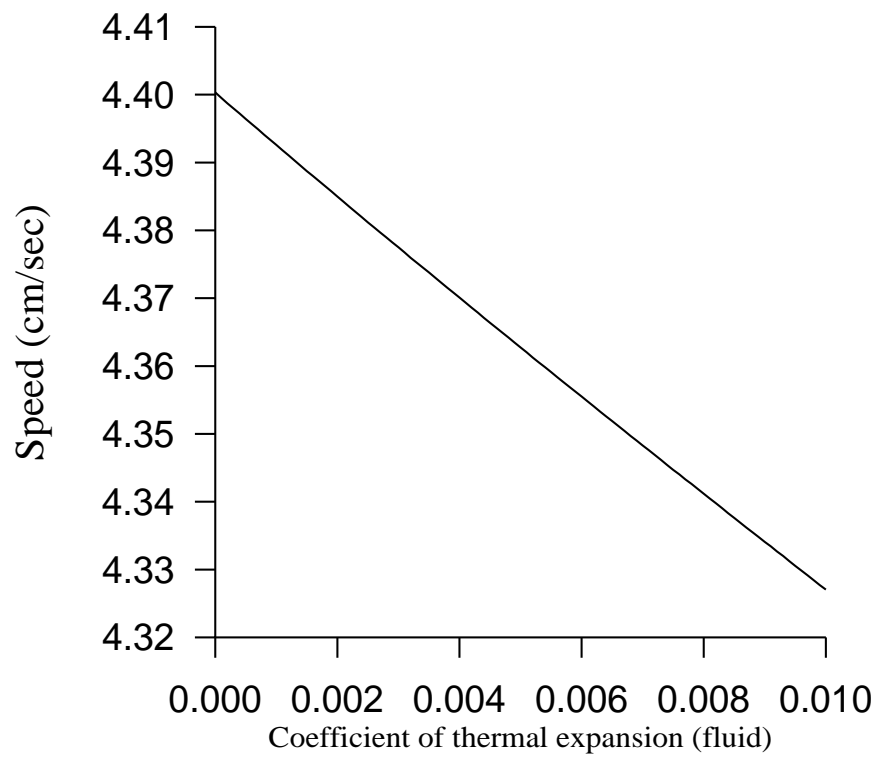


Figure 6. Variation of the speed of Rayleigh wave against coefficient of thermal expansion in fluid (α^f). (The values on vertical axis are without the multiplier 10^5)

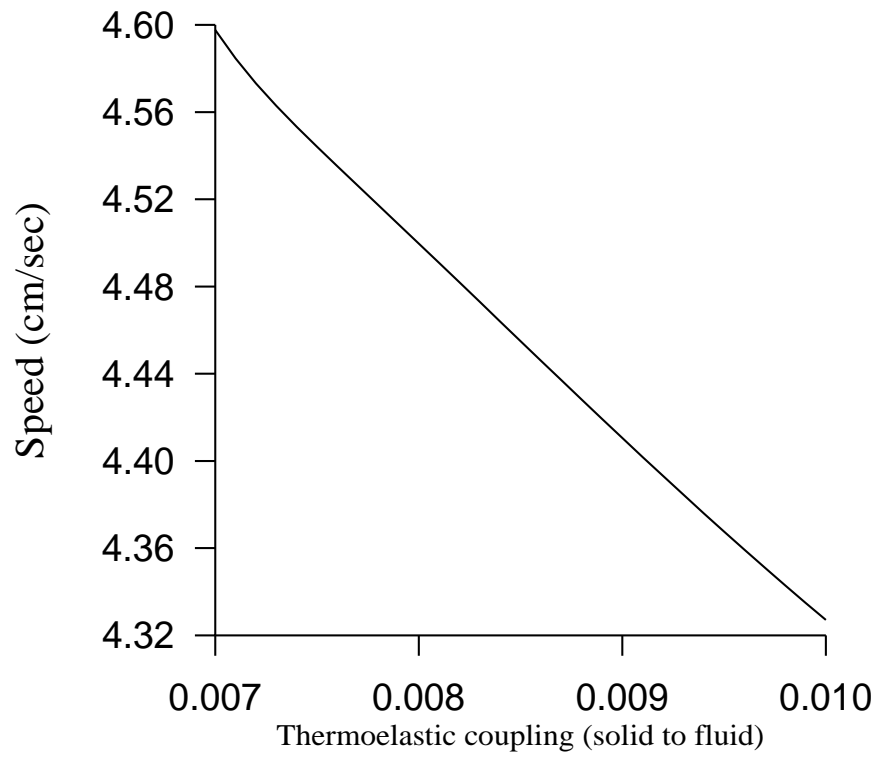


Figure 7. Variation of the speed of Rayleigh wave against thermoelastic coupling (α^{sf}). (The values on vertical axis are without the multiplier 10^5)

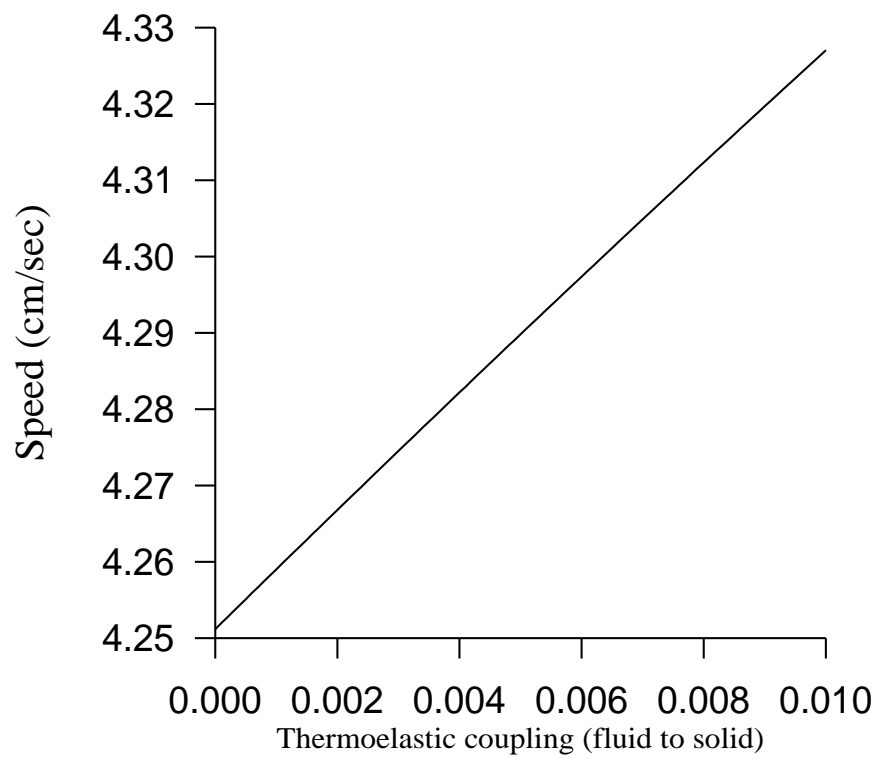


Figure 8. Variation of the speed of Rayleigh wave against thermoelastic coupling (α^{fs}). (The values on vertical axis are without the multiplier 10^5)

Chapter 2

On Rayleigh wave in a generalized porothermoelastic solid half-space

In this chapter, the governing equations of generalized porothermoelasticity are formulated in context of Green and Naghdi theory of thermoelasticity without energy dissipation. A problem on Rayleigh type surface in a generalized porothermoelastic solid half-space is considered. The governing equations are solved for particular surface wave solutions satisfying required radiation conditions in the half-space. A secular equation for Rayleigh wave speed is derived after applying these solutions to relevant boundary conditions at stress free thermally insulated surface of half-space. The Rayleigh wave speed is computed for relevant physical constants of material and plotted against various material parameters to observe the effects of porosity, coefficients of thermal expansion, coefficients of thermoelastic coupling and characteristics of solid and fluid phases.

1. INTRODUCTION

Linear poroelasticity has important applications in soils and rock materials saturated by groundwater. Fluid-saturated porous materials permeated by groundwater or oil are found on and below the surface of the earth. Water saturated ocean sediments are considered as fluid-saturated porous materials. Biot (1956a) gave the theory of fluid-saturated porous materials. Biot (1956b, 1962) also formulated a theoretical framework for isothermal wave propagation in fluid-saturated elastic

porous media for high and low frequency ranges. Many authors followed the Biot's theory and studied various problems on propagation of plane and surface waves in fluid-saturated porous materials. Some prominent contributors are Jones (1961), Deresiewicz and Rice (1962), Hajra and Mukhopadhyay (1982), Tajuddin (1984), Sharma and Gogna (1991), Carcione (1996), Khalili et al. (1999), Berrymann (2005), Tajuddin and Hussaini (2005), Lin et al. (2005), Albers and Wilmanski (2006), Wang et al. (2006), Sharma (2007), Li, et al. (2007), Zyserman and Santos (2007) and Nakagawa and Schoenberg (2007), Lo (2008), Sharma (2012), and many others.

Thermal and mechanical coupling between the phases made the thermo-mechanical coupling in the poroelastic medium more complex as compared to classical case. There are various areas like petroleum engineering, chemical engineering, pavement engineering and nuclear waste management, where the problems on wave propagation in saturated thermoelastic porous medium may find applications. Many researchers including Schiffman, 1971; Pecker and Dereziwicz, 1973; Mc Tigue, 1986; Coussy, 1989; Kurashige, 1989; Bear et al., 1992; Zhou et. al., 1998; Ghassemi and Diek, 2002; Shrefler, 2002; Abousleiman and Ekbote, 2005; Youssef, 2007, Singh, 2011, and Singh, 2013 have followed Biot (1956c) theory and contributed significant problems in porothermoelastic materials.

Following Biot (1956a, 1962) and Lord and Shulman (1967), Youssef (2007) developed a theory of generalized porothermoelasticity, in which he considered a homogeneous, isotropic, elastic matrix whose interstices are filled with a compressible ideal liquid, where both the solid and liquid form continuous and interacting regions and viscous stresses are neglected in the liquid. He also assumed that the liquid is capable of exerting a velocity-dependent friction force on the skeleton. This theory of generalized porothermoelasticity was applied by Singh (2011, 2013) to show the

existence of one shear and four kinds of coupled longitudinal waves and to study the reflection phenomena in a generalized porothermoelastic solid half-space.

In this chapter, the governing equations of generalized porothermoelasticity given in Youssef (2007) are simplified in context of Green and Naghdi (1993) theory of thermoelasticity without energy dissipation. A problem on Rayleigh type surface wave is considered in a generalized porothermoelastic solid half-space. A secular equation in Rayleigh wave speed is derived and solved numerically for a particular material. The wave speed is plotted to observe the effects of porosity and various thermal coefficients.

2. GOVERNING EQUATIONS

According to the theories of Youssef (2007) and Green and Naghdi (1993), the linear governing equations of isotropic and homogeneous generalized porothermoelasticity in absence of body forces and heat sources, are

(a) Constitutive equations

$$e_{ij} = \frac{1}{2}(u_{i,j} + u_{j,i}), \quad \epsilon = U_{i,i}, \quad (1)$$

$$\sigma_{ij} = 2\mu e_{ij} + (\lambda e_{kk} + Q\epsilon - R_{11}\Theta^s - R_{12}\Theta^f)\delta_{ij} \quad (2)$$

$$\sigma = Qe_{kk} + R\epsilon - R_{21}\Theta^s - R_{22}\Theta^f \quad (3)$$

$$\rho\eta^s = R_{11}e_{kk} + R_{21}\epsilon + \frac{F_{11}}{T_0}\Theta^s + \frac{F_{12}}{T_0}\Theta^f \quad (4)$$

$$\rho\eta^f = R_{12}e_{kk} + R_{22}\epsilon + \frac{F_{21}}{T_0}\Theta^s + \frac{F_{22}}{T_0}\Theta^f \quad (5)$$

(b) Equations of motion

$$\mu u_{i,jj} + (\lambda + \mu)u_{j,ij} + QU_{j,ij} - R_{11}\Theta_{,i}^s - R_{12}\Theta_{,i}^f = \rho_{11}\ddot{u}_i + \rho_{12}\ddot{U}_i, \quad (6)$$

$$RU_{j,ij} + Qu_{j,ij} - R_{21}\Theta_{,i^s} - R_{22}\Theta_{,i^f} = \rho_{12}\ddot{u}_i + \rho_{22}\ddot{U}_i, \quad (7)$$

(c) Heat Equations

$$K^s\Theta_{,ii^s} = \frac{\partial^2}{\partial t^2}(F_{11}\Theta^s + F_{12}\Theta^f + T_0R_{11}e_{ii} + T_0R_{21}\epsilon), \quad (8)$$

$$K^f\Theta_{,ii^f} = \frac{\partial^2}{\partial t^2}(F_{21}\Theta^s + F_{22}\Theta^f + T_0R_{12}e_{ii} + T_0R_{22}\epsilon), \quad (9)$$

where the meanings of all symbols are given in Appendix I.

Using the following Helmholtz's representations

$$u_1 = \phi_{,1^s} - \psi_{,2^s}, \quad u_2 = \phi_{,2^s} + \psi_{,1^s}, \quad (10)$$

$$U_1 = \phi_{,1^f} - \psi_{,2^f}, \quad U_2 = \phi_{,2^f} + \psi_{,1^f}, \quad (11)$$

the equations (6) to (9) reduce for $x_1 - x_2$ plane as

$$(\lambda + 2\mu)(\phi_{,11^s} + \phi_{,22^s}) + Q(\phi_{,11^f} + \phi_{,22^f}) - R_{11}\Theta^s - R_{12}\Theta^f = \rho_{11}\ddot{\phi}^s + \rho_{12}\ddot{\phi}^f, \quad (12)$$

$$R(\phi_{,11^f} + \phi_{,22^f}) + Q(\phi_{,11^s} + \phi_{,22^s}) - R_{21}\Theta^s - R_{22}\Theta^f = \rho_{12}\ddot{\phi}^s + \rho_{22}\ddot{\phi}^f, \quad (13)$$

$$K^s(\Theta_{,11^s} + \Theta_{,22^s})$$

$$= \frac{\partial^2}{\partial t^2}(F_{11}\Theta^s + F_{12}\Theta^f + T_0R_{11}(\phi_{,11^s} + \phi_{,22^s}) + T_0R_{21}(\phi_{,11^f} + \phi_{,22^f})), \quad (14)$$

$$K^f(\Theta_{,11^f} + \Theta_{,22^f})$$

$$= \frac{\partial^2}{\partial t^2}(F_{21}\Theta^s + F_{22}\Theta^f + T_0R_{12}(\phi_{,11^s} + \phi_{,22^s}) + T_0R_{22}(\phi_{,11^f} + \phi_{,22^f})), \quad (15)$$

$$\mu(\psi_{,11^s} + \psi_{,22^s}) = \rho_{11}\ddot{\psi}^s + \rho_{12}\ddot{\psi}^f, \quad (16)$$

$$0 = \rho_{12}\ddot{\psi}^s + \rho_{22}\ddot{\psi}^f, \quad (17)$$

3. SURFACE WAVE SOLUTIONS

We now consider a porothermoelastic half-space occupying the region $x_2 > 0$ in the reference configuration with boundary $x_2 = 0$ and Rayleigh surface waves propagating along the direction x_1 . The solutions of the equations (12) to (15) are now sought in the form

$$\{\phi^s, \phi^f, \Theta^s, \Theta^f\} = \{\bar{\phi}^s(y), \bar{\phi}^f(y), \bar{\Theta}^s(y), \bar{\Theta}^f(y)\}e^{ik(x_1-vt)}, \quad (18)$$

in which $\bar{\phi}^s, \bar{\phi}^f, \bar{\psi}^s, \bar{\psi}^f, \bar{\Theta}^s, \bar{\Theta}^f$ are functions of $y, y = kx_2, v$ is the phase speed and k is the wave number.

With the help of equation (18), the equations (12) to (15) lead to the following equation

$$a_0 D^8 - (4a_0 + a_1 \zeta) D^6 + (6a_0 + 3a_1 \zeta + a_2 \zeta^2) D^4 - (4a_0 + 3a_1 \zeta + 2a_2 \zeta^2 + a_3 \zeta^3) D^2 + (a_0 + a_1 \zeta + a_2 \zeta^2 + a_3 \zeta^3 + a_4 \zeta^4) = 0, \quad (19)$$

where $D = d/dx_2, \zeta = v^2$, and the expressions for a_0, a_1, a_2, a_3 and a_4 are given in Appendix II.

We require the following radiation conditions on $\bar{\phi}^s, \bar{\phi}^f, \bar{\Theta}^s, \bar{\Theta}^f$ for $x_2 \rightarrow \infty$

$$\bar{\phi}^s(x_2) \rightarrow 0, \bar{\phi}^f(x_2) \rightarrow 0, \bar{\Theta}^s(x_2) \rightarrow 0, \bar{\Theta}^f(x_2) \rightarrow 0, \quad (20)$$

The general solutions $\bar{\phi}^s(y), \bar{\phi}^f(y), \bar{\Theta}^s(y), \bar{\Theta}^f(y)$, which satisfy the radiation conditions (20) are

$$\bar{\phi}^s = \sum_{i=1}^4 A_i \exp(s_i y), \bar{\phi}^f = \sum_{i=1}^4 \xi_i A_i \exp(s_i y), \quad (21)$$

$$\bar{\theta}^s = \sum_{i=1}^4 \eta_i A_i \exp(s_i y), \bar{\theta}^f = \sum_{i=1}^4 \zeta_i A_i \exp(s_i y), \quad (22)$$

The expressions for $\xi_i, \frac{\eta_i}{k^2}, \frac{\zeta_i}{k^2}, (i = 1, 2, \dots, 4)$ and relations between $s_i, (i = 1, 2, \dots, 4)$, are given in Appendix III.

Similarly, the general solutions $\bar{\psi}^s(y), \bar{\psi}^f(y)$ of equations (16) and (17), which satisfy radiation conditions $\bar{\psi}^s(x_2) \rightarrow 0, \bar{\psi}^f(x_2) \rightarrow 0$, as $x_2 \rightarrow \infty$ are

$$\bar{\psi}^s = B \exp(my), \quad \bar{\psi}^f = \chi B \exp(my), \quad (23)$$

where $m = 1 - \frac{\rho_{11}\rho_{22} - \rho_{12}^2}{\mu\rho_{22}}v^2$ and $\chi = -\rho_{11}/\rho_{22}$.

4. BOUNDARY CONDITIONS

The suitable boundary conditions at free surface $x_2 = 0$ are vanishing of normal stress of solid, tangential stress of solid, liquid stress per unit area, solid heat flux and liquid heat flux

$$\sigma_{22} = 0, \quad \sigma_{12} = 0, \quad \sigma = 0, \quad \frac{\partial\theta^s}{\partial x_2} = 0, \quad \frac{\partial\theta^f}{\partial x_2} = 0, \quad (24)$$

where,

$$\sigma_{22} = \lambda \frac{\partial^2\phi^s}{\partial x_1^2} + (\lambda + 2\mu) \frac{\partial^2\phi^s}{\partial x_2^2} + 2\mu \frac{\partial^2\psi^s}{\partial x_1\partial x_2} + Q \left(\frac{\partial^2\phi^f}{\partial x_1^2} + \frac{\partial^2\phi^f}{\partial x_2^2} \right) - R_{11}\theta^s - R_{12}\theta^f,$$

$$\sigma_{12} = \mu \left(2 \frac{\partial^2\phi^s}{\partial x_1\partial x_2} + \frac{\partial^2\psi^s}{\partial x_1^2} - \frac{\partial^2\psi^s}{\partial x_2^2} \right),$$

$$\sigma = R \left(\frac{\partial^2\phi^f}{\partial x_1^2} + \frac{\partial^2\phi^f}{\partial x_2^2} \right) + Q \left(\frac{\partial^2\phi^s}{\partial x_1^2} + \frac{\partial^2\phi^s}{\partial x_2^2} \right) - R_{21}\theta^s - R_{22}\theta^f.$$

The solutions given by (21) to (23) satisfy the boundary conditions (24) and we obtain the following secular equation for Rayleigh wave

$$\begin{aligned} & (1 + m^2)[s_3s_4(a_1b_2 - a_2b_1)(\eta_3\zeta_4 - \eta_4\zeta_3) + s_2s_4(a_3b_1 - a_1b_3)(\eta_2\zeta_4 - \eta_4\zeta_2) \\ & + s_2s_3(a_1b_4 - a_4b_1)(\eta_2\zeta_3 - \eta_3\zeta_2) + s_1s_4(a_2b_3 - a_3b_2)(\eta_1\zeta_4 - \eta_4\zeta_1) \\ & + s_1s_3(a_4b_2 - a_2b_4)(\eta_1\zeta_3 - \eta_3\zeta_1) + s_1s_2(a_3b_4 - a_4b_3)(\eta_1\zeta_2 - \eta_2\zeta_1)] = 0, \end{aligned} \quad (25)$$

where

$$a_i = (\lambda + Q\xi_i)(s_i^2 - 1) + 2\mu s_i^2 - R_{11}\frac{\eta_i}{k^2} - R_{12}\frac{\zeta_i}{k^2}, \quad (i = 1, 2, \dots, 4),$$

$$b_i = (Q + R\xi_i)(s_i^2 - 1) - R_{21}\frac{\eta_i}{k^2} - R_{22}\frac{\zeta_i}{k^2}, \quad (i = 1, 2, \dots, 4).$$

5. RESULTS

The real part of wave speed of Rayleigh wave is computed for following physical constants at $T_0 = 27 \text{ }^\circ\text{C}$ (Yew and Jogi, 1976)

$$Q = 0.99663 \times 10^{11} \text{ dyne.cm}^{-2}, \quad R = 0.07435 \times 10^{11} \text{ dyne.cm}^{-2},$$

$$\lambda = 0.44363 \times 10^{11} \text{ dyne.cm}^{-2}, \quad \mu = 0.2765 \times 10^{11} \text{ dyne.cm}^{-2},$$

$$\rho_f^* = 0.82 \text{ gm.cm}^{-3}, \quad \rho_s^* = 2.6 \text{ gm.cm}^{-3}, \quad \rho_{11} = 0.002137 \text{ gm.cm}^{-3},$$

$$C_E^s = 2.1 \text{ cal.gm}^{-1}.^\circ\text{C}^{-1}, \quad C_E^f = 1.9 \text{ cal.gm}^{-1}.^\circ\text{C}^{-1}.$$

The variations of the wave speed of Rayleigh wave are shown graphically in figure 1 against the range $0.1 < \beta \leq 0.8$ of porosity when $\alpha^s = \alpha^f = \alpha^{sf} = \alpha^{fs} = 0.01$, $K^s = 0.5 \text{ cal.cm}^{-1}.s^{-1}.^\circ\text{C}^{-1}$, and $K^f = 0.4 \text{ cal.cm}^{-1}.s^{-1}.^\circ\text{C}^{-1}$ for porothermoelastic and poroelastic cases by solid and dashed lines, respectively. In porothermoelastic case, the value of wave speed is $1.24 \times 10^5 \text{ cm. s}^{-1}$ when $\beta = 0.1$. It increases very sharply and attains its maximum value $9.3448 \times 10^5 \text{ cm. s}^{-1}$ at $\beta = 0.3$. Thereafter, it decreases very sharply to a value $0.5048 \times 10^5 \text{ cm. s}^{-1}$ at $\beta = 0.8$. In absence of thermal effects, this variation reduces to a similar variation shown by dashed line in figure 1. The comparison of solid and dashed lines in figure 1 shows the effect of presence of porosity. This effect becomes more prominent in the range of porosity between 0.3 and 0.8.

For $\beta = 0.4, 0.5$ and 0.6 , the variations of the wave speed of Rayleigh wave are shown graphically in figure 2 against the range $0 \leq \alpha^s \leq 0.01$ of coefficient of thermal expansion in solid phase by solid, small dashed and long dashed lines, respectively when $\alpha^f = \alpha^{sf} = \alpha^{fs} = 0.01$, $K^s = 0.5 \text{ cal.cm}^{-1}.s^{-1}.^\circ\text{C}^{-1}$, and $K^f = 0.4 \text{ cal.cm}^{-1}.s^{-1}.^\circ\text{C}^{-1}$. For $\beta = 0.4$, it has its minimum value $1.1957 \times 10^5 \text{ cm. s}^{-1}$ at $\alpha^s = 0$. It increases to its maximum value $1.399 \times 10^5 \text{ cm. s}^{-1}$ at $\alpha^s = 0.01$.

By comparing the solid and dashed variations in figure 2, the effects of the presence porosity and coefficient of thermal expansion in solid phase are observed on wave speed of the Rayleigh wave.

For $\beta = 0.4, 0.5$ and 0.6 , the variations of the wave speed of Rayleigh wave are shown graphically in figure 3 against the range $0 \leq \alpha^f \leq 0.01$ of coefficient of thermal expansion in fluid phase by solid, small dashed and long dashed lines, respectively when $\alpha^s = \alpha^{sf} = \alpha^{fs} = 0.01$, $K^s = 0.5 \text{ cal.cm}^{-1}.\text{s}^{-1}.\text{ }^\circ\text{C}^{-1}$, and $K^f = 0.4 \text{ cal.cm}^{-1}.\text{s}^{-1}.\text{ }^\circ\text{C}^{-1}$. For $\beta = 0.4$, it has its maximum value $1.4838 \times 10^5 \text{ cm. s}^{-1}$ at $\alpha^f = 0$. It decreases to its minimum value $1.399 \times 10^5 \text{ cm. s}^{-1}$ at $\alpha^f = 0.01$. The comparison of solid and dashed variations in figure 3 shows the effects of the presence porosity and coefficient of thermal expansion in fluid phase are observed on wave speed of the Rayleigh wave.

For $\beta = 0.4, 0.5$ and 0.6 , the variations of the wave speed of Rayleigh wave are shown graphically in figure 4 against the range $0.002 \leq \alpha^{sf} \leq 0.01$ of thermoelastic coupling in solid phase by solid, small dashed and long dashed lines, respectively when $\alpha^s = \alpha^f = \alpha^{fs} = 0.01$, $K^s = 0.5 \text{ cal.cm}^{-1}.\text{s}^{-1}.\text{ }^\circ\text{C}^{-1}$, and $K^f = 0.4 \text{ cal.cm}^{-1}.\text{s}^{-1}.\text{ }^\circ\text{C}^{-1}$. For $\beta = 0.4$, it has a value $0.6875 \times 10^5 \text{ cm. s}^{-1}$ at $\alpha^{sf} = 0.002$. It increases sharply to its maximum value $1.4319 \times 10^5 \text{ cm. s}^{-1}$ at $\alpha^{sf} = 0.0078$ and then decreases slowly to a value $1.399 \times 10^5 \text{ cm. s}^{-1}$ at $\alpha^{sf} = 0.01$. By comparing the solid and dashed variations in figure 4, the effects of the presence porosity and thermoelastic coupling in solid phase are observed on wave speed of the Rayleigh wave.

For $\beta = 0.4, 0.5$ and 0.6 , the variations of the wave speed of Rayleigh wave are shown graphically in figure 5 against the range $0 \leq \alpha^{fs} \leq 0.01$ of thermoelastic coupling in fluid phase by solid, small dashed and long dashed lines, respec-

tively when $\alpha^s = \alpha^f = \alpha^{sf} = 0.01$, $K^s = 0.5 \text{ cal.cm}^{-1}.\text{s}^{-1}.\text{ }^\circ\text{C}^{-1}$, and $K^f = 0.4 \text{ cal.cm}^{-1}.\text{s}^{-1}.\text{ }^\circ\text{C}^{-1}$. For $\beta = 0.4$, it has a value $1.3810 \times 10^5 \text{ cm. s}^{-1}$ at $\alpha^{fs} = 0$. It increases very slowly to its maximum value $1.399 \times 10^5 \text{ cm. s}^{-1}$ at $\alpha^{fs} = 0.01$. The comparison of solid and dashed variations in figure 5 shows the effects of the presence porosity and thermoelastic coupling in fluid phase are observed on wave speed of Rayleigh wave.

For $\beta = 0.4, 0.5$ and 0.6 , the variations of the wave speed of Rayleigh wave are shown graphically in figure 6 against the range $0.4 \leq K^s \leq 1$ of the characteristic of solid phase by solid, small dashed and long dashed lines, respectively when $\alpha^s = \alpha^f = \alpha^{sf} = \alpha^{fs} = 0.01$ and $K^f = 0.4 \text{ cal.cm}^{-1}.\text{s}^{-1}.\text{ }^\circ\text{C}^{-1}$. For $\beta = 0.4$, it has a value $1.15 \times 10^5 \text{ cm. s}^{-1}$ at $K^s = 0.4$. It increases sharply to its maximum value $1.469 \times 10^5 \text{ cm. s}^{-1}$ at $K^s = 0.634$ and then decreases to a value $1.3207 \times 10^5 \text{ cm. s}^{-1}$ at $K^s = 1$. By comparing the solid and dashed variations in figure 6, the effects of the presence porosity and characteristic of solid phase are observed on wave speed of the Rayleigh wave.

For $\beta = 0.4, 0.5$ and 0.6 , the variations of the wave speed of Rayleigh wave are shown graphically in figure 7 against the range $0.25 \leq K^f \leq 1$ of the characteristic of fluid phase by solid, small dashed and long dashed lines, respectively when $\alpha^s = \alpha^f = \alpha^{sf} = \alpha^{fs} = 0.01$ and $K^s = 0.5 \text{ cal.cm}^{-1}.\text{s}^{-1}.\text{ }^\circ\text{C}^{-1}$. For $\beta = 0.4$, it has a value $1.2326 \times 10^5 \text{ cm. s}^{-1}$ at $K^f = 0.25$. It increases sharply to its maximum value $1.457 \times 10^5 \text{ cm. s}^{-1}$ at $K^f = 0.867$ and then decreases very slowly to a value $1.456 \times 10^5 \text{ cm. s}^{-1}$ at $K^f = 1$. The comparison of solid and dashed variations in figure 7 shows the effects of the presence porosity and characteristic of fluid phase are observed on wave speed of the Rayleigh wave.

6. CONCLUSIONS

The theory of Green and Naghdi generalized thermoelasticity is employed to study the Rayleigh wave on a thermally insulated stress free surface of a porothermoelastic solid half-space. With the help of particular surface wave solutions in half-space and relevant boundary conditions at free surface, a secular equation in wave speed of Rayleigh wave is obtained. The secular equation is solved numerically by a fortran program of iteration method. The real wave speed of Rayleigh wave is computed for relevant physical constants of porothermoelastic material (Yew and Jogi, 1976). To observe the dependence of wave speed of various material parameters, the wave speed of the Rayleigh wave is plotted against porosity, coefficients of thermal expansion in solid and fluid phases, thermoelastic coupling coefficients in solid and fluid phases and characteristics of solid and fluid phases. Some concluding remarks obtained from the numerical discussion of wave speed in these plots are given as

- (i) The wave speed of Rayleigh wave in Green-Naghdi porothermoelastic solid depends on porosity of the material. In absence of thermal parameters, the wave speed increases at each value of porosity in considered range. The thermal effect on wave speed becomes more prominent beyond $\beta = 0.3$.
- (ii) The effect of porosity on wave speed increases with the increase in value of coefficient of thermal expansion in solid phase.
- (iii) The effect of porosity on wave speed decreases with the increase in value of coefficient of thermal expansion in fluid phase.
- (iv) The effect of porosity on wave speed increases with the increase in values of coefficients of thermoelastic coupling for both solid to fluid and fluid to solid.
- (v) The wave speed of Rayleigh wave is affected significantly by characteristics of solid and fluid phases for different values of porosity.

Seismological observations provide the evidences of thermal-mechanical processes which control the formation and evolution of thermoelastic lithosphere below oceans. The present study may be useful in studying underground layers of porous solids saturated with oil or groundwater.

ACKNOWLEDGEMENT

Author is highly thankful to University Grants Commission, New Delhi for granting a Major Research Project (MRP-MAJOR-MATH-2013-2149).

APPENDIX I.

ρ^{f*} ; ρ^{s*} are the density of the fluid and solid phases, β is the porosity of the material,

$\rho^f = \beta\rho^{f*}$ are the density of the fluid phase per unit volume of the bulk,

$\rho^s = (1 - \beta)\rho^{s*}$ are the density of the solid phase per unit volume of the bulk,

$\rho_{11} = \rho^s - \rho_{12}$ are the mass coefficient of solid phase,

$\rho_{22} = \rho^f - \rho_{12}$ are the mass coefficient of fluid phase,

ρ_{12} is the dynamic coupling coefficient,

$u_i; U_i$ are the displacements of the skeleton and fluid phases,

$K^s; K^f$ are the characteristics of the solid and fluid phases,

$\eta^s; \eta^f$ are the entropy for the solid and fluid phases,

$\alpha^s; \alpha^f$ are the coefficients of thermal expansion of solid and fluid phases,

$\alpha^{sf}; \alpha^{fs}$ are the thermoelastic coupling between the phases, $\lambda; \mu; R; Q$, are the poroelastic coefficients,

$R_{11}; R_{12}; R_{21}; R_{22}, J$ are the mixed and thermal coefficients,

$C_E^s; C_E^f$ are the specific heat at constant strain of the phases,

$\rho = \rho^s + \rho^f; F_{11} = \rho C_E^s; F_{22} = \rho C_E^f; F_{12} = F_{21} = -JT_0;$

$R_{11} = \alpha^s P + \alpha^{fs} Q; R_{22} = \alpha^f R + 3\alpha^{sf} Q; R_{12} = \alpha^f Q + \alpha^{sf} P; R_{21} = 3\alpha^s Q + \alpha^{fs} R;$

$\Theta^s = T^s - T_0, (|\frac{\Theta^s}{T_0}| \ll 1); \quad \Theta^f = T^f - T_0, (|\frac{\Theta^f}{T_0}| \ll 1);$ where, in the reference state, $T^s = T^f = T_0$.

APPENDIX II.

The expressions for a_0, a_1, a_2, a_3 and a_4 are given as

$$a_0 = K^s K^f [(\lambda + 2\mu)R - Q^2],$$

$$a_1 = -K^s [F_{22}\{(\lambda + 2\mu)R - Q^2\} + T_0\{(\lambda + 2\mu)R_{22}^2 + RR_{12}^2 - 2QR_{12}R_{22}\}]$$

$$-K^f [F_{11}\{(\lambda + 2\mu)R - Q^2\} + T_0\{(\lambda + 2\mu)R_{21}^2 + RR_{11}^2 - 2QR_{11}R_{21}\}]$$

$$-K^s \bar{K}^f [(\lambda + 2\mu)\rho_{22} + R\rho_{11} - 2Q\rho_{12}],$$

$$a_2 = (F_{11}F_{22} - F_{12}F_{21})[(\lambda + 2\mu)R - Q^2] + (K^s F_{22} + K^f F_{11})[(\lambda + 2\mu)\rho_{22} + R\rho_{11} - 2Q\rho_{12}]$$

$$+ K^s T_0(\rho_{11}R_{22}^2 + \rho_{22}R_{12}^2 - 2\rho_{12}R_{12}R_{22}) + K^f T_0(\rho_{11}R_{21}^2 + \rho_{22}R_{11}^2 - 2\rho_{12}R_{11}R_{21})$$

$$+ K^s K^f (\rho_{11}\rho_{22} - \rho_{12}^2) + T_0^2 (R_{11}R_{22} - R_{12}R_{21})^2$$

$$+ T_0 [(\lambda + 2\mu)\{R_{21}^2 F_{22} + R_{22}^2 F_{11} - R_{21}R_{22}(F_{12} + F_{21})\}]$$

$$+ Q\{(F_{12} + F_{21})(R_{11}R_{22} + R_{12}R_{21}) - 2R_{11}R_{21}F_{22} - 2R_{12}R_{22}F_{11}\}$$

$$+ R\{R_{11}^2 F_{22} + R_{12}^2 F_{11} - R_{11}R_{12}(F_{12} + F_{21})\},$$

$$a_3 = (F_{12}F_{21} - F_{11}F_{22})[(\lambda + 2\mu)\rho_{22} + R\rho_{11} - 2Q\rho_{12}]$$

$$+ (\rho_{12}^2 - \rho_{11}\rho_{22})(K^s F_{22} + K^f F_{11})$$

$$+ T_0 [F_{11}(2\rho_{12}R_{12}R_{22} - \rho_{11}R_{22}^2 - \rho_{22}R_{12}^2)$$

$$+ (F_{12} + F_{21})(\rho_{22}R_{11}R_{12} + \rho_{11}R_{21}R_{22} - \rho_{12}R_{12}R_{21} - \rho_{12}R_{11}R_{22})$$

$$+ F_{22}(2\rho_{12}R_{11}R_{21} - \rho_{22}R_{11}^2 - \rho_{11}R_{21}^2)],$$

$$a_4 = (\rho_{11}\rho_{22} - \rho_{12}^2)(F_{11}F_{22} - F_{12}F_{21}).$$

APPENDIX III.

The expressions for $\xi_i, \frac{\eta_i}{k^2}, \frac{\zeta_i}{k^2}, (i = 1, 2, \dots, 4)$ are given as

$$\xi_i = \frac{(R_{12}q_i - R_{22}p_i) + (R_{11}R_{22} - R_{21}R_{12})\frac{\eta_i}{k^2}}{R_{22}q_i - R_{12}r_i},$$

$$\frac{\eta_i}{k^2} = \frac{f_i(q_i^2 - p_i r_i) - g(R_{22}q_i - R_{12}r_i)}{f_i(R_{21}q_i - R_{11}r_i) - e_i(R_{22}q_i - R_{12}r_i)},$$

$$\frac{\zeta_i}{k^2} = \frac{e_i(q_i^2 - p_i r_i) - g(R_{21}q_i - R_{11}r_i)}{e_i(R_{22}q_i - R_{12}r_i) - f_i(R_{21}q_i - R_{11}r_i)},$$

where

$$p_i = \rho_{11}v^2 + (\lambda + 2\mu)(s_i^2 - 1), \quad q_i = \rho_{12}v^2 + Q(s_i^2 - 1), \quad r_i = [\rho_{22}v^2 + R(s_i^2 - 1)],$$

$$e_i = T_0 R_{22} [K^s (s_i^2 - 1) + v^2 F_{11}] - T_0 R_{21} F_{21} v^2,$$

$$f_i = -T_0 R_{21} [K^f (s_i^2 - 1) + v^2 F_{22}] + T_0 R_{22} F_{12} v^2,$$

$$g = T_0 v^4 (R_{12} R_{21} - R_{11} R_{22}).$$

$$s_1^2 + s_2^2 + s_3^2 + s_4^2 = (4a_0 + a_1 \zeta) / a_0,$$

$$s_1^2 s_2^2 + s_2^2 s_3^2 + s_3^2 s_4^2 + s_4^2 s_1^2 + s_1^2 s_3^2 + s_2^2 s_4^2 = (6a_0 + 3a_1 \zeta + a_2 \zeta^2) / a_0,$$

$$s_1^2 s_2^2 s_3^2 + s_2^2 s_3^2 s_4^2 + s_1^2 s_3^2 s_4^2 + s_1^2 s_2^2 s_4^2 = (4a_0 + 3a_1 \zeta + 2a_2 \zeta^2 + a_3 \zeta^3) / a_0,$$

$$s_1^2 s_2^2 s_3^2 s_4^2 = (a_0 + a_1 \zeta + a_2 \zeta^2 + a_3 \zeta^3 + a_4 \zeta^4) / a_0.$$

REFERENCES

Abousleiman, Y., Ekbote, S., Solutions for the inclined borehole in a porothermoelastic transversely isotropic medium, *J. Appl. Mech.*, vol. **72**, pp. 102-114, 2005.

Albers, B., Wilmanski, K., Influence of coupling through porosity changes on the propagation of acoustic waves in linear poroelastic materials, *Arch. Mech.*, vol. **58**, pp. 313-325, 2006.

Bear, J., Sorek, S., Ben-Dor, G., Mazor, G., Displacement waves in saturated thermoelastic porous media. I. Basic equations, *Fluid Dyn. Res.*, vol. **9**, pp. 155-164, 1992.

Berryman, J.G., Confirmation of Biot's theory, *Appl. Phys. Lett.*, vol. **37**, pp. 382-384, 1980.

Berryman, J.G., Fluid effects on shear waves in finely layered porous media, *Geophys.*, vol. **70**, N1-N15, 2005.

Biot, M.A., General solutions of the equations of elasticity and consolidation for a

- porous material. *J. Appl. Mech.*, vol. **23**, pp. 91-96, 1956a.
- Biot, M.A., Theory of propagation of elastic waves in a fluid-saturated porous solid. I Low frequency range. II. Higher frequency range, *J. Acoust. Soc. Am.*, vol. **28**, pp. 168-191, 1956b.
- Biot, M.A., Mechanics of deformation and acoustic propagation in porous media, *J. Appl. Phys.*, vol. **33**, pp. 1482-1498, 1962.
- Biot, M.A., Thermoelasticity and irreversible thermodynamics. *J. Appl. Phys.*, vol. **27**, pp. 240-253, 1956c.
- Carcione, J.M., Wave propagation in anisotropic, saturated porous media: Plane-wave theory and numerical simulation, *J. Acoust. Soc. Am.*, vol. **99**, pp. 2655-2666, 1996.
- Charlez, P.A., O., Heugas, Measurement of thermoporoelastic properties of rocks: theory and applications. In: Hudson JA, editor, Proceedings of the Eurock 92, ISRM Symposium, pp. 421-446, 1992.
- Coussy, O., A general theory of thermoporoelastoplasticity for saturated porous materials. *Transport in porous media*, vol. **4**, pp. 281-293, 1989.
- Deresiewicz, H., Rice, J.T., The effect of boundaries on wave propagation in a liquid filled porous solid : III. Reflection plane waves at a free plane boundary (General Case), *Bull. Seismo. Soc. Am.*, vol. **52**, pp. 595-625, 1962.
- Gajo, A., Fedel, A., Mongiovi, L., Experimental analysis of the effects of fluid-solid couplings on the velocity of elastic waves in saturated porous media. *Geotech.*, vol. **47**, pp. 993-1008, 1997.
- Ghassemi, A., Diek, A., Porothermoelasticity for swelling shales, *J. Petro. Sci. Eng.*, vol. **34**, pp. 123-135, 2002.
- Green, A.E., Naghdi, P.M., Thermoelasticity without energy dissipation, *J. Elastic-*

ity, **31**, 189-209, 1993.

Hajra, S., Mukhopadhyay, A., Reflection and refraction of seismic waves incident obliquely at the boundary of liquid saturated porous solid, *Bull. Seismo. Soc. Am.*, vol. **72**, pp. 1509-1533, 1982.

Johnson, D.L., Plona, T.J., Kojima, H., Probing porous media with first and second sound. II. Acoustic properties of water-saturated porous media, *J. Appl. Phys.*, vol. **76**, pp. 115-125, 1994.

Jones, J.P., Rayleigh wave in a porous elastic saturated solid. *J. Acoust. Soc. Am.* vol. **33**, pp. 959-962, 1961.

Kelder, O., Smeulders, D.M.J., Observation of the Biot slow wave in water-saturated Nivelsteiner sandstone, *Geophys.*, vol. **62**, pp. 1794-1796, 1997.

Khalili, N., Yazdchi, M., Valliappan, S., Wave propagation analysis of two-phase saturated porous media using coupled finite-infinite element method, *Soil Dyn. Earth. Eng.*, vol. **18**, pp. 533-553, 1997.

Kurashige, M., A thermoelastic theory of fluid-filled porous materials. *Int. J. Solids Struct.*, vol. **25**, pp. 1039-1052, 1989.

Li, Y., Cui, Z.-W., Zhang, Y.-J., Wang, K.-X., Reflection of elastic waves at fluid/fluid saturated poroelastic solid interface *Rock Soil Mech.*, vol. **28**, pp. 1595-1599, 2007.

Lin, C-H., Lee, V.W., Trifunac, M.D., The reflection of plane waves in a poroelastic half-space saturated with inviscid fluid. *Soil Dyn. Earth. Eng.*, vol. **25**, 205-223, 2005.

Lo, W.-C., Propagation and attenuation of Rayleigh waves in a semi-infinite unsaturated poroelastic medium. *Adv. Water Resour.* vol. **31**, pp. 1399-1410, 2008.

Lord, H.W., Shulman, Y., A generalized dynamical theory of thermoelasticity. *J. Mech. Phys. Solids* , vol. **15**, pp. 299-309, 1967.

- Mc Namee, J., Gibson, R.E., Displacement functions and linear transforms applied to diffusion through porous elastic medium. *Quart. J. Mech. Appl. Math.*, vol. **13**, pp. 98-111, 1960.
- McTigue, D., Thermoelastic response of fluid-saturated porous rock. *J. Geophys. Res.*, vol. **91**, pp. 9533-9542, 1986.
- Nakagawa, N.K., Soga, K., Mitchell, J.K., Observation of Biot compressional wave of the second kind in granular soils. *Geotech.*, vol. **47**, pp. 133-147, 1997.
- Nakagawa, S., Schoenberg, M.A., Poroelastic modeling of seismic boundary conditions across a fracture, *J. Acoust. Soc. Am.*, vol. **122**, pp. 831-847, 2007.
- Pecker, C., Deresiewicz, H., Thermal effects on waves in liquid-filled porous media. *Acta Mech.*, vol. **16**, pp. 45-64, 1973.
- Plona, T.J., Observation of a second bulk compressional wave in a porous medium at ultrasonic frequencies, *Appl. Phys. Lett.*, vol. **36**, pp. 259-261, 1980.
- Schiffman, R.L., A thermoelastic theory of consolidation. In Environmental and Geophysical Heat Transfer, *ASME*, New York, vol. **99**, pp. 78-84, 1971.
- Shrefler, B.A. Mechanics and thermodynamics of saturated/unsaturated porous materials and quantitative solutions. *Appl. Mech. Rev.*, **55**, pp. 351-389, 2002.
- Sharma, M.D. and Gogna, M.L., Wave propagation in anisotropic liquid-saturated porous solids, *J. Acoust. Soc. Am.*, vol. **90**, pp. 1068-1073, 1991.
- Sharma, M.D., Wave propagation in a general anisotropic poroelastic medium: Biot's theories and homogenization theory, *J. Earth Syst. Sci.*, vol. **116**, pp. 357-367, 2007.
- Sharma, M.D., Rayleigh waves in a partially-saturated poroelastic solid. *Geophys. J. Int.* vol. **189**, pp. 1203-1214, 2012.
- Singh, B., On propagation of plane waves in generalized prothermoelasticity, *Bull.*

Seismo. Soc. Am., **101**, pp. 756-762, 2011.

Singh, B., Reflection of plane waves from a free surface of a porothermoelastic solid half-space, *J. Porous Media*, **16**, pp. 945-957, 2013.

Tajuddin, M. Rayleigh waves in a poroelastic half-space. *J. Acoust. Soc. Am.* vol. **75**, pp. 682-684, 1984.

Tajuddin, M., Hussaini, S.J., Reflection of plane waves at boundaries of a liquid filled poroelastic half-space, *J. Appl. Geophys.*, vol. **58**, pp. 59-86, 2005.

Wang, D., Zhang, H.-L., Wang, X.-M., A numerical study of acoustic wave propagation in partially saturated poroelastic rock, *Chinese J. Geophys.*, vol. **49**, pp. 524-532, 2006.

Yew, C.H., Jogi, P.N., Study of wave motion in fluid-saturated porous rocks, *J. Acoust. Soc. Am.*, vol. **60**, pp. 2-8, 1976.

Youssef, H.M., Theory of generalized porothermoelasticity, *Int. J. Rock Mech. Min. Sci.*, vol. **44**, pp. 222-227, 2007.

Yin, S., Dusseault, M.B., Rothenburg, L., Fully coupled numerical modeling of ground surface uplift in steam injection. *J. Can. Petro. Tech.* vol. **49**, pp. 16-21, 2010.

Yin, S., Dusseault, M.B., Rothenburg, L., Thermal reservoir modelling in petroleum geomechanics. *Int. J. Numer. Analyt. Methods Geomech.* vol. **33**, pp. 449-485, 2009.

Yin, S., Dusseault, M.B., Rothenburg, L., Multiphase poroelastic modeling in semi-space for deformable reservoirs. *J. Petro. Sci. Eng.* vol. **64**, pp. 45-54, 2009.

Yin, S., Towler, B.F., Dusseault, M.B., Rothenburg, L., Numerical experiments on oil sands shear dilation and permeability enhancement in a multiphase thermoporoelastoplasticity framework. *J. Petro. Sci. Eng.* vol. **69**, pp. 219-226, 2009.

Zhou, Y., Rajapakse, R.K.N.D., Graham, J., A coupled thermoporoelastic model with thermo-osmosis and thermal-filtration. *Int. J. Solids Struct.*, vol. **35**, pp. 4659-4683, 1998.

Zyserman, F.I., Santos, J.E., Analysis of the numerical dispersion of waves in saturated poroelastic media, *Comput. Methods Appl. Mech. Eng.*, vol. **196**, pp. 4644-4655, 2007.

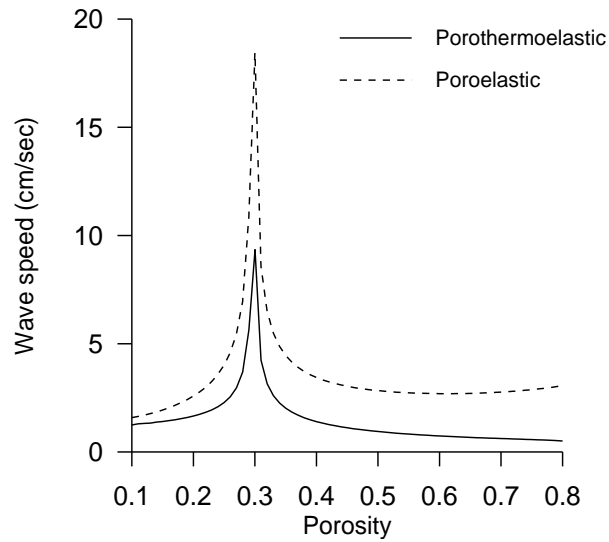


Figure 1. Variation of the speed of Rayleigh wave against porosity (β). (The values on vertical axis are without the multiplier 10^5)

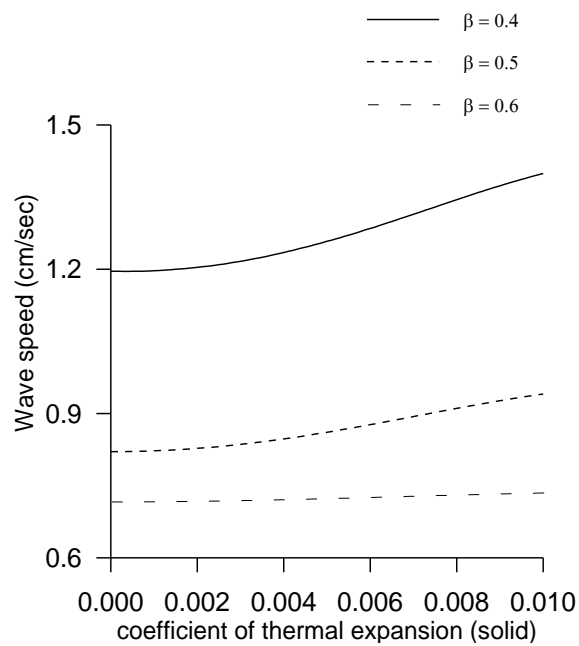


Figure 2. Variation of the speed of Rayleigh wave against coefficient of thermal expansion in solid (α^s). (The values on vertical axis are without the multiplier 10^5)

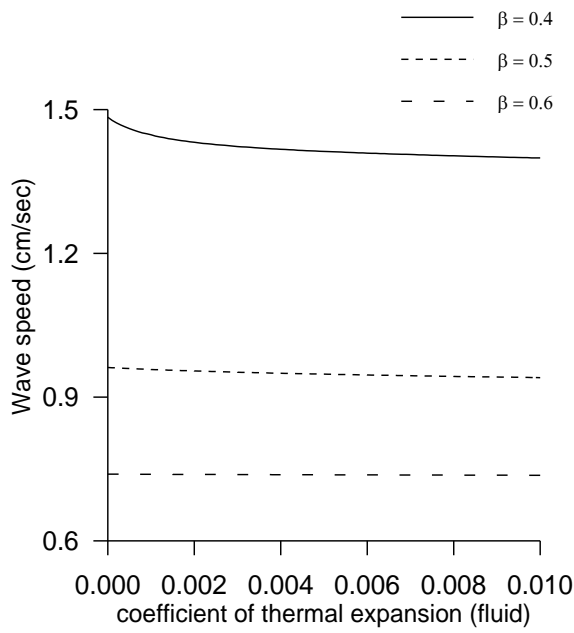


Figure 3. Variation of the speed of Rayleigh wave against coefficient of thermal expansion in fluid (α^f). (The values on vertical axis are without the multiplier 10^5)

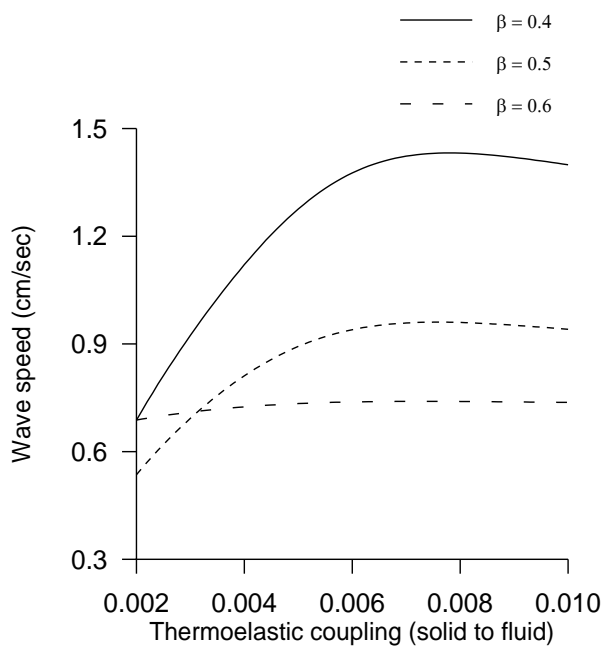


Figure 4. Variation of the speed of Rayleigh wave against thermoelastic coupling (α^{sf}). (The values on vertical axis are without the multiplier 10^5)

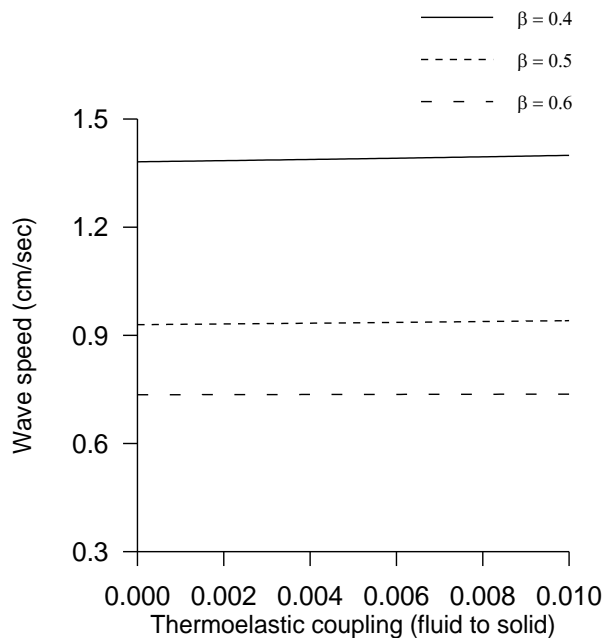


Figure 5. Variation of the speed of Rayleigh wave against thermoelastic coupling (α^{fS}). (The values on vertical axis are without the multiplier 10^5)

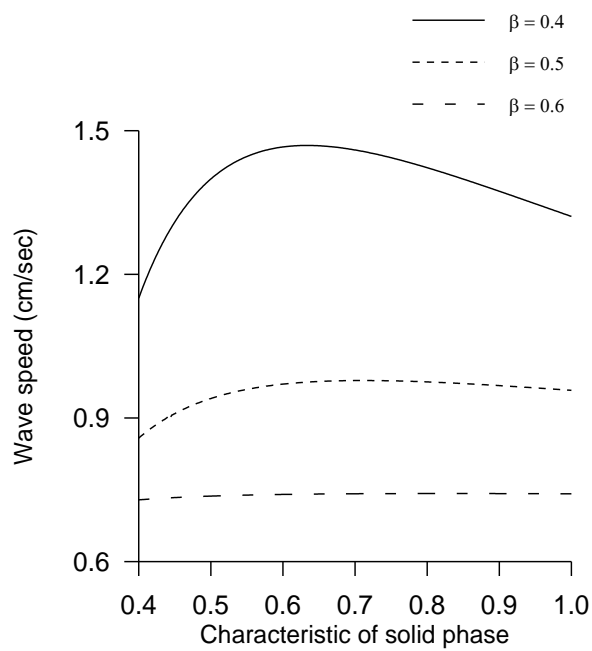


Figure 6. Variation of the speed of Rayleigh wave against characteristic of solid phase (K^S). (The values on vertical axis are without the multiplier 10^5)

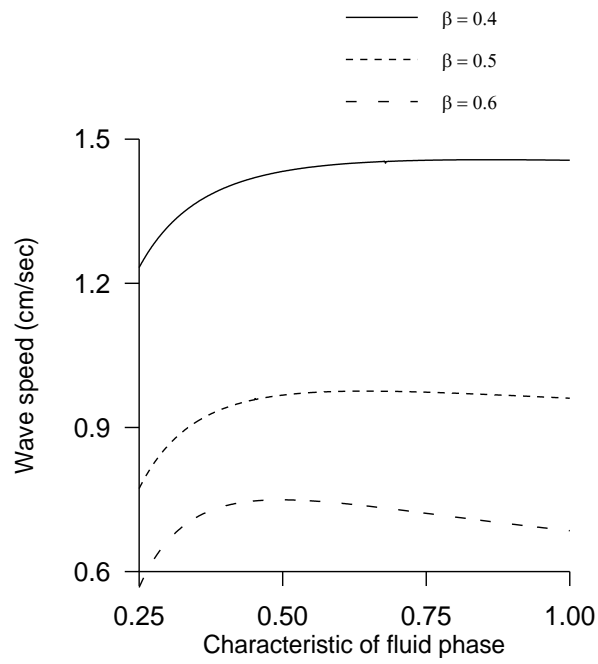


Figure 7. Variation of the speed of Rayleigh wave against characteristic of fluid phase (K^f). (The values on vertical axis are without the multiplier 10^5)

Chapter 3

Reflection of plane waves from surface of a thermoelastic saturated porous solid half-space with impedance boundary conditions

In this chapter, a problem on reflection of plane waves from a plane thermally insulated as well as isothermal surfaces of a half-space is studied in context of Lord-Shulman (*LS*) and Green-Naghdi (*GN*) theories of generalized thermoelasticity of saturated porous medium. The mechanical boundary conditions at surface of half-space are considered as impedance boundary conditions, where the normal and shear force tractions are assumed to vary linearly with the normal and tangential displacement components multiplied by the frequency, respectively. The impedance corresponds to the constants of proportionality. The governing equations are specialized in $x - z$ plane. The plane wave solution of these equations shows the existence of three coupled longitudinal waves and a shear vertical wave in a generalized thermoelastic saturated porous medium. For incident plane wave (longitudinal or shear), four reflected waves will propagate in the medium. The appropriate potentials for incident and reflected waves in a half-space are formulated, which satisfy the required boundary conditions with the help of a Snell's law. Finally, a non-homogeneous system of four equations is obtained in the amplitude ratios, where the ratios depend on material parameters, impedance parameter, angle of incidence, thermal relaxation and speeds of plane waves. For relevant material parameters, the amplitude ratios are computed numerically for certain ranges of impedance parameters and the angle of incidence. For validation purpose, the numerical results are compared with those without thermal and porous parameters.

1. INTRODUCTION

In crustal and reservoir rocks, the co-existence of porosity and thermoelasticity is a common, which may be crucial in non-destructive evaluation of composite materials and structures. Bear et al. (1992) and Levy et al. (1995) studied the fluid transport through porous media and obtained the fundamental equations for microscopic dynamism. Using Lagranges's equations, Biot (1956a, 1962a, b) derived the equations governing the motions of solid and fluid phases and developed a complete dynamic theory for wave propagation in fluid-saturated porous media. A large number of problems [for example, Lakes et al (1983); Kelder and Smeulders (1997); Gurevich et al (1999)] are studied to verify the Biot's theories.

Biot (1964) developed a coupled theory thermoelasticity, where dilatation based on the thermodynamics of irreversible process is derived and coupled it with elastic deformation. In this theory, the heat equation was of diffusion type, which predicts infinite speed for propagation of thermal signals. Lord and Shulman (1967) developed a theory of generalized thermoelasticity with one relaxation time for an isotropic body. In this theory, the conventional Fourier's law is replaced by a modified law of heat conduction including both the heat flux and its time derivative. The heat equation in this theory is hyperbolic, which eliminates the paradox of infinite speeds of propagation found in both the uncoupled and the coupled theories of thermoelasticity. Green and Lindsay (1972) also developed a generalised theory of thermoelasticity with two relaxation times. Chandrasekhariah (1986) reviewed the earlier research works on thermoelasticity. Green and Naghdi (1993) formulated another generalized theory of thermoelasticity without energy dissipation, which includes the thermal-displacement gradient among its independent constitutive variables and differs from the previous theories in that it does not accommodate dissipation of thermal energy. Various studies are conducted on wave propagation in thermoelastic materials

including McCarthy (1972), Chadwick (1979), Dhaliwal and Sheriff (1980), Sharma and Sidhu (1986), Gorodetskaya (2005), Sharma (2006), Arora and Tomar (2007), Singh (2013) and Goyal and Tomar (2015).

Biot (1956b) showed that the theory of porous media applies instantly to the theory of thermoelasticity. For example, the temperature and entropy replace the fluid pressure and relative fluid displacement, respectively. Norris (1992) used this analogy to translate the results from thermoelasticity for solving the problems of poroelasticity. The problems on wave propagation in saturated thermoelastic porous medium have useful applications in petroleum engineering, chemical engineering, pavement engineering and nuclear waste management. Sharma (2008) showed the existence of three longitudinal and one transverse waves in an isotropic thermoelastic porous solid saturated with a non-viscous fluid and analysed the velocities and attenuation of the three longitudinal waves numerically. Singh (2011) showed the existence of one shear and four kinds of coupled longitudinal waves in a generalized porothermoelastic solid half-space. Singh (2013) also studied the reflection phenomena in a generalized porothermoelastic solid half-space, where the reflection coefficients as well as energy ratios of reflected waves are obtained.

Impedance boundary conditions are a linear combination of unknown functions and their derivatives prescribed on the boundary. Impedance boundary conditions are commonly used in various fields of physics like acoustics and electromagnetism. However, these boundary conditions are not used much in seismology. Tiersten (1969) derived impedance-like boundary conditions to observe the effect of a thin layer of different material over an elastic half-space. Malischewsky (1987) investigated the Rayleigh waves with Tiersten's impedance boundary conditions and obtained a secular equation. Godoy et al. (2012) proved the existence and uniqueness of Rayleigh waves with impedance boundary conditions. Vinh and Hue (2014) discussed the propagation of Rayleigh waves in an orthotropic

and monoclinic half-space with impedance boundary conditions. Singh (2016) considered a problem on Rayleigh wave propagation in an isotropic generalized thermoelastic solid half-space with impedance boundary conditions. Recently, Vinh and Xuan (2017) studied the propagation of Rayleigh waves with impedance boundary condition and derived an exact formula for the velocity by using the complex function method. Using this formula, they also established the existence and uniqueness of the wave. However, the problems on reflection of elastic waves with impedance boundary conditions are not studied much in literature. The main purpose of this work is observe the effects of impedance boundary on reflection phenomena in a generalized thermoelastic saturated porous solid in context of Lord-Shulman and Green-Naghdi theories.

In the present chapter, we consider a generalized thermoelastic saturated porous solid half-space, whose surface is subjected to impedance boundary conditions as in Vinh and Hue [28], where the normal and tangential components of stress tensor depend linearly on normal and tangential displacement components times frequency, respectively. A problem on reflection of plane (longitudinal or shear) wave in a generalized thermoelastic saturated medium with these impedance boundary conditions is considered. The reflection coefficients (or amplitude ratios) of various reflected waves are analysed numerically to show the dependence on angle of incidence, thermal and porous parameters and impedance parameters.

2. BASIC EQUATIONS

Following Bear et al (1992), Levy et al (1995) and Lord and Shulman (1967), the stresses in porous aggregate in a thermally conducting isotropic porous solid saturated with a non-viscous fluid are

$$\tau_{ij} = \sigma_{ij} + \alpha(-p_f)\delta_{ij}, \quad (1)$$

where the effective stresses in the solid and fluid parts of the medium are

$$\sigma_{ij} = \lambda u_{k,k} \delta_{ij} + \mu(u_{i,j} + u_{j,i}) - \beta_s T \delta_{ij}, \quad (2)$$

$$-p_f = \alpha M u_{k,k} + M w_{k,k} - \beta_f T, \quad (3)$$

and β_s, β_f are the coefficients of thermal stress for solid and fluid, respectively. α is Biot's parameter to represent bulk coupling between fluid and solid phases. δ_{ij} is the Kronecker symbol. λ, μ are isothermal Lamé's constants for porous solid and M is an elastic parameter for isotropic bulk coupling of fluid and solid particles. w_i are the components of the averaged fluid motion relative to solid frame, where $w_i = f(U_i - u_i)$, f is the porosity of solid and u_i and U_i are displacement components in solid and fluid phases, respectively. T is small change in temperature. It is assumed that both the constituents of porous aggregate have the same constant temperature (T_0) in the undisturbed state.

The governing equations of motion in the deformed medium are

$$\tau_{ij,j} = \rho \ddot{u}_i + \rho_f \ddot{w}_i, \quad (4)$$

$$(-p_f)_{,i} = \rho_f \ddot{u}_i + q \ddot{w}_i, \quad (5)$$

$$KT_{,jj} - \rho C_e (\dot{T} + \tau_0 \ddot{T}) = T_0 \beta [\tau_0 (\ddot{u}_{j,j} + \ddot{w}_{j,j}) + (\dot{u}_{j,j} + \dot{w}_{j,j})], \quad (6)$$

where $\beta = \beta_s + \alpha \beta_f$. ρ and ρ_f are the densities of porous aggregate and pore fluid, respectively. τ_0 is relaxation time. The parameter q represents inertial coupling between pore-fluid and solid matrix of porous aggregate.

3. TWO-DIMENSIONAL SOLUTION

Making use of relations (1) to (3) in equations (4) to (6), the governing equations of a

generalized thermoelastic saturated porous medium are specialized in x-z plane as

$$(\lambda + 2\mu + \alpha^2 M) \frac{\partial^2 u_1}{\partial x^2} + (\lambda + \mu + \alpha^2 M) \frac{\partial^2 u_3}{\partial x \partial z} + \mu \frac{\partial^2 u_1}{\partial z^2} + \alpha M \left(\frac{\partial^2 w_1}{\partial x^2} + \frac{\partial^2 w_3}{\partial x \partial z} \right) - \beta \frac{\partial T}{\partial x} = \rho \frac{\partial^2 u_1}{\partial t^2} + \rho_f \frac{\partial^2 w_1}{\partial t^2}, \quad (7)$$

$$(\lambda + 2\mu + \alpha^2 M) \frac{\partial^2 u_3}{\partial z^2} + (\lambda + \mu + \alpha^2 M) \frac{\partial^2 u_1}{\partial x \partial z} + \mu \frac{\partial^2 u_3}{\partial x^2} + \alpha M \left(\frac{\partial^2 w_1}{\partial x \partial z} + \frac{\partial^2 w_3}{\partial z^2} \right) - \beta \frac{\partial T}{\partial z} = \rho \frac{\partial^2 u_3}{\partial t^2} + \rho_f \frac{\partial^2 w_3}{\partial t^2}, \quad (8)$$

$$\alpha M \left(\frac{\partial^2 u_1}{\partial x^2} + \frac{\partial^2 u_3}{\partial x \partial z} \right) + M \left(\frac{\partial^2 w_1}{\partial x^2} + \frac{\partial^2 w_3}{\partial x \partial z} \right) - \beta_f \frac{\partial T}{\partial x} = \rho_f \frac{\partial^2 u_1}{\partial t^2} + q \frac{\partial^2 w_1}{\partial t^2}, \quad (9)$$

$$\alpha M \left(\frac{\partial^2 u_1}{\partial x \partial z} + \frac{\partial^2 u_3}{\partial z^2} \right) + M \left(\frac{\partial^2 w_1}{\partial x \partial z} + \frac{\partial^2 w_3}{\partial z^2} \right) - \beta_f \frac{\partial T}{\partial z} = \rho_f \frac{\partial^2 u_3}{\partial t^2} + q \frac{\partial^2 w_3}{\partial t^2}, \quad (10)$$

$$K \left(\frac{\partial^2 T}{\partial x^2} + \frac{\partial^2 T}{\partial z^2} \right) = \beta T_0 \left[\left(1 + \tau_0 \frac{\partial}{\partial t} \right) \left\{ \frac{\partial u_1}{\partial t} + \frac{\partial u_3}{\partial t} + \frac{\partial w_1}{\partial t} + \frac{\partial w_3}{\partial t} \right\} \right] + \rho C_e \left(1 + \tau_0 \frac{\partial}{\partial t} \right) \frac{\partial T}{\partial t}. \quad (11)$$

Using the following Helmholtz,s representation

$$u_1 = \frac{\partial \phi}{\partial x} - \frac{\partial \psi}{\partial z}, \quad u_3 = \frac{\partial \phi}{\partial z} + \frac{\partial \psi}{\partial x}, \quad (12)$$

$$w_1 = \frac{\partial \Phi}{\partial x} - \frac{\partial \Psi}{\partial z}, \quad w_3 = \frac{\partial \Phi}{\partial z} + \frac{\partial \Psi}{\partial x}, \quad (13)$$

the equations (7) to (11) are written in terms of scalar potentials ϕ , ψ , Φ and Ψ as

$$\mu \left(\frac{\partial^2 \psi}{\partial x^2} + \frac{\partial^2 \psi}{\partial z^2} \right) = \rho \frac{\partial^2 \psi}{\partial t^2} + \rho_f \frac{\partial^2 \Psi}{\partial t^2}, \quad (14)$$

$$\rho_f \frac{\partial^2 \psi}{\partial t^2} + q \frac{\partial^2 \Psi}{\partial t^2} = 0, \quad (15)$$

$$(\lambda + 2\mu + \alpha^2 M) \left(\frac{\partial^2 \phi}{\partial x^2} + \frac{\partial^2 \phi}{\partial z^2} \right) + \alpha M \left(\frac{\partial^2 \Phi}{\partial x^2} + \frac{\partial^2 \Phi}{\partial z^2} \right) - \beta T = \rho \frac{\partial^2 \phi}{\partial t^2} + \rho_f \frac{\partial^2 \Phi}{\partial t^2}, \quad (16)$$

$$\alpha M\left(\frac{\partial^2\phi}{\partial x^2} + \frac{\partial^2\phi}{\partial z^2}\right) + M\left(\frac{\partial^2\Phi}{\partial x^2} + \frac{\partial^2\Phi}{\partial z^2}\right) - \beta_f T = \rho_f \frac{\partial^2\phi}{\partial t^2} + q \frac{\partial^2\Phi}{\partial t^2}, \quad (17)$$

$$K\left(\frac{\partial^2 T}{\partial x^2} + \frac{\partial^2 T}{\partial z^2}\right) = \beta T_0\left[\left(1 + \tau_0 \frac{\partial}{\partial t}\right)\left\{\frac{\partial^3\phi}{\partial x^2\partial t} + \frac{\partial^3\phi}{\partial z^2\partial t} + \frac{\partial^3\Phi}{\partial x^2\partial t} + \frac{\partial^3\Phi}{\partial z^2\partial t}\right\}\right] + \rho C_e\left(1 + \tau_0 \frac{\partial}{\partial t}\right)\frac{\partial T}{\partial t}. \quad (18)$$

We seek the plane wave solutions of equations (14) to (18) of the following form

$$\{\phi, \Phi, T, \psi, \Psi\} = \{A, B, C, D, E\} \exp[ik(\sin\theta x + \cos\theta z - Vt)], \quad (19)$$

where A, B, C, D and E are arbitrary constants. k is the wavenumber, V is the complex phase speed and θ is the angle of propagation. With the help of equation (19), the equations (14) to (18) lead to following two velocity equations

$$g_0 V^6 + g_1 V^4 + g_2 V^2 + g_3 = 0, \quad (20)$$

$$V^2 = \frac{\mu q}{\rho q - \rho_f^2} \quad (21)$$

where

$$\begin{aligned} g_0 &= \rho_f^2 - \rho q, \\ g_1 &= \rho M + q D_1 - 2\alpha \rho_f M + \frac{K}{\rho C_e \tau^*} (\rho q - \rho_f^2) + \frac{\beta T_0}{\rho C_e} (\rho \beta_f - \rho_f \beta_f - \rho_f \beta + q \beta), \\ g_2 &= M(\alpha^2 M - D_1) + \frac{\beta \beta_f T_0}{\rho C_e} (\alpha M - D_1) + \frac{\beta^2 T_0}{\rho C_e} M(\alpha - 1) + \frac{K}{\rho C_e \tau^*} M(2\alpha \rho_f - \rho) - D_1 q \frac{K}{\rho C_e \tau^*}, \\ g_3 &= \frac{K}{\rho C_e \tau^*} M(D_1 - \alpha^2 M), \quad D_1 = \lambda + 2\mu + \alpha^2 M, \quad \tau^* = \tau_0 + \frac{i}{w}. \end{aligned}$$

The velocity equation (20) shows the existence of three coupled longitudinal waves, namely, fast-P ($P1$), slow-P ($P2$) and thermal ($P3$) waves in a generalized thermoelastic saturated porous medium. If we write, $V_j^{-1} = v_j^{-1} - i\omega^{-1}q_j$, ($j = 1, 2, 3$), then clearly v_j and q_j are speeds of propagation and attenuations of the $P1, P2$ and $P3$ waves, respectively. The velocity equation (20) corresponds to Green and Naghdi (GN) theory for $\tau^* = 1$. The velocity equation (21) shows the existence of a Shear Vertical (SV) wave with speed $V = v_4$.

4. REFLECTION FROM A PLANE SURFACE

We consider a half-space of a generalized thermoelastic fluid-saturated porous medium. The plane surface of the half-space is taken along the x-axis. The negative z-axis is taken as normal into the half-space as shown in Figure 1. Following Vinh and Hue (2014), we assume that the surface of half-space is subjected to impedance boundary conditions, where the normal and tangential tractions are proportional to normal and tangential displacement components times frequency, respectively. Therefore, in the present problem, the impedance boundary conditions at $z = 0$ are expressed as

$$\sigma_{zz} + \omega Z_3 u_3 = 0, \quad \sigma_{zx} + \omega Z_1 u_1 = 0, \quad p_f = 0, \quad \frac{\partial T}{\partial z} + hT = 0, \quad (22)$$

where

$$\begin{aligned} \sigma_{zz} &= \lambda \frac{\partial u_1}{\partial x} + (\lambda + 2\mu) \frac{\partial u_3}{\partial z} - \beta_s T, & \sigma_{zx} &= \mu \left(\frac{\partial u_3}{\partial x} + \frac{\partial u_1}{\partial z} \right), \\ -p_f &= \alpha M \left(\frac{\partial u_1}{\partial x} + \frac{\partial u_3}{\partial z} \right) + M \left(\frac{\partial w_1}{\partial x} + \frac{\partial w_3}{\partial z} \right) - \beta_f T = 0, \end{aligned}$$

and $h \rightarrow 0$ corresponds to thermally insulated surface and $h \rightarrow \infty$ corresponds to isothermal surface. Z_1 and Z_3 are impedance parameters of dimension stress/velocity, which are assumed strictly real. For $Z_1 = 0; Z_3 = 0$, the impedance boundary conditions reduce to traction-free boundary conditions and $|Z_1| \rightarrow +\infty$ and $|Z_3| \rightarrow +\infty$ correspond to vanishing of tangential and normal components of displacement vector.

For an incident $P1$ or SV wave at plane surface $z = 0$, the reflected $P1, P2, P3$ and SV waves propagate in the half-space ($z < 0$). The appropriate potentials for incident and reflected waves in the half-space are:

$$\begin{aligned} \phi &= A_0 \exp\{ik_1(x \sin \theta_0 + z \cos \theta_0 - v_1 t)\} \\ &\quad + \sum_{j=1}^3 A_j \exp\{ik_j(x \sin \theta_j - z \cos \theta_j - v_j t)\}, \end{aligned} \quad (23)$$

$$\begin{aligned} \Phi &= p_1 A_0 \exp\{ik_1(x \sin \theta_0 + z \cos \theta_0 - v_1 t)\} \\ &\quad + \sum_{j=1}^3 p_j A_j \exp\{ik_j(x \sin \theta_j - z \cos \theta_j - v_j t)\}, \end{aligned} \quad (24)$$

$$\begin{aligned}
T = & q_1 A_0 \exp\{ik_1(x \sin \theta_0 + z \cos \theta_0 - v_1 t)\} \\
& + \sum_{j=1}^3 q_j A_j \exp\{ik_j(x \sin \theta_j - z \cos \theta_j - v_j t)\}, \tag{25}
\end{aligned}$$

$$\begin{aligned}
\psi = & B_0 \exp\{ik_4(x \sin \theta_0 + z \cos \theta_0 - v_4 t)\} \\
& + B_1 \exp\{ik_4(x \sin \theta_4 - z \cos \theta_4 - v_4 t)\}. \tag{26}
\end{aligned}$$

$$\begin{aligned}
\Psi = & r_1 B_0 \exp\{ik_4(x \sin \theta_0 + z \cos \theta_0 - v_4 t)\} \\
& + r_1 B_1 \exp\{ik_4(x \sin \theta_4 - z \cos \theta_4 - v_4 t)\}. \tag{27}
\end{aligned}$$

where the expressions for $p_m, \frac{q_m}{k_m^2}, (m = 1, 2, 3)$ and r_1 are obtained as

$$\begin{aligned}
p_m = & \frac{(\rho_f \beta - \rho \beta_f) v_m^2 + (\lambda + 2\mu + \alpha^2 M) \beta_f - \alpha M \beta}{(\rho_f \beta_f - q \beta) v_m^2 + (\beta M - \alpha M \beta_f)}, \quad r_1 = \frac{-\rho_f}{q}, \\
\frac{q_m}{k_m^2} = & \frac{(\rho_f^2 - \rho q) v_m^4 + (\rho M - 2\alpha M \rho_f + (\lambda + 2\mu + \alpha^2 M) q) v_m^2 - (\lambda + 2\mu) M}{(\rho_f \beta_f - q \beta) v_m^2 + (\beta M - \alpha M \beta_f)}.
\end{aligned}$$

The potentials given in equations (23) to (27) satisfy the boundary conditions if following relations (Snell's law) hold

$$\frac{\sin \theta_0}{(v_1 \text{ or } v_4)} = \frac{\sin \theta_1}{v_1} = \frac{\sin \theta_2}{v_2} = \frac{\sin \theta_3}{v_3} = \frac{\sin \theta_4}{v_4} \tag{28}$$

$$k_1 v_1 = k_2 v_2 = k_3 v_3 = k_4 v_4 \tag{29}$$

and with the help of these relations, we obtain a non-homogeneous system of four equations in amplitude ratios of four reflected waves as

(a) incident $P1$ wave

$$\sum_{j=1}^4 a_{ij} X_j = b_i, \quad (i = 1, 2, 3, 4) \tag{30}$$

where

$$X_j = \frac{A_j}{A_0}, \quad (j = 1, 2, 3), \quad X_4 = \frac{B_1}{A_0},$$

are reflection coefficients of reflected $P1, P2, P3$ and SV waves, and

$$a_{1m} = \left(\frac{v_1}{v_m}\right)^2 \left[\frac{\lambda + 2\mu \{1 - (\frac{v_m}{v_1})^2 \sin^2 \theta_0\} + \beta_s \frac{q_m}{k_m^2} + iv_m Z_3 \sqrt{1 - (\frac{v_m}{v_1})^2 \sin^2 \theta_0}}{\lambda + 2\mu \cos^2 \theta_0 + \beta_s \frac{q_1}{k_1^2} - iv_m Z_3 \cos \theta_0} \right],$$

$$a_{14} = \left(\frac{v_1}{v_4}\right) \sin \theta_0 \left[\frac{2\mu \sqrt{1 - (\frac{v_4}{v_1})^2 \sin^2 \theta_0} + iv_4 Z_3}{\lambda + 2\mu \cos^2 \theta_0 + \beta_s \frac{q_1}{k_1^2} - iv_m Z_3 \cos \theta_0} \right], \quad b_1 = -1,$$

$$a_{2m} = \left(\frac{v_1}{v_m}\right) \left[\frac{2\mu \sqrt{1 - (\frac{v_m}{v_1})^2 \sin^2 \theta_0} + iv_m Z_1}{2\mu \cos \theta_0 - iv_1 Z_1} \right], \quad (m = 1, 2, 3),$$

$$a_{24} = \left(\frac{v_1}{v_4}\right)^2 \left[\frac{(1 - 2(\frac{v_4}{v_1})^2 \sin^2 \theta_0) + iv_4 Z_1 \sqrt{1 - (\frac{v_4}{v_1})^2 \sin^2 \theta_0}}{\sin \theta_0 (2\mu \cos \theta_0 - iv_1 Z_1)} \right], \quad b_2 = 1,$$

$$a_{3m} = \left(\frac{v_1}{v_m}\right)^2 \left[\frac{(\alpha + p_m)M + \beta_f \frac{q_m}{k_m^2}}{(\alpha + p_1)M + \beta_f \frac{q_1}{k_1^2}} \right], \quad (m = 1, 2, 3), \quad a_{34} = 0, \quad b_3 = -1.$$

(i) Thermally insulated case

$$a_{4m} = \frac{q_m \left(\frac{v_1}{v_m}\right) \sqrt{1 - (\frac{v_m}{v_1})^2 \sin^2 \theta_0}}{q_1 \cos \theta_0}, \quad (m = 1, 2, 3), \quad a_{44} = 0, \quad b_4 = 1,$$

(ii) Isothermal case

$$a_{4m} = \frac{q_m}{q_1}, \quad (m = 1, 2, 3), \quad a_{44} = 0, \quad b_4 = -1,$$

and

(b) incident *SV* wave

$$\sum_{j=1}^4 c_{ij} Y_j = d_i, \quad (i = 1, 2, 3, 4) \quad (31)$$

where

$$Y_j = \frac{A_j}{B_0}, \quad (j = 1, 2, 3), \quad Y_4 = \frac{B_1}{B_0},$$

are reflection coefficients of reflected *P1*, *P2*, *P3* and *SV* waves, and

$$c_{1m} = \left(\frac{v_4}{v_m}\right)^2 \left[\frac{\lambda + 2\mu \{1 - (\frac{v_m}{v_4})^2 \sin^2 \theta_0\} + \beta_s \frac{q_m}{k_m^2} + iv_m Z_3 \sqrt{1 - (\frac{v_m}{v_4})^2 \sin^2 \theta_0}}{\mu \sin 2\theta_0 - iv_4 Z_3 \sin \theta_0} \right],$$

$$c_{14} = - \left[\frac{\mu \sin 2\theta_0 + iv_4 Z_3 \sin \theta_0}{\mu \sin 2\theta_0 - iv_4 Z_3 \sin \theta_0} \right], \quad (m = 1, 2, 3), \quad d_1 = -1,$$

$$c_{2m} = \left(\frac{v_4}{v_m}\right) \sin \theta_0 \left[\frac{2\mu \sqrt{(1 - (\frac{v_m}{v_4})^2 \sin^2 \theta_0)} + iv_m Z_1}{\mu \cos 2\theta_0 - iv_4 Z_1} \right], \quad (m = 1, 2, 3),$$

$$c_{24} = \frac{\mu \cos 2\theta_0 + iv_4 Z_1}{\mu \cos 2\theta_0 - iv_4 Z_1}, \quad d_2 = -1$$

$$c_{3m} = \left(\frac{v_1}{v_m}\right)^2 [(\alpha + p_m)M + \beta_f \frac{q_m}{k_m^2}], \quad (m = 1, 2, 3), \quad c_{34} = 0, \quad d_3 = 0,$$

(i) Thermally insulated case

$$c_{4m} = q_m \left(\frac{v_4}{v_m}\right) \sqrt{1 - \left(\frac{v_m}{v_4}\right)^2 \sin^2 \theta_0}, \quad (m = 1, 2, 3), \quad c_{44} = 0, \quad d_4 = 0,$$

(ii) Isothermal case

$$c_{4m} = q_m, \quad (m = 1, 2, 3), \quad c_{44} = 0, \quad d_4 = 0,$$

The above theoretical analysis reduces for traction free boundary case for $Z_1 = 0$ and $Z_3 = 0$.

5. RESULTS

To compute the numerical values of reflection coefficients of various reflected waves, the following physical constants of thermoelastic saturated porous medium are considered (Rasolofosaon and Zinszner, 2002)

$$\begin{aligned} \lambda &= 3.7 \times 10^9 N.m^{-1} & \mu &= 7.9 \times 10^9 N.m^{-1} & M &= 6.0 \times 10^9 N.m^{-1}, \\ \alpha &= 0.4, & f &= 0.16, & \rho &= 2216 kg.m^{-3}, & \rho_f &= 950 kg.m^{-3}, & q &= 1.05\rho_f/f, \\ C_e &= 1040 J.kg^{-1}K^{-1}, & K &= 170 W.m^{-1}K^{-1}, & T_0 &= 300K, & \tau_0 &= 10^{-11}s, \\ \beta_f/\mu &= 0.3 \times 10^{-3}K, & \beta_s &= 2\beta_f, & \omega &= 5s^{-1}. \end{aligned}$$

The velocity equation (20) is solved numerically for above physical constants and it is found that $v_1 > v_2 > v_3$, where v_1, v_2 and v_3 correspond to speeds of $P1$ (fast- P) wave, $P2$ (slow- P) wave and $P3$ (thermal wave), respectively. For above values of physical constants, the equations (30) and (31) are solved numerically to obtain the reflection coefficients of reflected waves for incidence of both $P1$ and SV .

(a) Incident $P1$ wave

The variations of reflection coefficients of reflected waves against the angle of incidence of $P1$ wave for LS and GN theories are shown in Figure 2 by solid and dashed curves respectively. Here the P_3 (or thermal wave) is affected significantly due to the presence of dissipation.

Numerical results in Figures 3 to 6 are restricted for Lord and Shulman theory only. The variations of reflection coefficients of all reflected waves against the angle of incidence of $P1$ wave are shown in Figure 3 for insulated, isothermal, without porous and without thermal cases by solid curve, solid curve with stars, solid curve with triangles and solid curve with rhombuses, respectively. Thermal and porous effects are observed on all the reflected waves, where the $P2$ and $P3$ waves does not exist in absence of porous and thermal parameters, respectively.

In Figure 4, three different sets of impedance boundary parameters are chosen to show the variations of reflection coefficients of all reflected waves against the angle of incidence of $P1$ wave. The variations for sets $Z_1 = -10, Z_3 = -10$; $Z_1 = 0, Z_3 = 0$ (traction free boundary); $Z_1 = 5, Z_3 = 5$ are shown in Figure 4 by solid curve with triangles, solid curve and solid curve with rhombuses, respectively. The comparison of different variations in Figure 4 shows the effect of impedance boundary on reflection coefficients of various reflected waves.

The variations of reflection coefficients of all reflected waves are plotted against the impedance parameters Z_1 and Z_3 in Figures 5 and 6 for insulated, without porous and without thermal cases by solid curve, small dashed curve and long dashed curve, respectively. The effects of thermal, porous and impedance parameters are observed in these figures at a particular incidence $\theta_0 = 45^\circ$, when $Z_3 = 0$. The peaks at $Z_1 = 0$ in Figure 5 and at $Z_3 = 0$ in Figure 6 correspond to the results for traction free surface.

(b) Incident SV wave

In Figure 7, the variations of reflection coefficients of all reflected waves are plotted against the angle of incident of SV wave for Lord and Shulman theory and Green Naghdi by solid and dashed curves respectively. Maximum effect of dissipation is observed on reflected $P3$ or thermal wave.

For Lord and Shulman theory, the variations of reflection coefficients of all reflected waves are plotted against the angle of incidence of SV wave in Figure 8 for insulated, isothermal, without porous and without thermal cases by solid curve, solid curve with stars, solid curve with triangles and solid curve with rhombuses, respectively. All reflected waves are affected due to the presence of thermal and porous parameters and the $P2$ and $P3$ waves does not exist in absence of porous and thermal parameters, respectively.

Using Lord and Shulman theory and for three different sets of impedance boundary parameters, the variations of reflection coefficients of all reflected waves are shown graphically against the angle of incidence of SV wave in Figure 9. The variations for sets $Z_1 = -10, Z_3 = -10$; $Z_1 = 0, Z_3 = 0$; $Z_1 = 5, Z_3 = 5$ are shown in Figure 9 by solid line with triangles, solid line and solid line with rhombuses, respectively. The comparison of these variations in Figure 9 shows the effect of impedance boundary on reflection coefficients of all reflected waves.

5. CONCLUDING REMARKS

A problem on reflection of plane waves from a plane surface of a generalized thermoelastic saturated porous solid half-space is considered, where the surface (thermally insulated or isothermal) is subjected to impedance boundary conditions. For incidence of both P and SV wave, the theory and numerical results suggest the following concluding remarks:

- (i) Thermal wave or $P3$ wave is most affected wave due to dissipation.
- (ii) The impedance boundary conditions affect significantly the reflection coefficients of various reflected waves in a thermoelastic saturated porous medium.
- (iii) The numerical results reduce for traction free boundary conditions for $Z_1 = 0$ and $Z_3 = 0$.
- (iv) In absence of impedance and porous parameters, the present results agree fairly with those obtained by Sharma et al. (2003).

(iv) The present theoretical and numerical results may be further explored by experimental seismologists working on earthquake estimation.

ACKNOWLEDGEMENTS

Author is highly thankful to University Grants Commission, New Delhi for granting a Major Research Project (MRP-MAJOR-MATH-2013-2149).

REFERENCES

- Arora, A. and Tomar, S.K., Elastic Waves at Porous/Porous Elastic Half-Spaces Saturated by Two Immiscible Fluids, *J. Porous Media*, vol. 10, pp. 751-768, 2007.
- Bear, J., Sorek, S., Ben-Dor, G., and Mazor, G., Displacement Waves in Saturated Thermoelastic Porous Media, I. Basic Equations, *Fluid Dyn. Res.*, vol. 9, pp. 155-164, 1992.
- Biot, M.A., The Theory of Propagation of Elastic Waves in a Fluid-Saturated Porous Solid, I. Low-Frequency Range II. Higher Frequency Range, *J. Acoust. Soc. Am.*, vol. 28, pp. 168-191, 1956a.
- Biot, M.A., Thermoelasticity and Irreversible Thermodynamics, *J. Appl. Phys.*, vol. 27, pp. 240-253, 1956b.
- Biot, M.A., Generalized Theory of Acoustic Propagation in Porous Dissipative Media, *J. Acoust. Soc. Am.*, vol. 34, pp. 1254-1264, 1962a.
- Biot, M.A., Mechanics of Deformation and Acoustic Propagation in Porous Media, *J. Appl. Phys.*, vol. 33, pp. 1482-1498, 1962b.
- Biot, M.A., Theory of Buckling of a Porous Slab and its Thermoelastic Analogy, *J. Appl. Mech.*, vol. 27, pp. 194-198, 1964.
- Chadwick, P., Basic Properties of Plane Harmonic Waves in a Pre-stressed Heat Conducting Elastic Material, *J. Thermal Stresses*, vol. 2, pp. 193-214, 1979.
- Chandrasekharaiah, D.S., Thermoelasticity with Second Sound, *Appl. Mech. Rev.*, vol. 39, pp. 355-376, 1986.

- Dhaliwal, R.S. and Sheriff, H.H., Generalised Thermoelasticity for Anisotropic Media, *Quart. Appl. Maths.*, vol. 38, pp. 1-8, 1980.
- Godoy, E., Duran, M., and Nedelec, J.C., On Existence of Surface Waves in an Elastic Half-Space with Impedance Boundary Conditions, *Wave Motion*, vol. 49, pp. 585-594, 2012.
- Gorodetskaya, N. S., Wave Reflection from the Free Boundary of Porous-Elastic Liquid-Saturated Half-Space, *Int. J. Fluid Mech. Res.*, vol. 32, pp. 327-339, 2005.
- Goyal, S., and Tomar, S. K., Reflection and Transmission of Inhomogeneous Waves at the Plane Interface Between Two Dissimilar Swelling Half-Spaces, *Special Topics Reviews Porous Media*, vol. 6, pp. 51-69, 2015.
- Green, A.E. and Lindsay, K.A., Thermoelasticity, *J. Elast.*, vol. 2, pp. 1-7, 1972.
- Green, A.E. and Naghdi, P.M., Thermoelasticity Without Energy Dissipation, *J. Elast.*, vol. 31, pp. 189-208, 1993.
- Gurevich, B., Kelder, O., and Smeulders, D.M.J., Validation of the Slow Compressional Wave in Porous Media: Comparison of Experiments and Numerical Simulations, *Trans. Porous Media*, vol. 36, pp. 149-160, 1999.
- Kelder, O. and Smeulders, D.M.J., Observations of the Biot Slow Wave in Water Saturated Nivelsteiner Sandstone, *Geophysics*, vol. 62, pp. 1794-1796, 1997.
- Lakes, R., Yoon, H.S., and Katz, J.L., Slow Compressional Wave Propagation in Wet Human and Bovine Cortical Bone, *Science*, vol. 220, pp. 513-515, 1983.
- Levy, A., Sorek, S., Ben-Dor, G., and Bear, J., Evolution of the Balance Equations in Saturated Thermoelastic Porous Media Following Abrupt Simultaneous Changes in Pressure and Temperature, *Trans. Porous Media*, vol. 21, pp. 241-268, 1995.
- Lord, H.W. and Shulman, Y., The Generalised Dynamic Theory of Thermoelasticity, *J. Mech. Phys. Solids*, vol. 15, pp. 299-309, 1967.

- Malischewsky, P.G., *Surface Waves and Discontinuities*, Elsevier, Amsterdam, 1987.
- Mc Carthy, M.F., Wave Propagation in Generalised Thermoelasticity, *Int. J. Eng. Sci.*, vol. 10, pp. 593-602, 1972.
- Norris, A.N., On the Correspondence Between Poroelasticity and Thermoelasticity, *J. Appl. Phys.*, vol. 71, pp. 1138-1141, 1992.
- Rasolofosaon, P.N.J. and Zinszner, B.E., Comparison Between Permeability Anisotropy and Elasticity Anisotropy of Reservoir Rocks, *Geophysics*, vol. 67, pp. 230-240, 2002.
- Sharma, J.N. and Sidhu, R.S., On the Propagation of Plane Harmonic Waves in Anisotropic Generalised Thermoelasticity, *Int. J. Eng. Sci.*, vol. 24, pp. 1511-1516, 1986.
- Sharma, J.N., Kumar, V., and Chand, D., Reflection of Generalized Thermoelastic Waves from the Boundary of a Half-Space, *J. Thermal Stresses*, vol. 26, pp. 925-942, 2003.
- Sharma, M.D., Wave Propagation in Anisotropic Generalized Thermoelastic Medium, *J. Thermal Stresses*, vol. 29, pp. 329-342, 2006.
- Sharma, M.D., Wave Propagation in a Thermoelastic Saturated Porous Medium, *J. Earth System Sci.*, vol. 117, pp. 951-958, 2008.
- Singh, B., On Propagation of Plane Waves in Generalized Porothermoelasticity, *Bull. Seismo. Soc. Am.*, vol. 101, pp. 756-762, 2011.
- Singh, B., Wave Propagation in Green-Naghdi Thermoelastic Solid with Diffusion, *Int. J. Thermophys.*, vol. 34, pp. 553-566, 2013.
- Singh, B., Reflection of Plane Waves from a Free Surface of a Porothermoelastic Solid Half-Space, *J. Porous Media*, vol. 16, pp. 945-957, 2013.
- Singh, B., Rayleigh Wave in a Thermoelastic Solid Half-Space with Impedance Boundary Conditions, *Meccanica*, vol. 51, pp. 1135-1139, 2016.
- Tiersten, H.F., Elastic Surface Waves Guided by Thin Films, *J. Appl. Phys.*, vol. 40, pp. 770-789, 1969.

Vinh, P.C. and Hue, T.T., Rayleigh Waves with Impedance Boundary Conditions in Anisotropic Solids, *Wave Motion*, vol. 51, pp. 1082-1092, 2014.

Vinh, P.C. and Xuan, N.Q., Rayleigh Waves with Impedance Boundary Condition: Formula for the Velocity, Existence and Uniqueness, *European J. Mech.- A/Solids*, vol. 61, pp. 180-185, 2017.

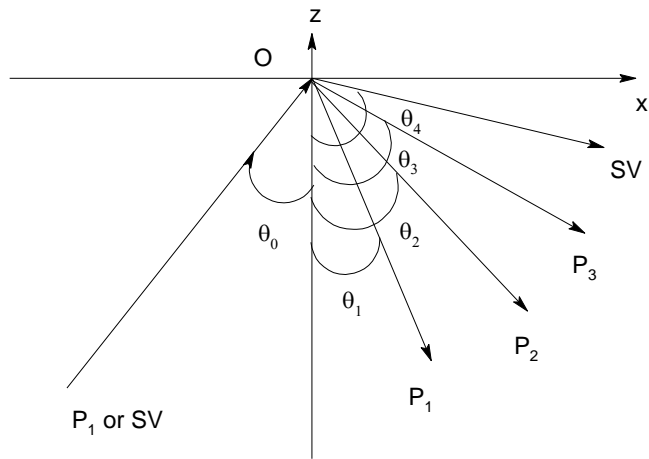


FIG. 1: Geometry showing incident and reflected waves in a thermoelastic saturated porous solid half-space.

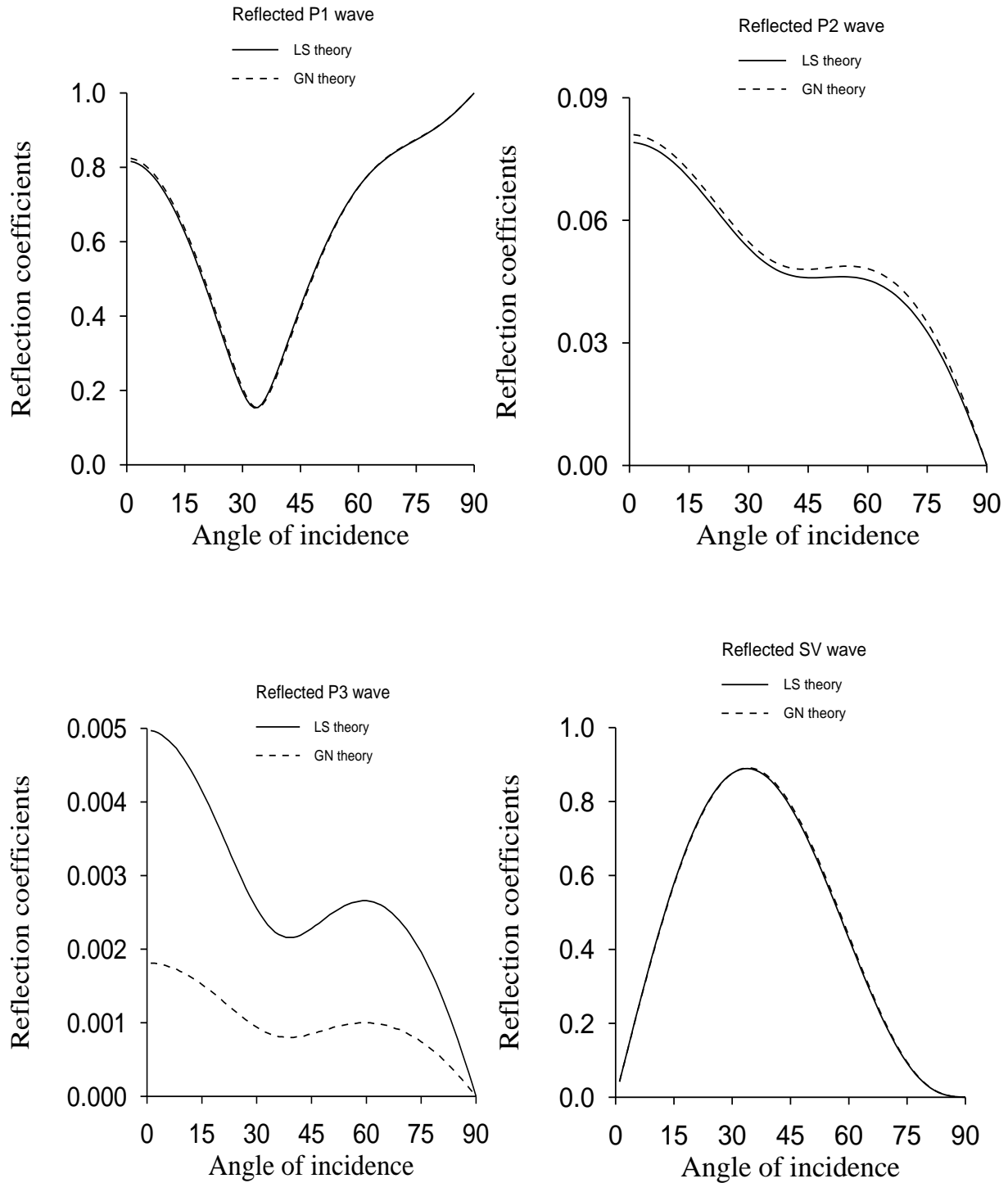


FIG. 2: Variations of reflection coefficients of reflected waves against the angle of incidence of P1 wave for LS and GN theories.

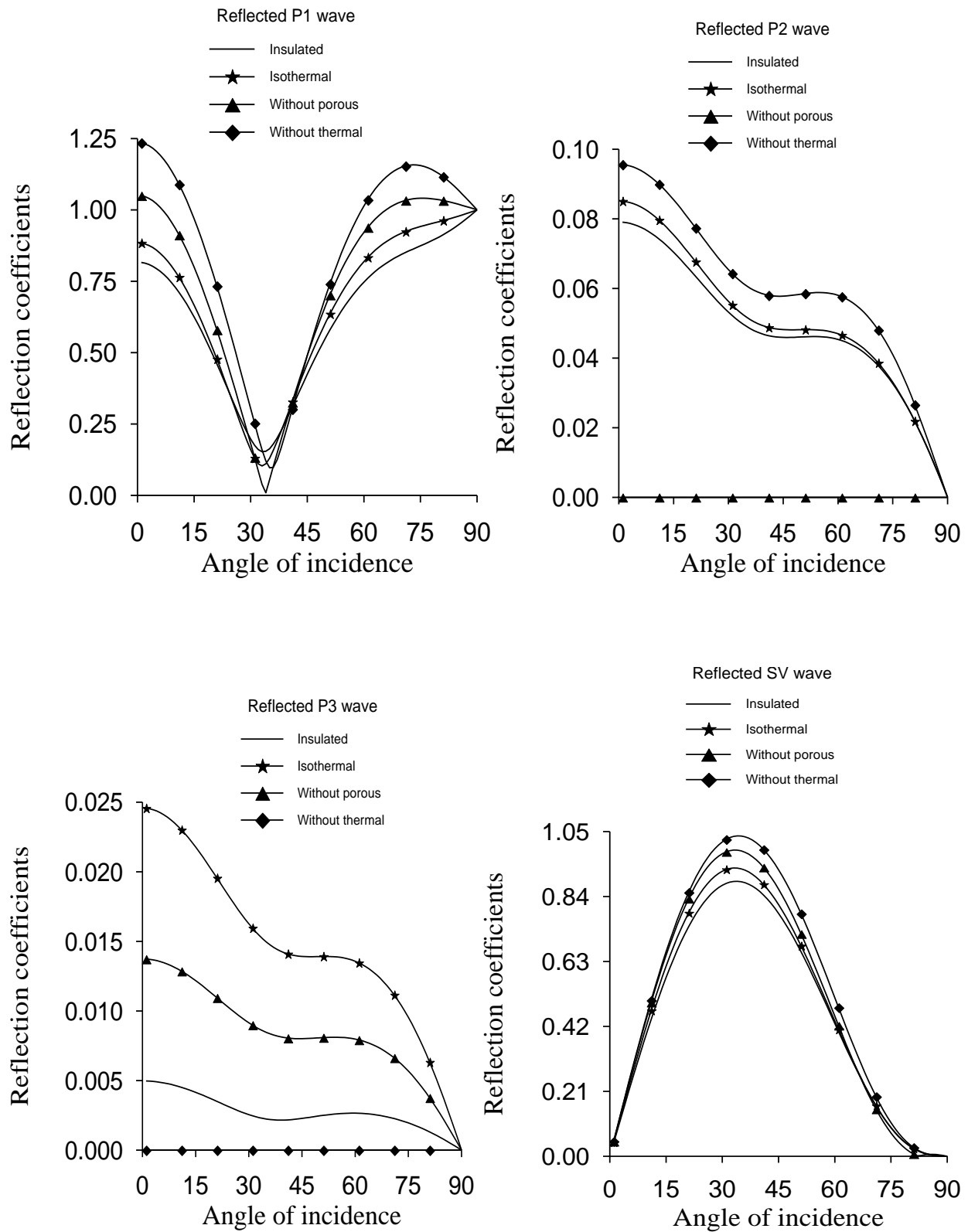


FIG. 3: Variations of reflection coefficients of reflected waves against the angle of incidence of P1 wave for insulated, isothermal, without porous and without thermal cases (LS theory only).

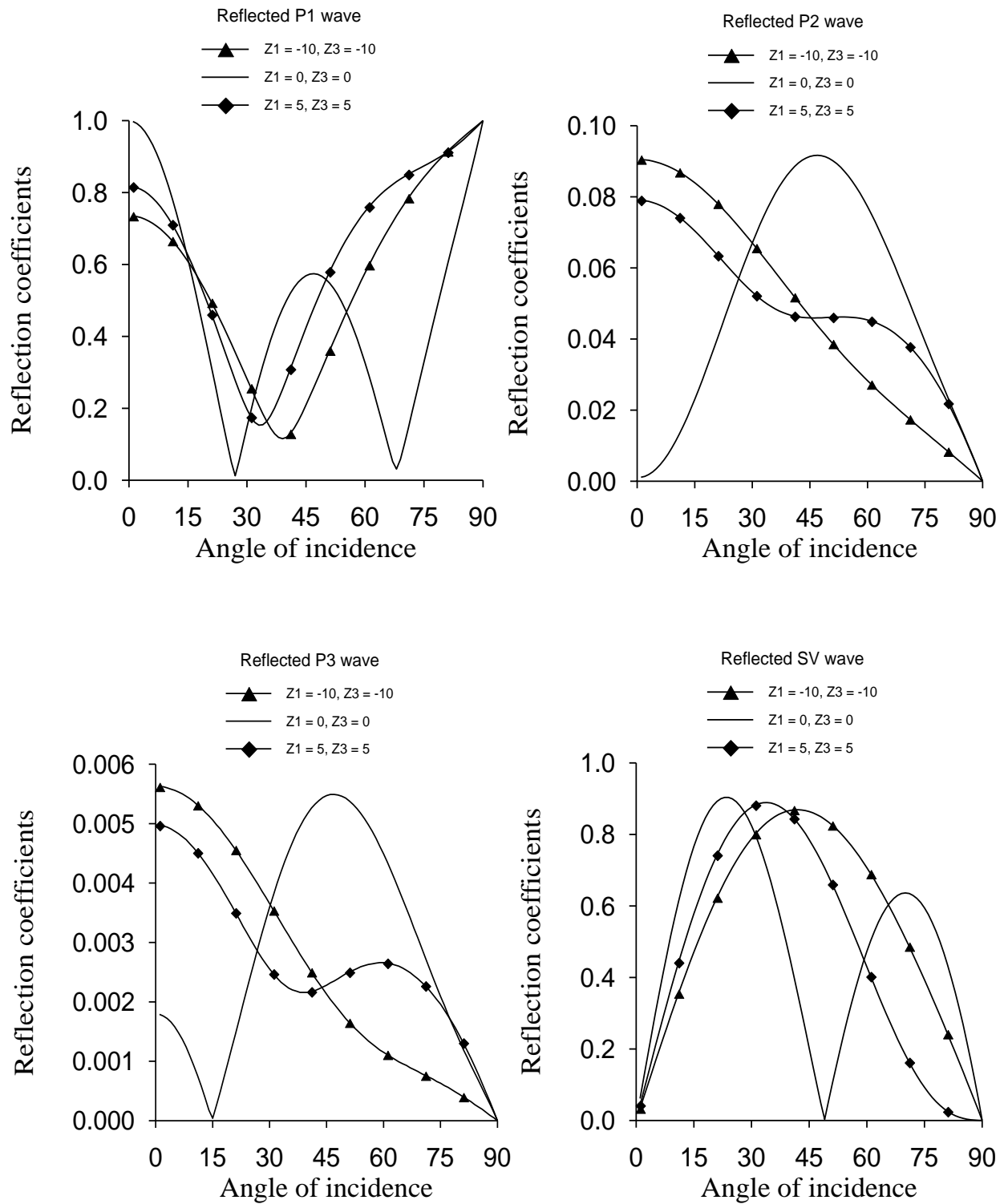


FIG. 4: Variations of reflection coefficients of reflected waves against the angle of incidence of P1 wave for different sets of impedance boundary parameters (LS theory only).

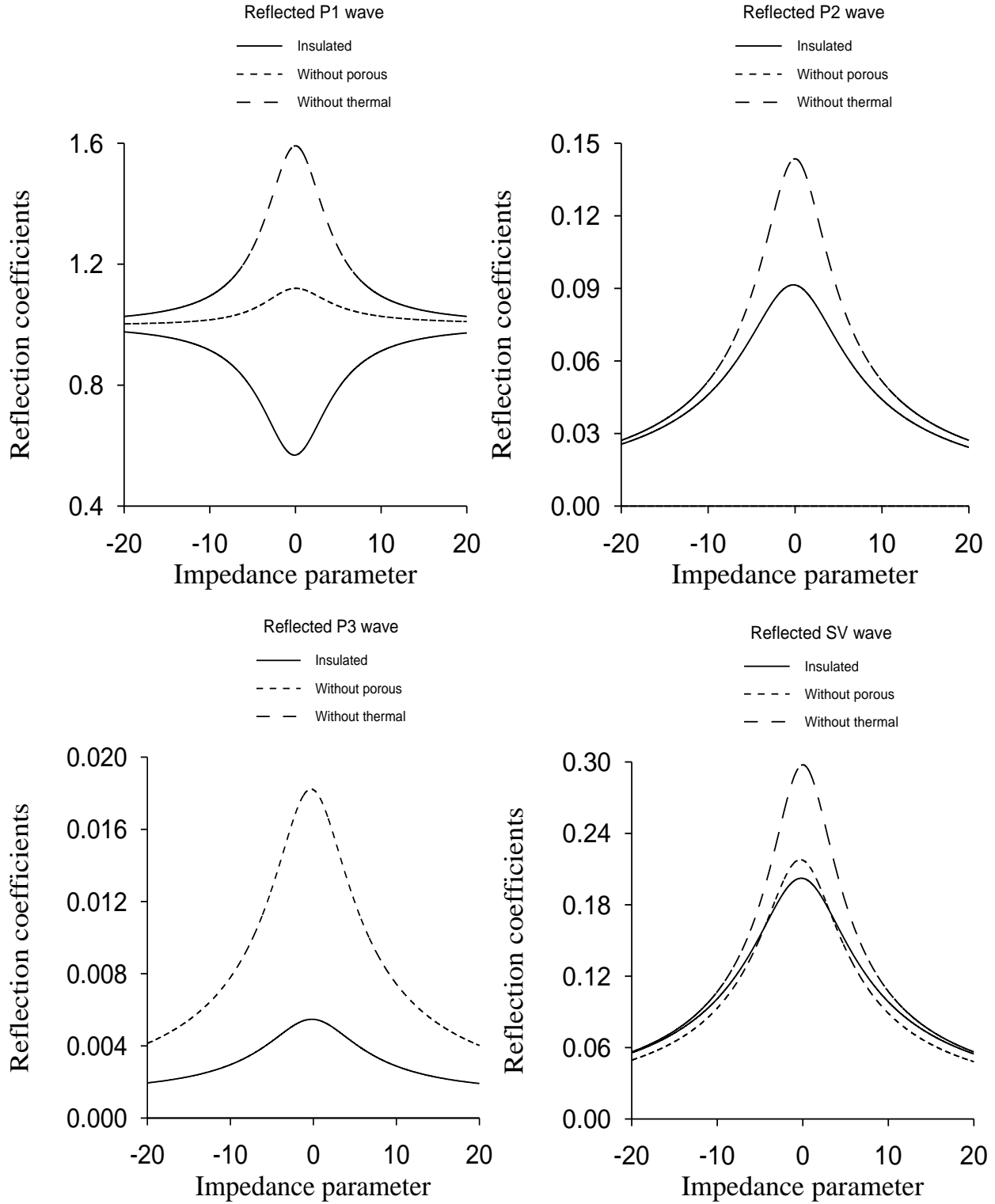


FIG. 5: Variations of reflection coefficients of reflected waves against the impedance parameter Z_1 for insulated, without porous and without thermal cases when $Z_3 = 0$ and $\theta_0 = 45^\circ$ (LS theory only).

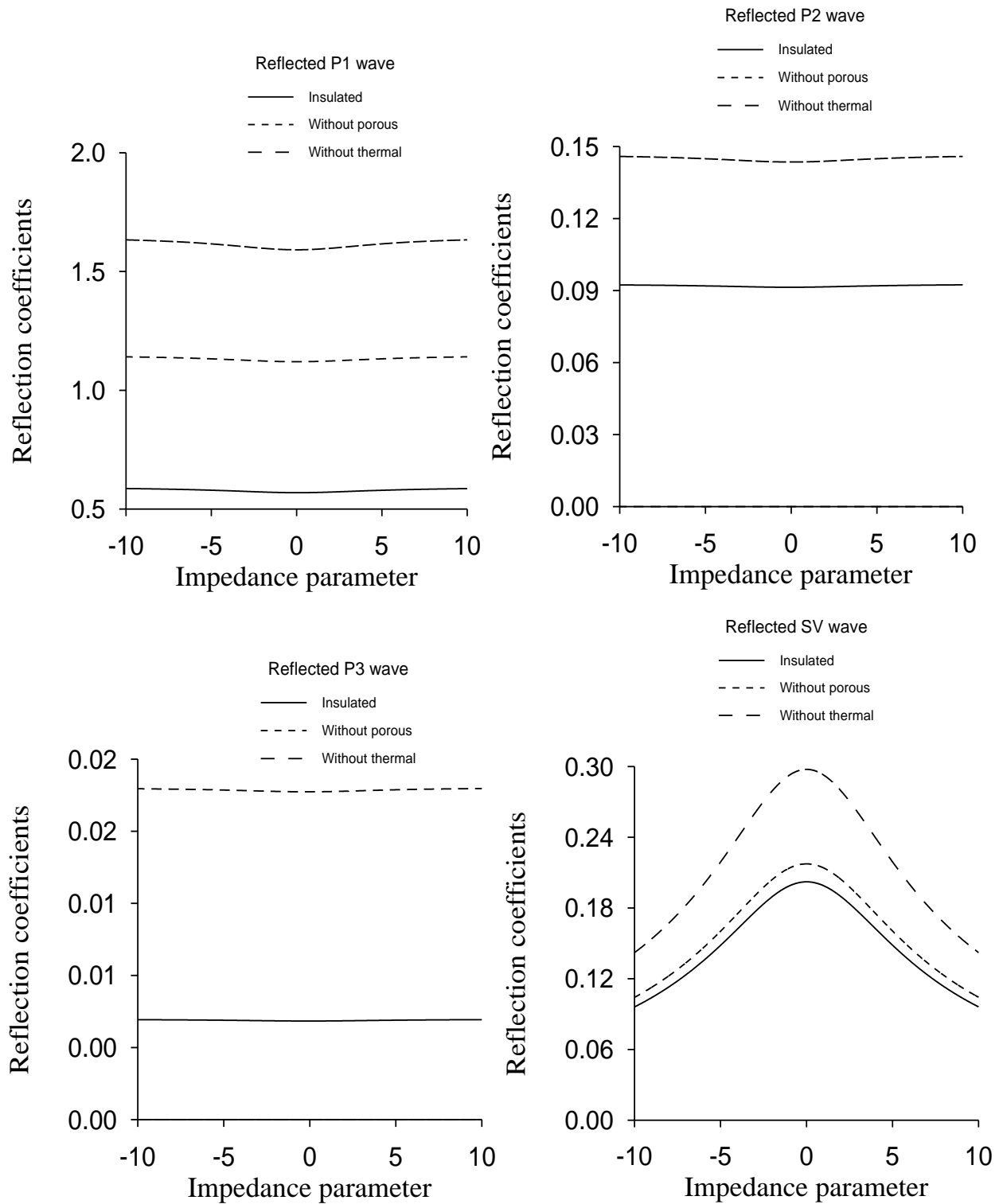


FIG. 6: Variations of reflection coefficients of reflected waves against the impedance parameter Z_3 for insulated, without porous and without thermal cases when $Z_1 = 0$ and $\theta_0 = 45^\circ$ (LS theory only).

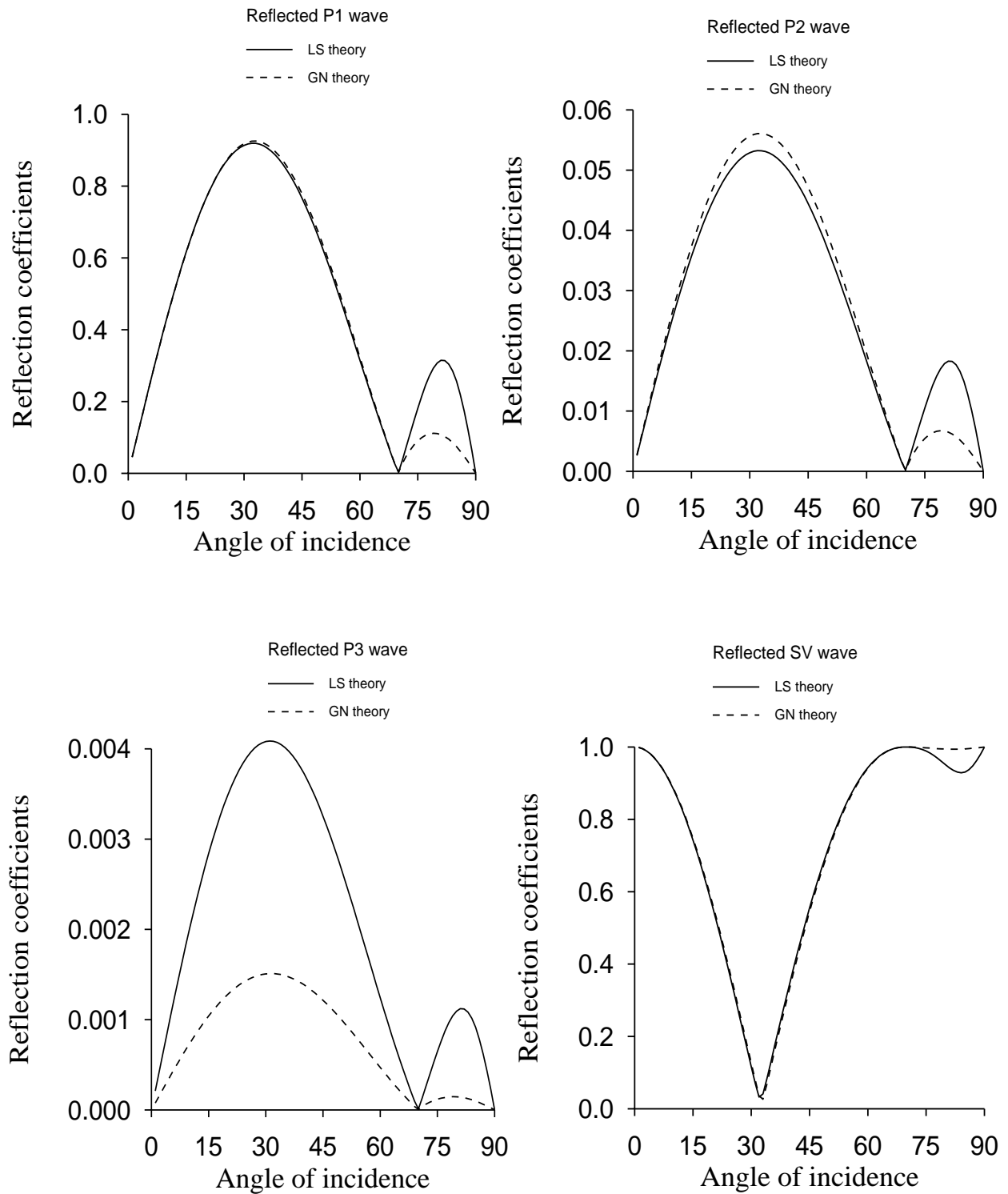


FIG. 7: Variations of reflection coefficients of reflected waves against the angle of incidence of SV wave for LS and GN theories.

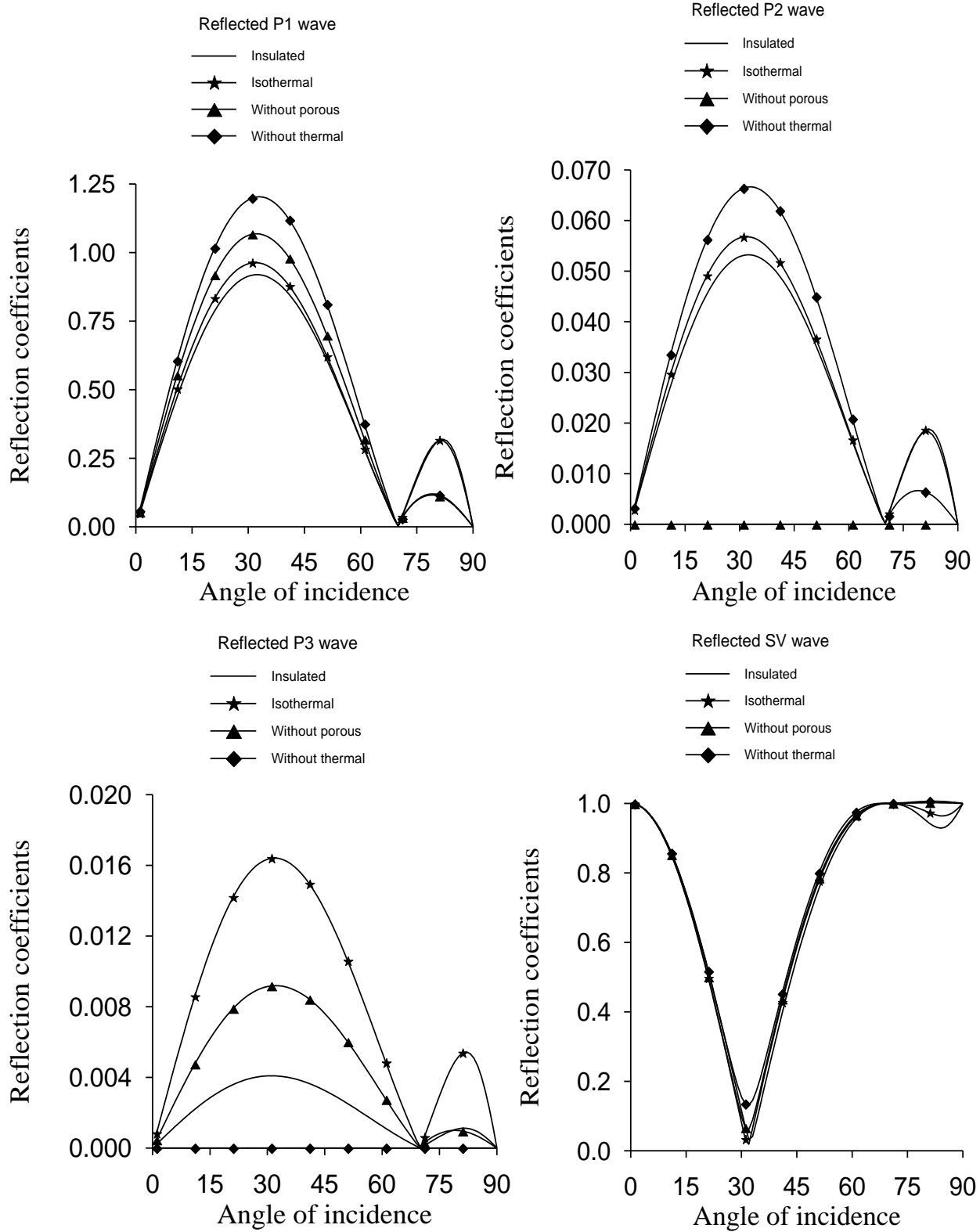


FIG. 8: Variations of reflection coefficients of reflected waves against the angle of incidence of SV wave for insulated, isothermal, without porous and without thermal cases (LS theory only).

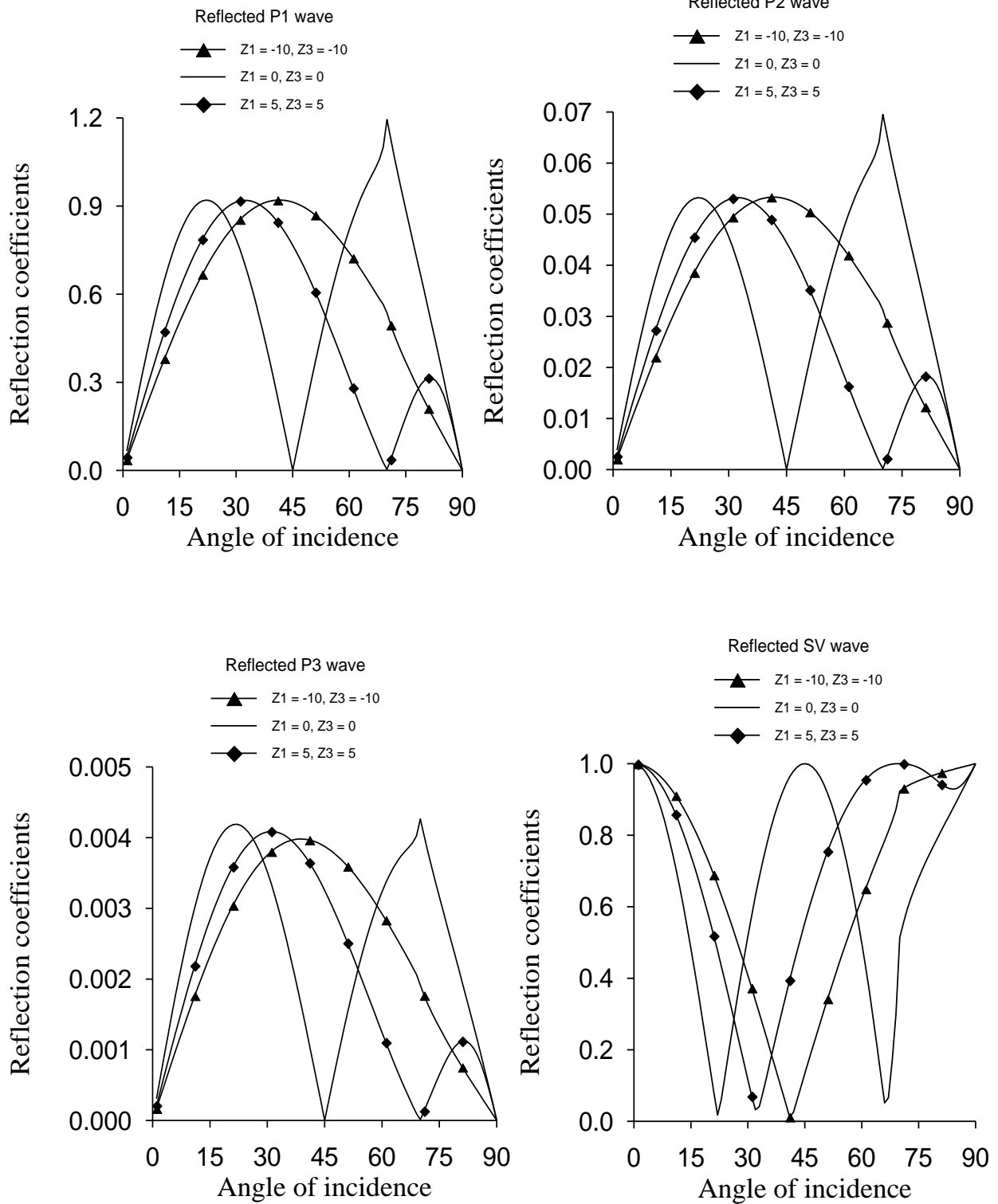


FIG. 9: Variations of reflection coefficients of reflected waves against the angle of incidence of SV wave for different set of impedance boundary parameters (LS theory only).

Chapter 4

Reflection of plane waves from surface of a generalized thermo-viscoelastic porous solid half-space with impedance boundary conditions

In this chapter, a phenomenon of reflection of plane waves from a thermally insulated surface of a solid half-space is studied in context of Lord-Shulman theory of generalized thermo-viscoelasticity with voids. The governing equations of generalized thermo-viscoelastic medium with voids are specialized in x-z plane. The plane wave solution of these equations shows the existence of three coupled longitudinal waves and a shear vertical wave in a generalized thermo-viscoelastic medium with voids. For incident plane wave (longitudinal or shear), three coupled longitudinal waves and a shear vertical wave reflect back in the medium. The mechanical boundary conditions at free surface of solid half-space are considered as impedance boundary conditions, in which the shear force tractions are assumed to vary linearly with the tangential displacement components multiplied by the frequency. The impedance corresponds to the constant of proportionality. The appropriate potentials of incident and reflected waves in the half-space will satisfy the required impedance boundary conditions. A non-homogeneous system of four equations in the amplitude ratios of reflected waves is obtained. These amplitude ratios are functions of material parameters, impedance parameter, angle of incidence, thermal relaxation and speeds of plane waves. Using relevant material parameters for

medium, the amplitude ratios are computed numerically and plotted against certain ranges of impedance parameter and the angle of incidence.

1. INTRODUCTION

Cowin and Nunziato [1] developed the theory of elastic material with voids. Iesan [2, 3] developed the theory of thermoelastic material with voids. Various dynamical problems and plane strain problems in theory of elasticity and thermoelasticity with voids have been appeared in literature. For example, Iesan [4], Ciarletta and Scalia [5], Chirita and Scalia [6], Chirita et al. [7], Iesan and Nappa [8], Chirita and D'Apice [9, 10] and Ciarletta et al. [11] have studied various outstanding dynamical problems in theory of thermoelasticity with voids. Various problems on plane wave propagation in elasticity and thermoelasticity with voids were also studied. For example, Puri and Cowin [12], Chandrasekharaiah [13, 14], Singh [15], Ciarletta and Straughan [16], Ciarletta, et al. [17] and Bucur et al. [18].

Iesan [19, 20] developed theories of thermoviscoelastic materials with voids by incorporating the memory effects. Some problems on waves and vibrations in thermoviscoelastic material with voids were studied by Sharma and Kumar [21], Svanadze [22], Tomar et al. [23], Chirita [24], Chirita and Danescu [25], D'Apice and Chirita [26] and Bucur [27]. Exploring various problems on wave propagation in thermoviscoelastic materials with voids is useful in civil engineering, seismology, nano-technology and bio-materials [28]. In the present paper, we consider a generalized thermoviscoelastic solid half-space with voids, whose surface is subjected to impedance boundary conditions as in Godoy [29], where the tangential components of stress tensor depends linearly on tangential displacement components times frequency, respectively. A problem on reflection of plane (longitudinal or shear) wave in

a generalized thermoviscoelastic medium with voids under these impedance boundary conditions is considered. The reflection coefficients (or amplitude ratios) of various reflected waves are analysed numerically to show the dependence on angle of incidence, viscous, thermal and voids parameters and impedance parameters.

2. BASIC EQUATIONS

Following Iesan [19] and Lord and Shulman [30], the system of field equations for isotropic and homogeneous generalized thermoviscoelastic porous solid in absence of body forces and heat sources are:

(a) the equations of motion

$$t_{sr,s} = \rho \ddot{u}_r, \quad (1)$$

$$H_{r,r} + g = \rho K^* \ddot{\phi}, \quad (2)$$

(b) the energy equation

$$\rho T_0 \dot{\eta} = Q_{r,r}, \quad (3)$$

(c) the constitutive equations

$$t_{rs} = \lambda_0 e_{mm} \delta_{rs} + 2\mu_0 e_{rs} + b_0 \phi \delta_{rs} - \beta T \delta_{rs}, \quad (4)$$

$$H_r = \alpha_0 \phi_{,r} + \tau^* T_{,r}, \quad (5)$$

$$g = -b_0 e_{mm} - \xi_0 \phi + mT, \quad (6)$$

$$\rho \eta = \beta e_{mm} + aT + m\phi, \quad (7)$$

$$Q_r + \tau_0 \dot{Q}_r = \kappa T_{,r} + \zeta \dot{\phi}_{,r}, \quad (8)$$

$$e_{rs} = \frac{1}{2}(u_{r,s} + u_{s,r}), \quad (9)$$

Using equations (4) to (9) in equations (1) to (3), we can obtain following equations

$$\mu_0 u_{s,rr} + (\lambda_0 + \mu_0) u_{m,ms} + b_0 \phi_{,s} - \beta T_{,s} = \varrho \ddot{u}_s, \quad (10)$$

$$\alpha_0 \phi_{,rr} - \gamma_0 u_{r,r} - \xi_0 \phi + \tau^* T_{,rr} + mT = \varrho K^* \ddot{\phi}, \quad (11)$$

$$\kappa T_{,rr} + \zeta \dot{\phi}_{,rr} = \beta T_0 (\dot{u}_{r,r} + \tau_0 \ddot{u}_{r,r}) + mT_0 (\dot{\phi} + \tau_0 \ddot{\phi}) + C_e (\dot{T} + \tau_0 \ddot{T}), \quad (12)$$

where the following notations are used

$$C_e = aT_0, \quad \lambda_0 = \lambda + \lambda^* \frac{\partial}{\partial t}, \quad \mu_0 = \mu + \mu^* \frac{\partial}{\partial t}, \quad b_0 = b + b^* \frac{\partial}{\partial t}, \quad \alpha_0 = \alpha + \alpha^* \frac{\partial}{\partial t}, \quad \gamma_0 = b + \gamma^* \frac{\partial}{\partial t}, \quad \xi_0 = \xi + \xi^* \frac{\partial}{\partial t}.$$

and t_{rs} are the components of the stress tensor, H_r are the components of the equilibrated stress vector, g is the intrinsic equilibrated body force, η is the entropy per unit mass, Q_r are the components of the heat flux vector, e_{rs} are the components of the strain tensor, ϱ is the mass density of the medium, K^* is the equilibrated inertia, u_r are the components of the displacement vector, ϕ is the void volume fraction, θ is the change in temperature from the constant reference temperature T_0 and δ_{rs} are the components of the Kronecker delta, λ and μ are well known Lamé's constant parameters, b , α , ξ and ξ^* are the constant parameters corresponding to voids present in the medium, β , τ^* , m , κ , ζ and a are the constant thermal parameters and λ^* , μ^* , b^* , α^* and γ^* are the constant viscoelastic parameters, τ_0 is thermal relaxation time.

Equations (10) to (12) are specialized in x-z plane as

$$\mu_0 (u_{1,11} + u_{1,33}) + (\lambda_0 + \mu_0) (u_{1,11} + u_{3,31}) + b_0 \phi_{,1} - \beta T_{,1} = \varrho \ddot{u}_1 \quad (13)$$

$$\mu_0(u_{3,11} + u_{3,33}) + (\lambda_0 + \mu_0)(u_{1,13} + u_{3,33}) + b_0\phi_{,3} - \beta T_{,3} = \rho\ddot{u}_3 \quad (14)$$

$$\alpha_0(\phi_{,11} + \phi_{,33}) - \gamma_0(u_{1,1} + u_{3,3}) - \xi_0\phi + \tau^*(T_{,11} + T_{,33}) + mT = \rho K^*\ddot{\phi}, \quad (15)$$

$$\begin{aligned} \kappa(T_{,11} + T_{,33}) + \zeta(\dot{\phi}_{,11} + \dot{\phi}_{,33}) - \beta T_0\{(\dot{u}_{1,1} + \dot{u}_{3,3}) + \tau_0(\ddot{u}_{1,1} + \ddot{u}_{3,3})\} \\ -mT_0(\dot{\phi} + \tau_0\ddot{\phi}) - C_e(\dot{T} + \tau_0\ddot{T}) = 0, \end{aligned} \quad (16)$$

Using the following Helmholtz representations of displacement components in terms of potentials

$$u_1 = \frac{\partial q}{\partial x} - \frac{\partial \psi}{\partial z}, \quad u_3 = \frac{\partial q}{\partial z} + \frac{\partial \psi}{\partial x} \quad (17)$$

the equations (13) to (16) result into the following equations

$$\mu_0\left(\frac{\partial^2 \psi}{\partial x^2} + \frac{\partial^2 \psi}{\partial z^2}\right) = \rho\ddot{\psi} \quad (18)$$

$$(\lambda_0 + 2\mu_0)\left(\frac{\partial^2 q}{\partial x^2} + \frac{\partial^2 q}{\partial z^2}\right) + b_0\phi - \beta T = \rho\ddot{q} \quad (19)$$

$$\alpha_0\left(\frac{\partial^2 \phi}{\partial x^2} + \frac{\partial^2 \phi}{\partial z^2}\right) - \gamma_0\left(\frac{\partial^2 q}{\partial x^2} + \frac{\partial^2 q}{\partial z^2}\right) - \xi_0\phi + \tau^*\left(\frac{\partial^2 T}{\partial x^2} + \frac{\partial^2 T}{\partial z^2}\right) + mT = \rho K^*\ddot{\phi} \quad (20)$$

$$\begin{aligned} \kappa\left(\frac{\partial^2 T}{\partial x^2} + \frac{\partial^2 T}{\partial z^2}\right) + \zeta\left(\frac{\partial^2 \dot{\phi}}{\partial x^2} + \frac{\partial^2 \dot{\phi}}{\partial z^2}\right) - \beta T_0\left\{\left(\frac{\partial^2 \dot{q}}{\partial x^2} + \frac{\partial^2 \dot{q}}{\partial z^2}\right) + \tau_0\left(\frac{\partial^2 \ddot{q}}{\partial x^2} + \frac{\partial^2 \ddot{q}}{\partial z^2}\right)\right\} \\ -mT_0(\dot{\phi} + \tau_0\ddot{\phi}) - C_e(\dot{T} + \tau_0\ddot{T}) = 0. \end{aligned} \quad (21)$$

We seek the plane wave solutions of equations (18) to (21) of the following form

$$\{q, \phi, T, \psi\} = \{A, B, C, D\} \exp[ik(\sin \theta x + \cos \theta z - Vt)], \quad (22)$$

where A, B, C, D and E are arbitrary constants. k is the wavenumber, V is the complex phase speed and θ is the angle of propagation. With the help of (22), the

non-trivial plane wave solution of equation (18) leads to

$$V^2 = \frac{\mu_0}{\rho}. \quad (23)$$

which is the speed of shear vertical (*SV*) wave.

With the help of (22) the plane wave solutions of equations (19) to (21) lead to following cubic velocity equation

$$\begin{aligned} & \left(\frac{1 - \bar{\xi}_0}{\rho} - \epsilon_2 \bar{m} \right) \Gamma^3 - \left[\bar{\kappa} (1 - \bar{\xi}_0) + \frac{c_2}{\rho} + \epsilon_3 c_3 + \epsilon_3 \bar{m} + \frac{c_1 (1 - \bar{\xi}_0)}{\rho} - \epsilon_2 c_1 \bar{m} + \frac{b_0 \bar{\gamma}_0}{\rho} + \epsilon_1 b_0 \bar{m} \right. \\ & \left. + \beta \gamma_0 \epsilon_2 + \beta \epsilon_1 (1 - \bar{\xi}_0) \right] \Gamma^2 + \left[\bar{\kappa} c_2 - \epsilon_3 c_3 + \bar{\kappa} c_1 (1 - \bar{\xi}_0) + \frac{c_1 c_2}{\rho} - c_1 c_3 \epsilon_3 + c_1 \bar{m} \epsilon_3 \right. \\ & \left. + b_0 \bar{\gamma}_0 \bar{\kappa} - b_0 c_3 \epsilon_1 - \beta \epsilon_3 \bar{\gamma}_0 + \beta c_2 \epsilon_1 \right] \Gamma - (c_1 c_2 \bar{\kappa} - c_1 c_3 \epsilon_3) = 0, \end{aligned} \quad (24)$$

where

$$\Gamma = \rho v^2, \quad c_1 = \lambda_0 + 2\mu_0, \quad c_2 = \frac{\alpha_0}{K^*}, \quad c_3 = -\frac{\tau^*}{K^*}, \quad \epsilon_1 = \frac{\beta T_0}{\rho C_e},$$

$$\epsilon_2 = \frac{m T_0}{\rho C_e}, \quad \epsilon_3 = \frac{\zeta^* \omega^2}{C_e}, \quad \bar{\kappa} = \frac{\kappa}{C_e (\tau_0 + \frac{i}{\omega})}, \quad \bar{\gamma}_0 = \frac{\gamma_0}{\rho K^* \omega^2},$$

$$\bar{m} = \frac{m}{\rho K^* \omega^2}, \quad \bar{\xi}_0 = \frac{\xi_0}{\rho K^* \omega^2}, \quad \zeta^* = \frac{i \zeta}{\omega (\tau_0 + \frac{i}{\omega})}.$$

The real parts of the roots of cubic velocity equation (24) correspond to the speeds of three coupled longitudinal (*P1*, *P2* and *P3*) waves.

3. REFLECTION FROM A PLANE SURFACE

We consider a half-space of a generalized thermoviscoelastic medium with voids. The plane surface of the half-space is taken along the x-axis. The negative z-axis is taken as normal into the half-space as shown in Figure 1. Following Godoy et al.

[29], we assume that the surface of half-space is subjected to impedance boundary conditions, where the tangential tractions are proportional to tangential displacement components time frequency, respectively. Therefore, in the present problem, the impedance boundary conditions at $z = 0$ are expressed as

$$t_{33} = 0, \quad t_{31} + \omega Z u_1 = 0, \quad H_3 = 0, \quad Q_3 = 0, \quad (25)$$

where

$$t_{33} = \lambda_0(e_{11} + e_{33}) + 2\mu_0 e_{33} + b_0 \phi - \beta T, \quad t_{31} = 2\mu_0 e_{31},$$

$$Q_3 = \kappa \frac{\partial T}{\partial z} + \zeta \frac{\partial \dot{\phi}}{\partial z}, \quad H_3 = \alpha_0 \frac{\partial \phi}{\partial z} + \tau^* \frac{\partial T}{\partial z},$$

and ω is frequency of wave and Z is impedance parameters of dimension stress/velocity, which is assumed strictly real. For $Z = 0$, the impedance boundary conditions reduce to traction-free boundary conditions and $|Z| \rightarrow +\infty$ corresponds to vanishing of tangential component of displacement vector. For an incident P_1 or SV wave at plane surface $z = 0$, the reflected P_1, P_2, P_3 and SV waves propagate in the half-space ($z < 0$). The appropriate potentials for incident and reflected waves in the half-space are:

$$q = A_0 \exp\{ik_1(x \sin \theta_0 + z \cos \theta_0 - v_1 t)\}$$

$$+ \sum_{j=1}^3 A_j \exp\{ik_j(x \sin \theta_j - z \cos \theta_j - v_j t)\}, \quad (26)$$

$$\phi = p_1 A_0 \exp\{ik_1(x \sin \theta_0 + z \cos \theta_0 - v_1 t)\}$$

$$+ \sum_{j=1}^3 p_j A_j \exp\{ik_j(x \sin \theta_j - z \cos \theta_j - v_j t)\}, \quad (27)$$

$$T = q_1 A_0 \exp\{ik_1(x \sin \theta_0 + z \cos \theta_0 - v_1 t)\}$$

$$+ \sum_{j=1}^3 q_j A_j \exp\{ik_j(x \sin \theta_j - z \cos \theta_j - v_j t)\}, \quad (28)$$

$$\begin{aligned}\psi = & B_0 \exp\{ik_4(x \sin \theta_0 + z \cos \theta_0 - v_4 t)\} \\ & + B_1 \exp\{ik_4(x \sin \theta_4 - z \cos \theta_4 - v_4 t)\}.\end{aligned}\quad (29)$$

where $v_i = \text{Re}(V_i)$, ($i = 1, 2, \dots, 4$) and the expression for $\frac{p_j}{k_j^2}$, $\frac{q_j}{k_j^2}$, ($j = 1, 2, 3$) are

given as

$$\begin{aligned}\frac{p_j}{k_j^2} &= \frac{(\tau^* - \frac{m}{k_j^2})(\lambda_0 + 2\mu_0 - \varrho v_j^2) + \frac{\beta \gamma_0}{k_j^2}}{b_0(\tau^* - \frac{m}{k_j^2}) + \beta(\alpha_0 + \frac{\xi_0}{k_j^2} - \varrho K^* v_j^2)}, \\ \frac{q_j}{k_j^2} &= \frac{-(\alpha_0 + \frac{\xi_0}{k_j^2} - \varrho K^* v_j^2)(\lambda_0 + 2\mu_0 - \varrho v_j^2) + \frac{b_0 \gamma_0}{k_j^2}}{b_0(\tau^* - \frac{m}{k_j^2}) + \beta(\alpha_0 + \frac{\xi_0}{k_j^2} - \varrho K^* v_j^2)}.\end{aligned}$$

The potentials given in equations (26) to (29) satisfy boundary conditions (25) if following relations (Snell's law for present problem) hold

$$\frac{\sin \theta_0}{v_1 \text{ or } v_4} = \frac{\sin \theta_1}{v_1} = \frac{\sin \theta_2}{v_2} = \frac{\sin \theta_3}{v_3} = \frac{\sin \theta_4}{v_4} \quad (30)$$

$$k_1 v_1 = k_2 v_2 = k_3 v_3 = k_4 v_4 \quad (31)$$

and

(a) incident P wave

$$\sum_{j=1}^4 a_{ij} Z_j = b_i, \quad (i = 1, 2, \dots, 4) \quad (32)$$

where

$Z_j = \frac{A_j}{A_0}$, ($j = 1, 2, 3$) and $Z_4 = \frac{B_1}{A_0}$ are reflection coefficients of reflected P_1, P_2, P_3 and SV waves, and

$$b_1 = -1, \quad b_2 = -1, \quad b_3 = 1, \quad b_4 = 1,$$

$$a_{1j} = \frac{(\frac{v_1}{v_j})^2 [(\lambda - iw\lambda^*) + 2(\mu - iw\mu^*)(1 - (\frac{v_j}{v_1})^2 \sin^2 \theta_0) - (b - iw b^*) \frac{p_j}{k_j^2} + \beta \frac{q_j}{k_j^2}]}{(\lambda - iw\lambda^*) + 2(\mu - iw\mu^*) \cos^2 \theta_0 - (b - iw b^*) \frac{p_1}{k_1^2} + \beta \frac{q_1}{k_1^2}},$$

$$\begin{aligned}
a_{14} &= -\frac{2(\mu - i\omega\mu^*)\frac{v_1}{v_4} \sin \theta_0 \sqrt{1 - (\frac{v_4}{v_1})^2 \sin^2 \theta_0}}{(\lambda - i\omega\lambda^*) + 2(\mu - i\omega\mu^*) \cos^2 \theta_0 - (b - i\omega b^*)\frac{p_1}{k_1^2} + \beta\frac{q_1}{k_1^2}}, \\
a_{2j} &= \left(\frac{v_1}{v_j}\right) \left[\frac{2\sqrt{1 - (\frac{v_j}{v_1})^2 \sin^2 \theta_0} + iZ_j}{-2 \cos \theta_0 + iZ_1} \right], \quad Z_j = \frac{v_j Z}{\mu - i\omega\mu^*}, \quad (j = 1, 2, 3), \\
a_{24} &= \left(\frac{v_1}{v_4}\right)^2 \left[\frac{1 - 2(\frac{v_4}{v_1})^2 \sin^2 \theta_0 + iZ_4 \sqrt{1 - (\frac{v_4}{v_1})^2 \sin^2 \theta_0}}{\sin \theta_0 (-2 \cos \theta_0 + iZ_1)} \right], \quad Z_4 = \frac{v_4 Z}{\mu - i\omega\mu^*}, \\
a_{3j} &= \frac{(\frac{v_1}{v_j})(\omega p_j \zeta + i q_j \kappa) \sqrt{1 - (\frac{v_j}{v_1})^2 \sin^2 \theta_0}}{(\omega p_1 \zeta + i q_1 \kappa) \cos \theta_0}, \quad (j = 1, 2, 3), \quad a_{34} = 0, \\
a_{4j} &= \frac{(\frac{v_1}{v_j})[(\alpha - i\omega\alpha^*)p_j + \tau^* q_j] \sqrt{1 - (\frac{v_j}{v_1})^2 \sin^2 \theta_0}}{[(\alpha - i\omega\alpha^*)p_1 + \tau^* q_1] \cos \theta_0}, \quad (j = 1, 2, 3), \quad a_{44} = 0, \\
\text{(b) incident } SV \text{ wave:}
\end{aligned}$$

$$\sum_{j=1}^4 c_{ij} Y_j = d_i, \quad (i = 1, 2, \dots, 4) \tag{33}$$

where

$Y_j = \frac{A_j}{B_0}$ ($j = 1, 2, 3$) and $Y_4 = \frac{B_1}{B_0}$ are reflection coefficients of reflected P_1, P_2, P_3 and SV waves, and,

$$d_1 = -1, \quad d_2 = -1, \quad d_3 = 0, \quad d_4 = 0,$$

$$c_{1j} = \frac{(\frac{v_4}{v_j})^2 [(\lambda - i\omega\lambda^*) + 2(\mu - i\omega\mu^*) [1 - (\frac{v_j}{v_4})^2 \sin^2 \theta_0] - (b - i\omega b^*)\frac{p_j}{k_j^2} + \beta\frac{q_j}{k_j^2}]}{(\mu - i\omega\mu^*) \sin 2\theta_0},$$

$$c_{14} = -1,$$

$$c_{2j} = \sin \theta_0 \left(\frac{v_4}{v_j}\right) \left[\frac{2\sqrt{1 - (\frac{v_j}{v_4})^2 \sin^2 \theta_0} + iZ_j}{1 - 2 \sin^2 \theta_0 - iZ_4 \cos \theta_0} \right], \quad (j = 1, 2, 3),$$

$$c_{24} = \frac{1 - 2 \sin^2 \theta_0 + iZ_4 \cos \theta_0}{1 - 2 \sin^2 \theta_0 - iZ_4 \cos \theta_0},$$

$$c_{3j} = \left(\frac{v_4}{v_j}\right)(w\zeta p_j + i\kappa q_j) \sqrt{1 - \left(\frac{v_j}{v_4}\right)^2 \sin^2 \theta_0}, \quad (j = 1, 2, 3), \quad c_{34} = 0,$$

$$c_{4j} = \left(\frac{v_4}{v_j}\right)[(\alpha - iw\alpha^*)p_j + \tau^* q_j] \sqrt{1 - \left(\frac{v_j}{v_4}\right)^2 \sin^2 \theta_0}, \quad (j = 1, 2, 3), \quad c_{44} = 0.$$

4. RESULTS

To get an idea about the dependence of amplitude ratios of various reflected waves on angle of incidence, impedance parameter and other material parameters, the copper is treated as a thermoviscoelastic material with voids. The following physical constants of copper material are considered

$$\begin{aligned} \lambda &= 7.76 \times 10^{11} \text{ dyn/cm}^2, & \mu &= 3.86 \times 10^{11} \text{ dyn/cm}^2, & \rho &= 8.954 \text{ gm/cm}^3, \\ c &= 3.4303 \times 10^4 \text{ dyn/cm}^2 \text{ } ^\circ\text{C}, & b &= 2 \times 10^3 \text{ dyn/cm}^2, & \alpha &= 1.688 \text{ dyn}, \\ \beta &= 0.4 \times 10^{-1} \text{ dyn/cm}^2 \text{ } ^\circ\text{C}, & \xi &= 1.475 \text{ dyn/cm}^2, & m &= 0.2 \times 10^7 \text{ dyn/cm}^2 \text{ } ^\circ\text{C}, \\ \kappa &= 0.386 \times 10^8 \text{ dyn/s } ^\circ\text{C}, & T_0 &= 293 \text{ K}, & K^* &= 1.75 \times 10^{-11} \text{ cm}^2, \end{aligned}$$

and we set

$$\begin{aligned} \lambda^* &= 0.1 \text{ dyn s/cm}^2, & \mu^* &= 0.2 \text{ dyn s/cm}^2, & b^* &= 0.1 \times 10^{-3} \text{ dyn s/cm}^2, \\ \xi^* &= 0.3 \text{ dyn s/cm}^2, & \alpha^* &= 0.1 \text{ dyn s}, & \gamma^* &= 0.5 \times 10^{-7} \text{ dyn s/cm}^2, \\ \tau^* &= 0.3 \times 10^{-7} \text{ dyn/ } ^\circ\text{C}, & \zeta &= 1.5 \times 10^{-11} \text{ dyn}. \end{aligned}$$

For above values of material parameters, the non-homogeneous systems (32) and (33) of linear equations in amplitude ratios of reflected waves are solved by using Fortran program of Gauss elimination method. For incident $P1$ wave, the amplitude ratios of reflected waves are plotted against the range $0^\circ \leq \theta_0 \leq 90^\circ$ of angle of incidence in Figure 2 by solid lines, when impedance parameter $Z = 0$. The amplitude ratios of reflected $P1$ wave is 0.98 at $\theta_0 = 0^\circ$ (normal incidence). It decreases to a value 0.6695 at $\theta_0 = 55^\circ$ and then increases to a value one at $\theta_0 = 90^\circ$ (grazing incidence). The amplitude ratios of reflected $P2$ and $P3$ waves are very smaller

in comparison to that of $P1$ wave. The maximum values of the amplitude ratios of reflected $P2$ and $P3$ waves are $0.4841e-05$ and $0.4825e-05$ at normal incidence. These reduce to zero at grazing incidence. The amplitude ratios of reflected SV is 0.9742 at normal incidence and it also reduces to zero at grazing incidence. Similar variations for impedance parameters $Z = -5$ and $Z = 5$ are also shown in Figure 2 by dashed line and dashed line with star as center symbols, respectively. The comparison of these dashed lines with solid line shows the effect of impedance parameter at each angle of incidence of $P1$ wave.

For incident $P1$ wave, the amplitude ratios of reflected waves are plotted against the range $-20 \leq Z \leq 20$ of impedance parameter in Figure 3 by dashed line, dashed line with squares and solid line with stars for $\theta_0 = 30^\circ, 60^\circ$ and 90° , respectively. The comparison of these three variations shows the effect of three different angle of incidences in a particular range of impedance parameter. It is observed that there is no impact of impedance at grazing incidence.

For incident $SV1$ wave, the amplitude ratios of reflected waves are plotted against the range $1^\circ \leq \theta_0 \leq 45^\circ$ of angle of incidence in Figure 4 by solid lines, when impedance parameter $Z = 0$. Beyond $\theta_0 > 45^\circ$, a phase change occurs. The amplitude ratios of reflected $P1$ wave is zero at $\theta_0 = 1^\circ$ (near normal incidence). It increases to its maximum value 0.5472 at $\theta_0 = 34^\circ$ and then decreases sharply to its minimum value zero at $\theta_0 = 90^\circ$ (grazing incidence). In this case also, the amplitude ratios of reflected $P2$ and $P3$ waves are observed very smaller in comparison to that of $P1$ wave. The maximum values of the amplitude ratios of reflected $P2$ and $P3$ waves are $0.7350e - 04$ and $0.7355e - 04$ at $\theta_0 = 25^\circ$. These amplitude ratios of reflected $P2$ and $P3$ waves reduce to zero at 1° and 45° . The amplitude ratios of reflected SV is one at $\theta_0 = 1^\circ$ and it reduces to 0.5416 at $\theta_0 = 39^\circ$ and increases

sharply to one at 45° . Similar variations for impedance parameters $Z = -5$ and $Z = 5$ are also shown in Figure 4 by dashed line and dashed line with star as center symbols, respectively. The comparison of these dashed lines with solid line shows the effect of impedance parameter at each angle of incidence of SV wave.

For incident SV wave, the amplitude ratios of reflected waves are plotted against the range $-20 \leq Z \leq 20$ of impedance parameter in Figure 5 by dashed line, dashed line with stars and solid line with squares for $\theta_0 = 15^\circ, 30^\circ$ and 45° , respectively. The comparison of these three variations shows the effect of three different angle of incidences in a particular range of impedance parameter. It is observed that there is no impact of impedance at $\theta_0 = 45^\circ$.

5. CONCLUSIONS

Plane waves in a thermoviscoelastic medium with voids is studied in context of Lord and Shulman theory of generalized thermoelasticity. The solution of specialized governing equations of medium shows the existence of three coupled longitudinal waves ($P1, P2$ and $P3$) and a shear vertical (SV) wave. The relations between the amplitude ratios of various reflected waves are obtained for incidence of both $P1$ and SV waves. For a particular material representing the medium, the amplitude ratios of the reflected waves are computed and plotted against the angle of incidence and impedance parameter. The numerical discussion of these plots provide some vital observations:

- (i) The introduction of impedance parameter in tangential stress component changes significantly the amplitude ratios of reflected waves for incidence of both $P1$ and SV waves.
- (ii) For incident $P1$ wave, the impedance parameter significantly changes the amplitude ratios of reflected waves at each angle of incidence except grazing incidences.

From figure 2, it is also observed that the presence of impedance parameter changes significantly the amplitude ratios of reflected shear vertical wave at normal incidence and the amplitude ratios of reflected longitudinal waves remain unaffected at normal incidence.

(iii) For incident SV wave, the impedance parameter significantly changes the amplitude ratios of reflected waves at each angle of incidence except at $\theta_0 = 45^\circ$. Again from figure 4, it is also observed that the presence of impedance parameter changes significantly the amplitude ratios of reflected shear vertical wave at normal incidence and the amplitude ratios of reflected longitudinal waves remain unaffected at normal incidence.

ACKNOWLEDGEMENT

Author is highly thankful to University Grants Commission, New Delhi for granting a Major Research Project (MRP-MAJOR-MATH-2013-2149).

REFERENCES

- [1] S.C. Cowin, J.W.Nunziato,Linear theory of elastic materials with voids,J. Elastic 13(1983)125-147.
- [2] D. Iesan,A theory of thermoelastic materials with voids,Acta Mech. 60(1986)67-89.
- [3] D. Iesan,Thermoelastic Models of Cortinua, Kluwer Academic Publishers ,Boston, Dordrecht, London, 2004.
- [4] D. Iesan,Some theorems in the theory of elastic materials with voids,J. Elasticity 15(1985)215-224.
- [5] M. Ciarletta,A. Scalia,On uniqueness and reciprocity in linear thermoelasticity of materials with voids,J. Elasticity 32(1993)1-17.
- [6] S. Ciarletta,A. Scalia,On the spatial and temporal behaviour in linear thermoe-

- lasticity of materials with voids, *J. Therm. Stresses* 24(2001)433-455.
- [7] S. Ciarletta, M. Ciarletta, V. Tibullo, Rayleigh surface waves on a Kelvin-Voigt viscoelastic half-space, *J. Elasticity* 115(2014)61-76.
- [8] D. Iesan, L. Nappa, Thermal stresses in plane strain of porous elastic bodies, *Meccanica* 39(2004)125-138.
- [9] S. Chirita, C.D'Apice, On Saint-Venant's principle for a linear poroelastic material in plane strain, *J. Math. Anal. Appl.* 363(2010)454-467.
- [10] S. Chirita, C.D'Apice, On Saint-Venant's principle in a poroelastic arch-like region, *Math. Methods Appl. Sci.* 33(2010) 1743-1754.
- [11] M. Ciarletta, F. Passarella, M. Svanadze, Plane waves and uniqueness theorems in the coupled linear theory of elasticity for solids with double porosity, *J. Elasticity* 114(2014)55-68.
- [12] P. Puri, S.C. Cowin, Plane waves in linear elastic materials with voids, *J. Elasticity* 15(1985) 167-183.
- [13]. D.S. Chandrasekharaiah, Surface waves in an elastic half-space with voids, *Acta Mech.* 62(1986) 77-85.
- [14] D.S. Chandrasekharaiah, Rayleigh Lamb waves in an elastic plate with voids, *J. Appl. Mech.* 54(1987) 509-512.
- [15] B. Singh, Wave propagation in a generalized thermoelastic material with voids, *Appl. Math. Comp.*, 189 (2007) 698-709.
- [16] M. Ciarletta, B. Straughan, Thermo-poroacoustic acceleration waves in elastic materials with voids, *J. Math. Anal. Appl.* 333(2007)142-150.
- [17] M. Ciarletta, M. Svanadze, L. Buonanno, Plane waves and vibrations in the theory of micropolar thermoelasticity for materials with voids, *Eur. J. Mech., A solid* 28(2009) 897-903.

- [18] A.V.Bucur,F. Passarella,V. Tibullo, Rayleigh surface waves in the theory of thermoelastic materials with voids,Meccanica 49(2014) 2069-2078.
- [19] D. Iesan, On a theory of thermoviscoelastic materials with voids, J. Elastic 104(2011) 369-384.
- [20] D. Iesan, On the Nonlinear Theory of Thermoviscoelastic Materials with Voids, J. Elast., 128 (2017) 1-16.
- [21] K.Sharma, P.Kumar,Propagation of plane waves and fundamental solution in thermoviscoelastic medium with voids,J. Therm. Stresses 36(2013) 94-111.
- [22] M.M. Svanadze, Potential method in the linear theory of viscoelastic materials with voids,J. Elasticity 114(2014) 101-126.
- [23] S.K. Tomar, J. Bhagwan, H. Steeb, Time harmonic waves in a thermo-viscoelastic materials with voids, J. Vib. Control 20(2014) 1119-1136.
- [24] S. Chirita, On the spatial behaviour of the steady-state vibrations in thermo-viscoelastic porous materials, J. Therm. Stresses 38(2015) 96-109.
- [25] S. Chirita and A. Danescu, Surface waves problem in a thermoviscoelastic porous half-space, Wave Motion, 54 (2015) 100-114.
- [26] C. D'Apice, S. Chirita, Plane harmonic waves in the theory of thermoviscoelastic materials with voids, J. Therm. Stresses, 39 (2016)<http://dx.doi.org/10.1080/01495739.2015.112>
- [27] A. Bucur, Rayleigh surface waves problem in linear thermoviscoelasticity with voids, Acta Mechanica, 227 (2016) 1199-1212.
- [28] R.S.Lakes, Viscoelastic Materials,Cambridge University Press, Cambridge, 2009.
- [29] E. Godoy, M. Durn, J.-C. Ndlec, On the existence of the surface waves in an elastic half-space with impedance boundary conditions. Wave Motion, 49 (2012) 585-594.
- [30] H. Lord and Y. Shulman, A generalised dynamical theory of thermoelasticity,

J. Mech. Phys. Solids, 15 (1967) 299-309.

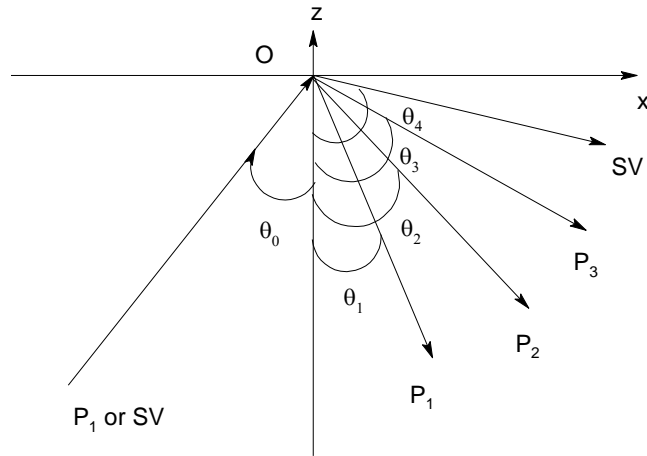


Figure1. Reflection of plane waves at a stress-free surface of a poro-thermo-viscoelastic solid half-space.

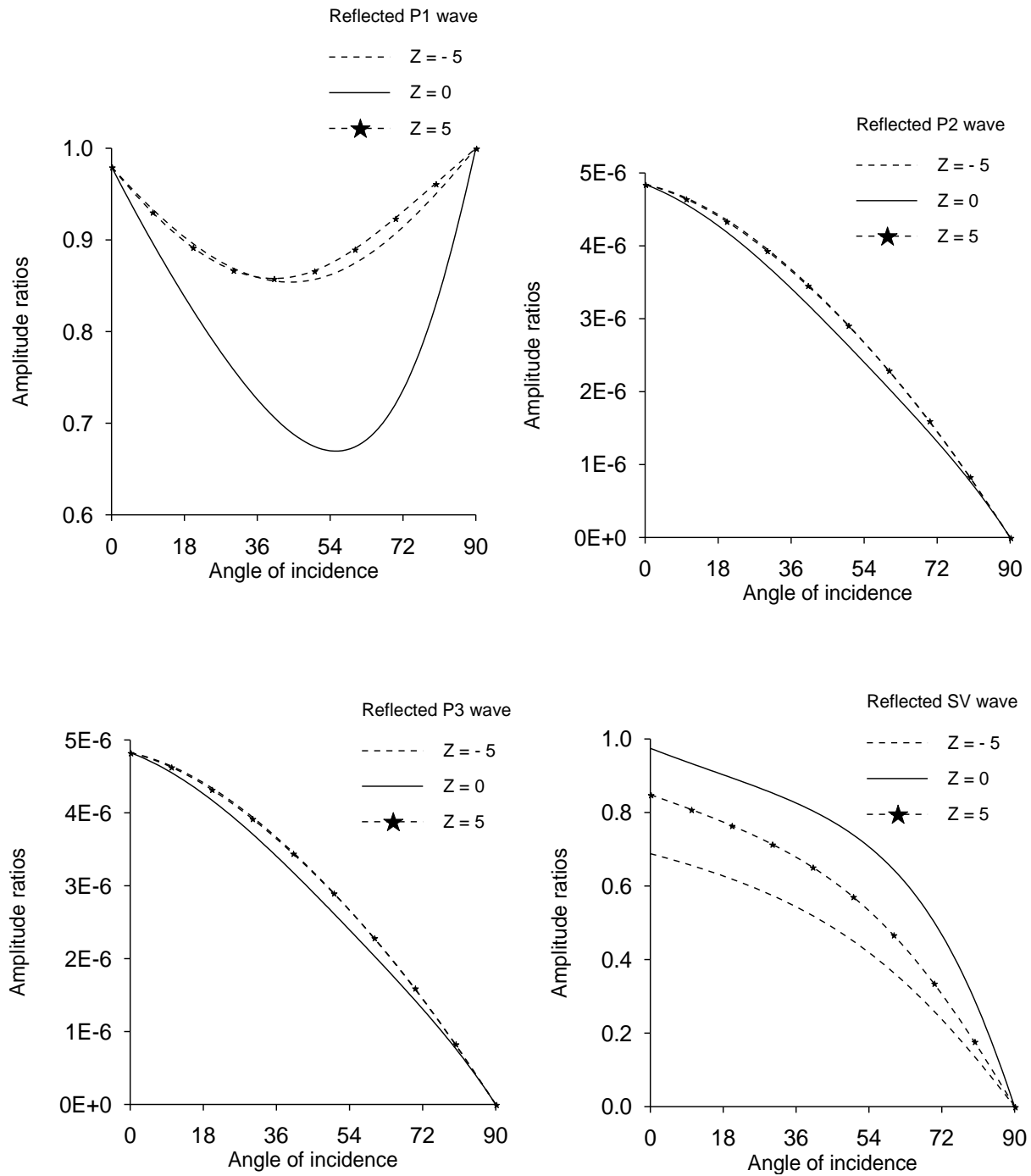


Figure 2. Variations of the amplitude ratios of reflected P1, P2, P3 and SV waves against the angle of incidence θ_0 of incident P1 wave when $Z = -5, 0$ and 5 .

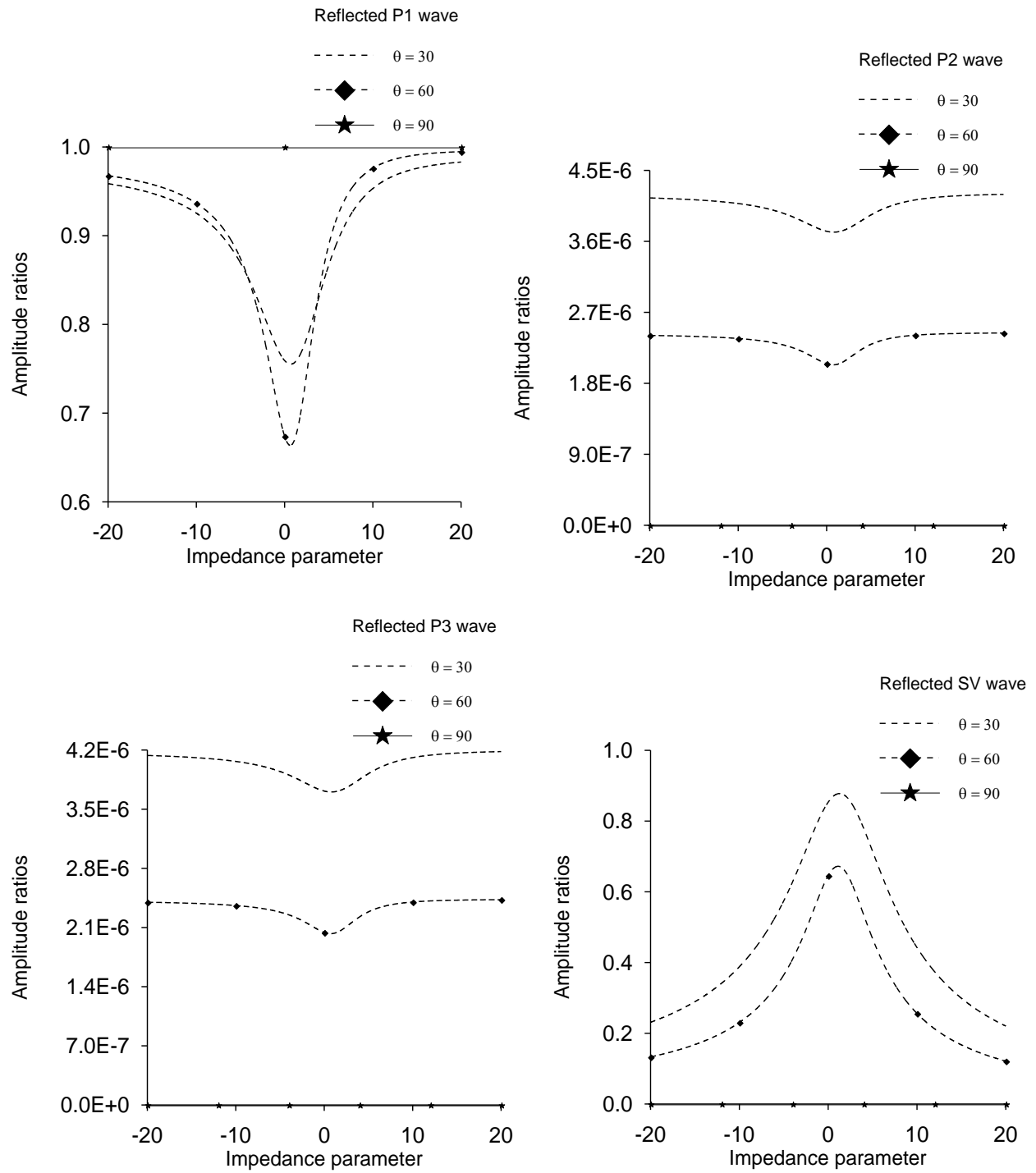


Figure 3. Variations of the amplitude ratios of reflected P1, P2, P3 and SV waves against the impedance parameter Z for incident P1 wave when $\theta_0 = 30^\circ$, 60° and 90° .

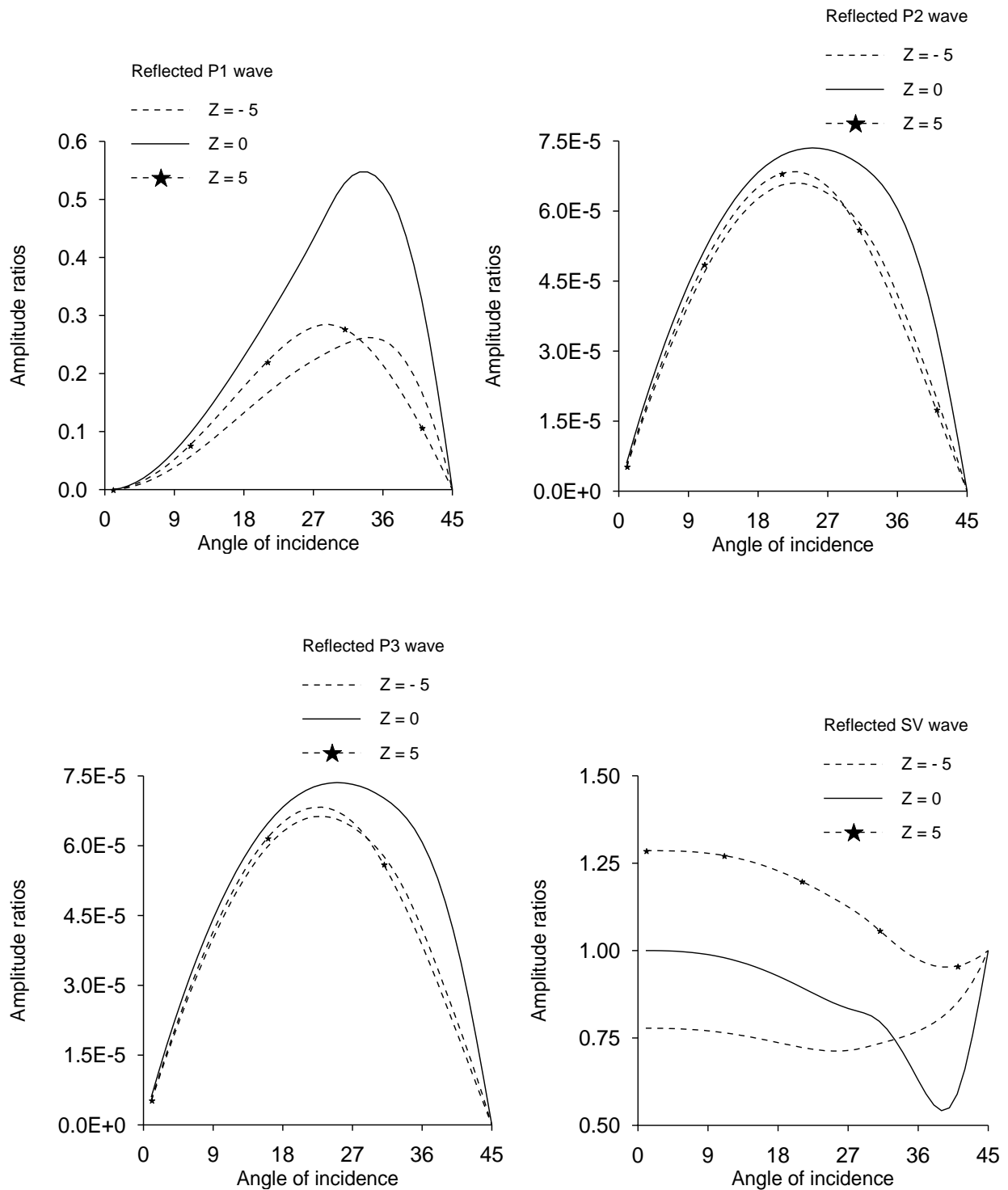


Figure 4. Variations of the amplitude ratios of reflected P1, P2, P3 and SV waves against the angle of incidence θ_0 of incident SV wave when $Z = -5, 0$ and 5 .

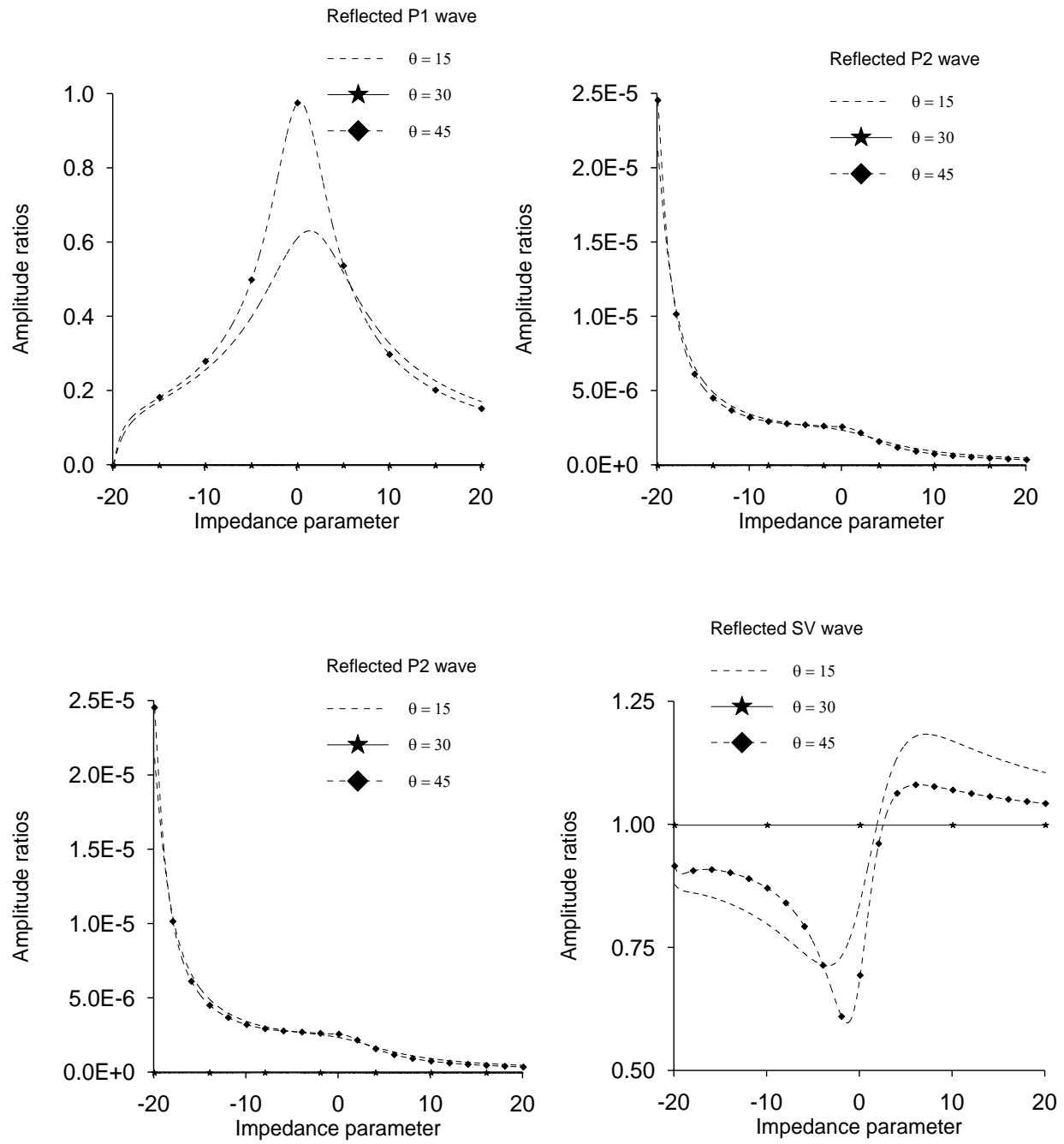


Figure 5. Variations of the amplitude ratios of reflected P1, P2, P3 and SV waves against the impedance parameter Z for incident SV wave when $\theta_0 = 15^\circ, 30^\circ$ and 45° .

Summary

1. A problem on the Rayleigh wave at a traction free surface of a generalized porothermoelastic solid half-space is considered. The governing equations of generalized porothermoelasticity are solved for surface wave solutions. The general solutions satisfying the required radiation conditions are obtained in a half-space of the material. These solutions satisfy the suitable boundary conditions at the free surface of the half-space to obtain the secular equation for wave speed of Rayleigh wave. The wave speed of Rayleigh wave is computed for relevant physical constants of material to observe the effects of porosity, frequency, thermal relaxation times, coefficients of thermal expansion and thermoelastic coupling.
2. The governing equations of generalized porothermoelasticity are formulated in context of Green and Naghdi theory of thermoelasticity without energy dissipation. A problem on Rayleigh type surface in a generalized porothermoelastic solid half-space is considered. The governing equations are solved for particular surface wave solutions satisfying required radiation conditions in the half-space. A secular equation for Rayleigh wave speed is derived after applying these solutions to relevant boundary conditions at stress free thermally insulated surface of half-space. The Rayleigh wave speed is computed for relevant physical constants of material and plotted against various material parameters to observe the effects of porosity, coefficients of thermal expansion, coefficients of thermoelastic coupling and characteristics of solid and fluid phases.
3. A problem on reflection of plane waves from a plane thermally insulated as

well as isothermal surfaces of a half-space is studied in context of Lord-Shulman (LS) and Green-Naghdi (GN) theories of generalized thermoelasticity of saturated porous medium. The mechanical boundary conditions at surface of half-space are considered as impedance boundary conditions, where the normal and shear force tractions are assumed to vary linearly with the normal and tangential displacement components multiplied by the frequency, respectively. The impedance corresponds to the constants of proportionality. The governing equations are specialized in $x-z$ plane. The plane wave solution of these equations shows the existence of three coupled longitudinal waves and a shear vertical wave in a generalized thermoelastic saturated porous medium. For incident plane wave (longitudinal or shear), four reflected waves will propagate in the medium. The appropriate potentials for incident and reflected waves in a half-space are formulated, which satisfy the required boundary conditions with the help of a Snell's law. Finally, a non-homogeneous system of four equations is obtained in the amplitude ratios, where the ratios depend on material parameters, impedance parameter, angle of incidence, thermal relaxation and speeds of plane waves. For relevant material parameters, the amplitude ratios are computed numerically for certain ranges of impedance parameters and the angle of incidence. For validation purpose, the numerical results are compared with those without thermal and porous parameters.

4. A phenomenon of reflection of plane waves from a thermally insulated surface of a solid half-space is studied in context of Lord-Shulman theory of generalized thermo-viscoelasticity with voids. The governing equations of generalized thermo-viscoelastic medium with voids are specialized in $x-z$ plane. The plane wave solution of these equations shows the existence of three coupled longitudinal waves and a shear vertical wave in a generalized thermo-viscoelastic medium with voids.

For incident plane wave (longitudinal or shear), three coupled longitudinal waves and a shear vertical wave reflect back in the medium. The mechanical boundary conditions at free surface of solid half-space are considered as impedance boundary conditions, in which the shear force tractions are assumed to vary linearly with the tangential displacement components multiplied by the frequency. The impedance corresponds to the constant of proportionality. The appropriate potentials of incident and reflected waves in the half-space will satisfy the required impedance boundary conditions. A non-homogeneous system of four equations in the amplitude ratios of reflected waves is obtained. These amplitude ratios are functions of material parameters, impedance parameter, angle of incidence, thermal relaxation and speeds of plane waves. Using relevant material parameters for medium, the amplitude ratios are computed numerically and plotted against certain ranges of impedance parameter and the angle of incidence.

These theoretical and numerical results may be useful in the detection and study of underground layers of porous solids saturated with oil or groundwater. Water-saturated porous medium can be a more realistic seismic model for oceanic bed. At the ocean bottom, lithosphere is formed by upwelling of hot material at ridges which spreads around and cools with time. The evidences for thermal-mechanical processes that control the formation and evolution of thermoelastic lithosphere below oceans are provided by the seismological observations. Therefore, the applications of this theoretical and numerical study are geophysical, for example, for the exploration of the oceanic crust, structural engineering or to hydrocarbon/geothermal processes.